UNIVERSITÀ DEGLI STUDI DI MILANO

DOCTORAL SCHOOL IN BIOCHEMICAL SCIENCE

DIPARTIMENTO DI BIOTECNOLOGIE MEDICHE E MEDICINA TRASLAZIONALE

PHD COURSE IN BIOCHEMISTRY

XXX Cycle

PhD THESIS

BIOCHEMICAL AND FUNCTIONAL PROFILE OF SPONTANEOUSLY DIFFERENTIATED HUMAN MONOCYTE-DERIVED MACROPHAGES IN PATIENTS WITH ISCHEMIC HEART DISEASE

R25

Susanna Fiorelli

Matricola R10987

TUTOR: Professor Donatella Caruso

COORDINATORE DEL DOTTORATO: Professor Sandro Sonnino

ANNO ACCADEMICO 2016/2017

1. ABSTRACT **5**

2. RIASSUNTO **7**

3. INTRODUCTION **9**

3.1 Atherosclerosis **10**

3.1.1 Definition 10

3.1.2 Etiology 10

3.1.3 Formation and development of atherosclerotic plaque 11

3.1.3.1 Classification of atherosclerotic lesion 13

3.1.4 Clinical manifestation of atherosclerosis 15

3.2 Macrophages **17**

3.2.1 Origin 17

3.2.2 Macrophages heterogeneity 19

3.2.3 MDMs in atherosclerotic disease 20

3.2.3.1 Recruitment of monocytes and transmigration in the atherosclerotic plaque 20

3.2.3.2 Differentiation of monocytes in the two different macrophage phenotypes 21

3.2.3.3 Foam cells formation 22

3.2.3.4 Macrophage proliferation 23

3.2.3.5 Macrophage apoptosis 23

3.3 Efferocytosis **25**

3.3.1 Role of efferocytosis in atherosclerotic disease 29

3.4 Transglutaminase 2 **31**

3.4.1 Role of TG2 in atherosclerotic disease 33

3.5 Tissue Factor **34**

3.5.1 Role of TF in atherosclerosis 36

3.6 Oxidative stress **37**

3.6.1 Antioxidant response 38

3.6.1.1 GSH 38

3.6.1.2 Nrf2/HO-1 pathway 39

3.6.2 Oxidative stress and antioxidant response in atherosclerosis 40

3.7 Fatty Acids **42**

3.7.1 Biosynthesis of fatty acids 43

3.7.2 Macrophages fatty acid compositions 46

4. OBJECTIVE **48**

5. MATERIAL AND METHODS **50**

5.1 Patient population **51**

5.2 Blood collection **52**

5.3 Methodologies **52**

5.3.1 Monocyte isolation and culture 52

5.3.2 Western Blot 53

5.3.3 Immunofluorescence 53

5.3.3.1 Quantitative image analysis 53

5.3.4 Apoptosis of Jurkat-T cells 54

5.3.5 Efferocytosis assay 54

5.3.6 Thrombin generation measurement 54

5.3.7 Enzyme activity assay 55

5.3.8 Mass spectrometry analysis 55

5.3.8.1 GSH/GSSG determination 55

5.3.8.2 Total and free fatty acid composition assessment 56

5.3.9 OCT analysis 57

5.3.9.1 OCT image analysis 57

5.3.9.2 OCT macrophage analysis 58

5.4 Biochemical signatures **59**

5.5 Functional analyses **59**

5.6 Oxidative stress evaluation **59**

5.7 Statistical analysis **60**

6. RESULTS **61**

6.1 Study population **62**

6.2 Morphological characterization of MDMs **64**

6.3 Biochemical and functional profile assessment **65**

6.3.1 Efferocytosis of MDMs 65

6.3.2 Evaluation of TG2 levels 65

6.3.3 Evaluation of TF levels 67

6.3.4 Thrombin generation 68

6.4 Matrix Metalloproteinase-9 Activity **69**

6.4.1 Evaluation of GSH/GSSG ratio 69

6.4.2 Evaluation of Nrf2 and HO-1 levels 70

6.5 Fatty acid composition **73**

6.6 MDMs: biochemical and morphological characteristics and OCT plaque features **76**

6.6.1 MDMs morphology 77

6.6.2 MDMs TF levels 79

6.6.3 MDM oxidative stress profile and plaque features analyzed by OCT 80

7. DISCUSSION **83**

8. FUTURE PERSPECTIVES **94**

8. REFERENCES **96**

1. Abstract

Background: Atherosclerosis is a chronic inflammatory disease in which oxidative stress and macrophages play fundamental roles. Macrophages are heterogeneous cells in term of morphology and function and the prevalence of a specific morpho-phenotype may influence the progression or the regression of the plaque. Human coronary plaque macrophages are not easily obtainable and monocyte-derived macrophages (MDMs) are widely accepted as a good surrogate. Our previous study has reported that healthy subjects show two dominant MDM morphotypes, spindle and round, present in the same percentage.

Aim: The aims of the study were to assess the biochemical and functional profile of MDMs obtained from CAD patients and to investigate the relationship between these characteristics and plaque features detected *in vivo*.

Material and methods: ninety CAD patients and twenty-five healthy volunteers were enrolled. MDMs were obtained by culturing monocytes for 7 days in medium supplemented with 10% autologous serum. Transglutaminase2 (TG2), tissue factor (TF), nuclear factor erythroid 2–related factor 2 (Nrf2) and heme-oxygenase (HO-1) were determined by western blotting and immunofluorescence. The uptake of apoptotic Jurkat T cells was detected by flow cytometry and thrombin formation was assessed by thrombinoscope. Fatty acids composition and oxidative stress status, determined as the ratio between the reduced and oxidized forms of glutathione (GSH and GSSG, respectively) were analyzed by liquid-chromatography tandem mass spectrometry (LC-MS/MS). Plaque features were detected *in vivo* by optical coherence tomography (OCT).

Results: MDMs obtained from CAD patients were characterized by the predominance of round cells. These cells exhibited a lower efferocytic capacity and higher capacity to generate thrombin in respect to those of healthy subjects, reflecting the low expression of TG2 and the enhance of TF levels. Moreover, MDMs of CAD patients showed a higher oxidative stress status, evidenced by the lower GSH/GSSG ratio, in respect to those of healthy subjects. Finally, we found a positive correlation between oxidative stress status and membrane fluidity (MFI) as evidenced by the ratio of C18:1 (oleic acid)/C18:2 (linoleic acid), as well as MFI and capacity to engulf apoptotic cells. Regarding OCT analysis, patients with a higher round MDMs prevalence exhibited more frequently a lipid rich plaque, a TCFA (thin cap fibroatheroma), a greater intra-plaque macrophage content, and a ruptured plaque, characteristics of vulnerable plaque. Furthermore,

patients with high TF levels more frequently presented a intra-plaque macrophages accumulation, a ruptured plaque and a presence of thrombus. In addition, vulnerable plaque characteristics were associated with high HO-1 levels.

Conclusions: MDMs of CAD patients present a pro-inflammatory and high thrombogenic profile in respect to those of healthy volunteers. The high oxidative stress present in these cells influences the membrane fluidity that in turn influences the efferocytic capability. This specific cellular profile detected in *in vitro* obtained MDMs is associated with the detection of high-risk and rupture-prone coronary plaques *in vivo*, at OCT investigation.

Different MDM phenotypes might be novel diagnostic and therapeutic target able to counteract the progression of atherosclerosis.

2. Riassunto

Razionale: Lo stress ossidativo e l'infiammazione svolgono un ruolo fondamentale in tutti gli stadi della patologia aterosclerotica. I macrofagi sono cellule caratterizzate da un'elevata eterogeneità morfologica e funzionale e la prevalenza di un determinato fenotipo può influenzare la progressione e/o la regressione della placca. Nell'uomo, i macrofagi della placca coronarica non sono facilmente ottenibili e i macrofagi ottenuti per differenziamento *in vitro* di monociti (MDM) sono considerati un buon surrogato. Un precedente studio condotto nel nostro laboratorio ha evidenziato che gli MDM ottenuti da soggetti sani si presentano come una popolazione morfologicamente eterogenea con cellule tonde e cellule lunghe presenti in egual misura.

Obiettivo: Delineare un profilo biochimico e funzionale e definire la prevalenza dei due diversi morfotipi (a cellule lunghe e tonde) dei macrofagi ottenuti dal differenziamento di monociti isolati da pazienti con patologia coronarica (CAD). Inoltre, nei pazienti queste caratteristiche saranno messe in relazione con le caratteristiche della placca coronarica analizzata *in vivo*.

Materiali e metodi: Sono stati arruolati 90 pazienti CAD e 25 soggetti sani. Gli MDM sono stati ottenuti in seguito al differenziamento dei monociti isolati dal sangue periferico e coltivati per 7 giorni in terreno contenente il 10% di siero autologo. I livelli di transglutaminasi 2 (TG2), di fattore tissutale (TF), del fattore di trascrizione nucleare eritroide-2 (Nrf2) e di eme ossigenasi (HO-1) sono stati valutati mediante western blotting e immunofluorescenza. L'efferocitosi di queste cellule è stata analizzata mediante citofluorimetria a flusso e la formazione di trombina mediante trombinoscopio. Gli acidi grassi e lo stress ossidativo, valutato come rapporto tra la forma ridotta del glutatione e quella ossidata (GSH e GSSG, rispettivamente), sono stati analizzati mediante cromatografia liquida accoppiata a spettrometria di massa. Le caratteristiche della placca sono state valutate *in vivo* mediante tomografia ottica a coerenza di fase (OCT).

Risultati: Gli MDM ottenuti dai pazienti CAD sono caratterizzati da una prevalenza di cellule tonde. Queste cellule mostrano una ridotta efferocitosi con più bassi livelli di TG2, e da una maggior capacità di generare trombina che riflette i più alti livelli di TF presenti. Inoltre, gli MDM ottenuti dai pazienti CAD mostrano livelli di stress ossidativo più alti, evidenziati da un basso rapporto GSH/GSSG, rispetto a quelli ottenuti dai volontari sani. Infine è stata osservata una correlazione positiva tra la fluidità di membrana (MFI), espressa dal rapporto tra acido oleico/acido linoleico, e lo stress ossidativo, così come tra MFI e la capacità efferocitica. L'analisi

della placca mediante OCT, ha evidenziato che i pazienti con una aumentata prevalenza di cellule tonde presentavano più frequentemente una placca ricca in lipidi, un cappuccio fibroso sottile, un alto contenuto di macrofagi intra-placca e una placca lesionata, caratteristiche tipiche della placca vulnerabile. Inoltre, i pazienti con livelli di TF più alti presentavano un maggiore accumulo di macrofagi intra-placca, una placca rotta e la presenza di trombo. Infine, è stato osservato che la vulnerabilità di placca si associa con più alti livelli di HO-1.

Conclusioni: Gli MDM dei pazienti CAD presentano un profilo pro-infiammatorio e pro-trombotico rispetto a quello dei soggetti sani, e un alto livello di stress ossidativo associato ad alterazioni della fluidità della membrana. Questo specifico profilo riscontrato negli MDM ottenuti *in vitro* risulta essere associato con la presenza di placche ad alto rischio e prone alla rottura evidenziate mediante OCT. I diversi fenotipi macrofagici potrebbero quindi rappresentare un nuovo bersaglio diagnostico e terapeutico per contrastare la progressione dell'aterosclerosi.

3. Introduction

3.1 Atherosclerosis

3.1.1 Definition

Atherosclerosis (the term derives from the Greek word ἀρτηρία (athere), meaning gruel (lipid's accumulation), and σκλήρωσις (sclerosis) for hardening) is currently considered as a chronic inflammatory disease in which immune mechanism interact with metabolic risk factors to initiate, propagate, and activate lesions in the arterial tree [1].

3.1.2 Etiology

The cause of atherosclerosis is still unknown but many epidemiological studies have identified several risk factors that can contribute to the pathogenesis of the disease. In particular, atherosclerosis risk factors can be classified into two categories, non-modifiable or modifiable:

a) Non-modifiable risk factors:

- *age*: atherosclerosis is an age-related disease; the incidence is lower in people under 40 years, and increased in elderly people [2]
- *sex*: women generally have a lower risk for developing cardiovascular disease (CVD) compared to men of similar age [3] but this protection is lost during menopause suggesting the importance of sex steroid hormone signaling [4]
- *family history of premature coronary heart disease*: genetic predisposition to developing atherosclerotic disease is related to alterations of genes involved in lipid, sugar and amino acid metabolisms. For example, subjects with a gene mutation in LDL lipoprotein receptor, a pathological condition known as familial hypercholesterolemia, have cholesterol levels twice that of the normal population and they are at high risk to develop cardiovascular disease [5].

b) modifiable risk factors:

- *lifestyle and diet*: a diet rich in animal protein and saturated fat, cholesterol, sodium and sugar associated with a sedentary lifestyle can contribute to increase the incidence of atherosclerosis [6]. Epidemiological studies have shown that cardiovascular disease is higher in western countries than in the eastern ones, where a diet with low calories intake, low in saturated fat and high fiber content, is followed [7]. An unbalanced diet

can favor the insurgence of various pathological conditions associated with atherosclerosis such as diabetes and insulin resistance, obesity and hypertension.

- *hyperlipidemia:* cholesterol is transported by several classes of lipoproteins, such as very low density lipoprotein (VLDL), low density lipoprotein (LDL) and high density lipoprotein (HDL). High levels of plasma cholesterol are related to a high synthesis of LDL, which levels are related to the onset of atherosclerosis [8].
- *hypertension*: the mechanism through which hypertension can promote the onset and the progression of atherosclerosis is still unclear, but it is known that the increase in blood pressure can lead to endothelium damage, with the subsequent increase in the permeability and the retention of LDL in the vessel wall. In addition, hypertensive patients exhibit elevated levels of angiotensin II, a vasoconstrictor mediator that is involved in the atherosclerotic process [9].
- *smoke*: according to World Health Organization data, smoke is responsible for 10% of all CVD cases [10]. Smoke plays a strong role not only in CVD initiation but it also contributes to disease progression and fatal cardiovascular outcomes. The key processes in smoking-induced atherogenesis initiation are endothelial dysfunction and damage, increase in oxidation of proatherogenic lipids, as well as decrease of HDL. Moreover, smoke induces inflammation and tissue factor (TF) expression that contributes to shift toward a procoagulant status [11].
- *diabetes*: hyperglycemia induces non-enzymatic glycosylation processes that may alter the lipoprotein structure and exert adverse effects on the vascular endothelium, promoting an oxidative stress condition [12]. In addition, insulin resistance was associated with hypertriglyceridemia and low levels of HDL. The increase in circulating levels of insulin favors the onset and the development of atheromasic plaque by inducing vascular wall changes, by promoting smooth muscle cell (SMC) proliferation and activating cholesterol synthesis [13].

3.1.3 Formation and development of atherosclerotic plaque

The first step of atherosclerotic plaque formation is the endothelium dysfunction (ED). Vascular endothelium has a pivotal role in the modulation of vascular function and structure, mainly

through the synthesis of nitric oxide (NO). Thereby, many pathophysiological states, mainly by reducing endothelium-dependent vasodilation, evoke ED [14]. ED is defined an early phase as endothelial activation, a switch from a quiescent phenotype toward one that involves host defense response. ED is caused by an increase in radical oxygen species (ROS) generation (free oxygen radicals, superoxide anions and peroxides) and a reduction of NO bioavailability in vascular endothelium. At moderate concentrations ROS act as signaling molecules and play an important role in the regulation of vascular tone, oxygen sensing, cell growth and proliferation, apoptosis, and inflammatory responses [15]. In contrast to these regulatory functions under physiological conditions, excessive or sustained ROS production, exceeding the available antioxidant defense systems, leads to oxidative stress. Radical species mediate the endothelium nitric oxide synthase (eNOS) "uncoupling" that is responsible of the generation of superoxide rather than NO [16]. Another mechanism responsible for the reduction of NO is via the regulation of the levels of the NO synthesis inhibitor asymmetric dimethylarginine (ADMA) [17]. In particular, ROS reduce the activity of dimethyl arginine dimethyl aminohydrolase (DDAH), protein involved in the catabolism of ADMA, upregulate the expression of protein methyl transferases, enzymes involved in ADMA production, resulting in increase ADMA levels [17]. Also, vascular inflammation is highly associated with ED and plays a major role in the development of atherosclerosis.

ED induces the increase of the endothelium permeability causing the retention of LDL into the intima of the vessels. At this level, LDL may undergo to oxidative modification by ROS from surrounding cells and modified LDL participate to the activation of the endothelial cells [18]. Healthy endothelium does not interact with leukocytes; however, activated endothelial cells express adhesion molecules and secrete chemoattractant signals leading to the recruitment of leukocytes from the bloodstream at the site of damage [19]. Among the molecules that are involved in cell adhesion, the selectin family, specifically E- and P-selectin, is responsible for the early attachment of leukocytes. One of the mechanisms involved is represented by the interaction between monocyte P-selectin glycoprotein ligand-1 and the endothelium. Monocytes are anchored to the endothelium through the endothelial intergrins vascular cell adhesion molecule-1 (VCAM-1) and intercellular adhesion molecule-1 (ICAM-1) [19]. In response to the accumulation of modified LDL into the intima, activated edothelium secretes several molecules, such as the chemokine monocyte chemoattractant protein-1 (MCP-1), that promote the

infiltration of monocytes into the vessel wall [18, 20]. At this level, monocytes differentiate into macrophages under the action of different stimuli, particular macrophage colony-stimulating factor [21]. Monocyte derived macrophages (MDM) uptake modified lipoproteins via scavenger receptors, resulting in the formation of lipid laden macrophages known as foam cells. The accumulation of foam cell is the very first event for the formation of early fatty streak [22]. Subsequent chemokine and cytokine secretion by foam cells and resident vascular wall cells induces the migration of SMC from the media into the intima [23]. This migration and the consequent proliferation leads to the secretion of extracellular matrix molecules, such as collagen, proteoglycans and elastin fibers, which are involved in the formation of the fibrous cap, which covers and stabilizes the plaque. Plaque stability depends on cap thickness and its thinning can provoke the plaque rupture. This event promote the exposure of the necrotic core, consisting of lipids, numerous macrophages and SMCs, to the blood flow of the artery causing thrombus formation and often leading to artery occlusion, cardiac event, myocardial infarction or stroke [24].

3.1.3.1 Classification of atherosclerotic lesion

The atheromatous plaques have been reclassified in the 1990s by the American Heart Association (AHA) Consensus Group [25]. This latter classification includes six categories: type I, adaptive intimal thickening; type II, fatty streak; type III, transitional or intermediate lesions; type IV, atheroma; type V, fibroatheroma; type VI, complicated plaques with surface defects, and/or hematoma-hemorrhage, and/or thrombosis (Figure 1).

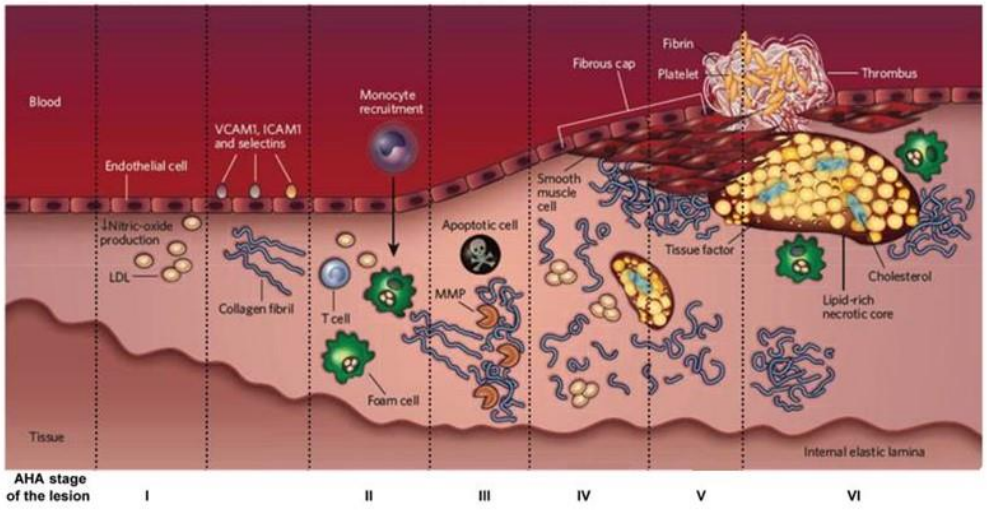

Figure 1. AHA classification of atherosclerotic plaques.

Type I lesion: consists of atherogenic lipoproteins and mononuclear cells infiltration at the intima level. The histological changes are minimal and consist in thickening of the vascular wall. Type I lesions have been described in most infants and children.

Type II lesion: is characterized by fatty streaks formation. This lesion consist of macrophage, foam cells, and smooth muscle cells infiltrated into the intima. The extracellular space contains small quantities of lipid droplets and vesicles. The arteries of children generally contain type II lesions as the only grossly visible lesions.

Type III lesion: is also known as intermediate lesion. It is characterized by the presence of visible extracellular lipid droplets and particles.

Type IV lesion: is also defined atheroma. It is characterized by the presence of the lipid core containing macrophages, smooth muscle cells, lymphocytes and mast cells. Frequently these cell types are more concentrated in the limits of lesion.

Type V lesions: are also known as fibroatheromas. They are lesions in which new fibrous connective tissue has been formed. There are different type of lesions:

- type Va: lesions may be multilayered with the presence of lipid cores close into the media, separated by thick layers of connective tissue;
- type Vb: lesions containing a large amount of calcium and increased content of fibrous connective tissue;
- type Vc: lesions where the normal intima is replaced and thickened with fibrous connective tissue, while lipid is minimal or absent.

Type VI lesion: is also known as complicated lesions. It is a type IV or V lesion in which disruptions of the lesion surface, hematoma or hemorrhage, and/or thrombotic deposits are present. Type VI lesions may be subdivided into:

- type VIa: with the presence of disruption of the surface;
- type VIb : with the presence of hematoma or hemorrhage;
- type VIc: with the presence of thrombosis;
- type VIabc: with the presence of all three features.

3.1.4 Clinical manifestation of atherosclerosis

In the recent decades, cardiovascular diseases have become the leading cause of morbidity and mortality worldwide [26]. CAD, also known as ischemic heart disease includes several clinical states of the disease: stable angina (SA), unstable angina (UA), myocardial infarction, and sudden cardiac death [27]. A common symptom is chest pain or discomfort which may travel into the shoulder, arm, back, neck, or jaw. SA is characterized by chest pain that occurs regularly with activity, after eating, or at other predictable times and is associated with narrowings of the arteries of the heart. SA patients present a partial occlusion of coronary artery with consequent reduction of myocardial perfusion. They present normal electrocardiogram (ECG) between the attacks, with a temporary ST segment depression during the events, but do not present blood biomarker of myocardial infarction such as troponin and creatine kinase-MB (CK-MB) increase. Angina that changes in intensity, features or frequency is termed unstable. UA is characterized by the presence of chest pain in rest condition and may precede myocardial infarction. It is distinguished from myocardial infarction without ST segment elevation for the absence or the modest increase in myocardial necrosis markers [28]. Myocardial infarction is due to a limited blood flow to the heart that cause ischemia (cell starvation secondary to a lack of oxygen) of the myocardial cells. The cause of blood flow limitation is atherosclerotic plaque growth, which protrudes into the channel of the artery, causing a partial obstruction. Myocardial infarction present two acute clinical manifestations: myocardial infarction that presents with the ST-segment elevation (STEMI), the most severe condition, and the one that does not present with the ST-segment elevation (NSTEMI). STEMI represents a complete occlusion of a coronary artery leading to full-thickness myocardial infarction, and its diagnosis is based on the presence of ST-

segment elevation on the electrocardiogram (ECG) that meets specific STEMI criteria [29]. In NSTEMI patient there is not a total occlusion of the vessel but there is myocardial cell death. From a diagnostic point of view, these patients can be identified by ECG changes [28].

3.2 Macrophages

Macrophages, identified for the first time at the end of 19th century by Metchnikoff by their phagocytic nature, are cells belong to immunity system. They have key roles not only in immunity but also in numerous biological processes from development, homeostasis, and tissue repair to inflammation [30].

3.2.1 Origin

In 1960s van Furth observed that all macrophages derived from a pro-monocyte present in the bone marrow [31]. Nowadays, it is well established that tissue macrophages derives not only from monocytes that differentiate in the tissue and are unable to proliferate, but also may have an embryonic origin with the capacity of in situ self-renewal [32]. MDMs originate in the bone marrow from hematopoietic stem cells (HSCs) that differentiated toward more committed cell population. In detail, the master regulator PU.1 induces the differentiation of HSCs into common myeloid progenitors (CMP) through the inhibition of c-Myc [33]. Moreover, PU.1 through the activation of colony stimulating factor-1 (CSF-1) and IL-34 [34] not only directs lineage commitment of HSCs toward CMP but also of granulocyte-macrophage progenitors (GMP) toward monocyte-macrophage DC progenitors (MDP). Monocytes originate from MDP afterwards inflammatory stimulus through a chemotactic mechanism [35] (Figure 2).

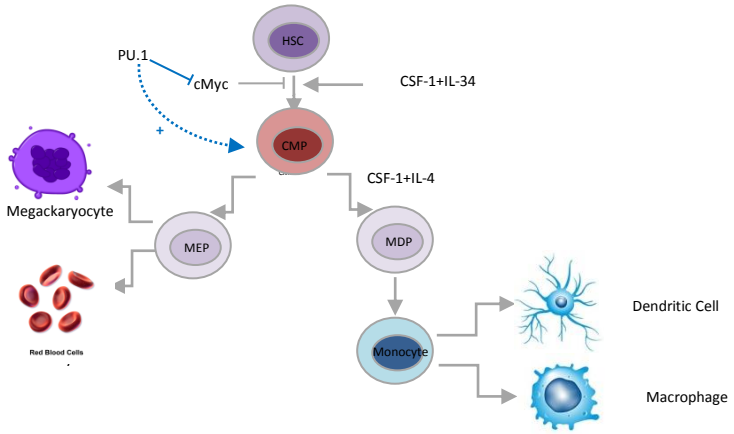

Figure 2. Origin of macrophages

The release of monocytes from the bone marrow into the blood stream involves the chemokine receptor 2 (CCR2) and its ligand chemokine (C-C motif) ligand 7 (CCL7). Monocytes have been considered as a homogenous cell population until the late 1980s, when Bernward Passlick,

Dimitri Flieger and Löms Ziegler-Heitbrock demonstrated for the first time the existence of distinct subsets of monocytes [36]. Today, circulating monocytes are classified into three main populations based on the different expression of surface markers, chemokines, and adhesion molecules [37]. The majority of circulating monocytes belong to the 'classical monocytes' that are characterized by high expression of CD14 receptor (that is involved in the recognition of lipopolysaccharide (LPS)) and no expression of CD16 (immunoglobulin Fcγ receptor). These monocytes CD14++CD16- show high phagocytic capacity and high myeloperoxidase activity. Moreover, they are big cells in term of size and are able to produce high levels of ROS and interleukin 6 (IL-6). CD14+CD16++ , known as 'non classical' monocytes, are smaller in term of size as compared to the 'classical' and they express high levels of fraktaline (CX3CR1) and C-C chemokine receptor (CCR) type 5 ; conversely, they do not express CCR2 and they produce tumor necrosis factor-α (TNF-α) and interleukin (IL)-1. Thus, this subpopulation present pro-inflammatory characteristics.The number of 'non classical' monocytes is higher in subjects affected by acute inflammation [38], obesity [39], hypercholesterolemia [40] and CAD [41]. The 'intermediate' monocytes, CD14+CD16+, share some characteristics with 'classical' monocytes and others with 'non classical'. In particular, they express CCR1, CCR2 and C-X-C chemokine receptor (CXCR) 2 that are present in 'classical' monocytes but not in 'non classical', and they express CX3CR1 and CCR5 that are express by 'non classical' but not by 'classical' monocytes. Furthermore, 'intermediate' monocytes are characterized by a high inflammatory potential and they produced TNF-α and IL-1 after stimulation with LPS.

Monocytes circulate in the bloodstream for about one to three days and then migrate, through the endothelium, into the intima where they differentiate into macrophages and participate to local immune defense [31]. Under physiological conditions, macrophages represent about 10-15% of total number of cells present in the organism and this percentage can grow in response to inflammatory stimuli. Macrophages play a fundamental role in immunity response: they are involved in killing pathogens, in the elimination and degradation of apoptotic and necrotic cells, in the uptake of cellular debris and toxic molecules [42]. Moreover, they have a key role in inflammation and in the resolution of inflammation and in tissue repair [43].

3.2.2 Macrophages heterogeneity

Tissue macrophages have different nomenclatures and functions that are peculiar of the tissue where they are localized. In particular, bone macrophages are known as osteoclasts and are highly specialized in bone resorption [44]. Alveolar macrophages are present in the lung and are responsible for recycling of surfactant molecules [45]. The brain macrophages (microglia) sustain the brain development through trophic functions (regulation of neuronal precursor and production of neurotrophic factors) [46]. Kupffer cells in the liver ensure protection during infections and maintain iron homeostasis [47]. In the skin, macrophages (also known as Langerhans cells) are involved in the immune functions and in the epidermis/skin homeostasis [48]. In the spleen, red pulp macrophages are involved in the processing of heme and iron from senescent erythrocytes [49], while macrophages in the splenic marginal zone are important for the capture of blood-borne antigens [50]. Macrophages in the bone marrow have a crucial role in the retention of HSCs into bone marrow itself [51]. Intestinal macrophages in the muscularis mucosae are involved in the crosstalk with surrounding muscle cells and enteric neurons to ensuring normal intestinal peristalsis [52]. Resident macrophages maintain and control the tissue homeostasis, and, an alteration of steady state leads to a recruitment of high number of inflammatory cells that can change microenvironment inside the tissues. Macrophages are cells with great plasticity and they can easily change their phenotype inside the tissue in relation to microenvironmental changes. In response to the stimulus, macrophages are activated through a polarization towards two opposite states, the M1 or classical, and the M2 or alternative activation [53, 54]. M1 activation is induced by pathogens, wall components of bacterial cell, lipoproteins and cytokines such as interferon gamma (IFN-γ) and TNF-α. In particular, macrophages M1 show high microbicidal capacity [55] and secrete pro-inflammatory cytokynes like IL-1β, IL-6, IL-23 and TNF-α. Moreover, they are able to degrade the extracellular matrix (ECM) and they present high levels of major hystocompatibility complex (MHC) proteins [53]. The M2 activation is induced by fungal cells, parasites, immune complexes, complements, apoptotic cells, macrophage colony stimulating factor (M-CSF), IL-4, IL-13, IL-10, and trasforming growth factor-β (TGF-β) [55]. Macrophages M2 show high phagocytic capability and are involved in tissue repair and tissue remodeling [56, 57]. Moreover, the M1/M2 paradigm is not able to define the complexity and plasticity of mononuclear phagocytes, indeed *in vivo*, macrophages can adopt a variety of functional phenotypes depending on continuous changes in the tissue

microenvironment. Therefore, the M1/M2 macrophages description may be taken as a simplified framework describing a continuum of several functional states, of which M1 and M2 activation states represent the two extremes [54]. In addition, M2 population has been further classified into M2a-d macrophages based on inducing agents, marker expression and functionality irrespective of tissue residence. In particular, the M2a is induced by IL-4 and IL-13 and express high level of the mannose receptor (CD206), the decoy receptor IL-1RII and release IL-1 receptor antagonist. M2b macrophages are obtained after exposure to immune complexes and Toll-like receptor (TLR) agonists or IL-1 receptor ligands; they show the typical M2 characteristics, but also produce pro-inflammatory cytokines such as TNF-α, IL-1β and IL-6 [58]. After IL-10 and glucocorticoids stimulation we have the highly efferocytic M2c macrophages that are characterized by the expression of pentraxin-3 and high amounts of TGF-β and IL-10. Moreover, they display high levels of the Mer receptor kinase (MerTK), which is crucial for their intense efferocytic activity [58, 59]. Finally, the stimulation of adenosine A (2A) receptor by TLR agonists induces the differentiation of macrophage into M2d phenotype. Adenosine signaling suppresses TNF-α, IL-1 and IFN-γ expression and confers a pro-angiogenic profile to macrophages, inducing the expression of vascular endothelial growth factor (VEGF) and IL-10 [60].

3.2.3 MDMs in atherosclerotic disease

3.2.3.1 Recruitment of monocytes and transmigration in the atherosclerotic plaque

During all stages of atherosclerotic disease, macrophages and T-lymphocytes mediate the inflammatory response, whereas neutrophils and granulocytes that are less present in atherosclerotic plaques less contribute to this process [61]. Moreover, as previously mentioned, monocytes and macrophages are involved in all steps of lesion development like lipids accumulation, releasing of pro-inflammatory factors and cytokines, and ECM remodeling. A chronic inflammatory state enhances the recruitment of monocytes and lymphocytes from the blood circulation and favors their proliferation inside the plaque. At plaque level, the presence of growth factors and cytokines determines the monocytes differentiation into macrophages. The subsequent uptake of oxidized LDL (ox-LDL) induces the transformation of macrophages into foam cells [22] which contribute to the formation of the necrotic core, a typical feature of advanced lesions [62]. Monocytes penetrate into the subendothelial space through a process

called diapedesis which requires the activation of a complex system of interactions between adhesion molecules and chemotactic factors. The adhesion molecules involved in the endothelial recruitment of monocytes belong to four families: selectine, immunoglobulins, integrins and glycoproteins (mucin-like). The family of selectine, transmembrane monomeric glycoproteins, is composed by several classes, that differ for their localization. L-selectin, or CD62L, is expressed at leukocytes surface levels, interacts with the endothelium ligands and allows transient adhesion; E-selectin (or CD62E) is present on cytokine activated endothelial cells, and binds the sialylated carbohydrate groups of proteins on the leukocyte surface; P-selectin (or CD62P) is localized both on endothelial cells and platelets. P-selectin under physiological conditions, is present at intracellular compartment in secretion granules; during inflammation the release of chemical mediators stimulates its translocation on the cell surface making it available for interaction with leukocyte ligands [61]. In addition, member of immunoglobulins superfamily, such as VCAM-1 and ICAM-1, are express on the endothelial surface and represent ligands for leukocytes integrins [63]. Integrins are heterodimeric transmembrane receptors formed by α and β subunits: monocytes express integrins β1 that recognize VCAM-1, and integrins β2, LFA-1 and Mac-1 that bind ICAM-1. Also the α4β1 integrin known as VLA-4 (very late antigen -4) plays an important role in adhesion of monocytes to the endothelial surface, through the binding to some fibronectin isoforms and VCAM-1 [61, 64]. Macrophages localization in the atherosclerotic lesion contribute to the recruitment and to the migration of monocytes; in fact they secrete cytokines such as TNF-α and IL-1, that induce expression of ligands for integrins, especially VCAM-1 and ICAM-1, on endothelium. In response to lipid oxidation, macrophages also produce chemokines (chemotactic cytokines) such as MCP-1 (or CCL2) involved in the recall and amplify of the recruitment process of circulating monocytes in the arterial wall [65].

3.2.3.2 Differentiation of monocytes in the two different macrophage phenotypes

Monocytes differentiate into macrophages inside the intima of vessels. The atherosclerotic plaque is characterized by a heterogeneous macrophage population that reflects the complexity and diversity of the microenvironment to which the cells are exposed after crossing the vascular wall. The presence of cytokines and growth factors during the monocytes differentiation process of monocytes induces polarization towards different phenotypes that have very different properties, even opposed. As previously mentioned, M1 macrophages have pro-inflammatory

characteristics, and when stimulated with LPS or interferon γ, they produce IL-1, IL-6, IL-8, IL-12 and TNF-α. These cytokines, by activating endothelial cells and SMCs, enhance endothelial dysfunction state and promote oxidative stress [66]. While M1 macrophages promote necrotic core expansion and favor plaque development [67], the M2 phenotype is characterized by the presence of CD163 scavenger receptor and CD206 [68] that have an atheroprotective role. Moreover, they secrete TGF-β and anti-inflammatory cytokines such as IL-10 and reduce recruitment of pro-inflammatory cells [68]. Distribution of macrophages subpopulation in atherosclerotic lesions is different. It has been observed that murine lesions at an early stage contain predominantly M2 macrophages, whereas advanced lesions exhibit a predominance of M1. This evidence suggests that macrophages can modify their phenotype as a result of changes in the microenvironment present in the atherosclerotic plaque [69]. In contrast, in human atheromas, the phenotype M1 and M2 appear to be simultaneously present throughout the evolution of the plaque, as evidenced by a recent study on different lesion stages even if with different localization [70]. Specifically, M1 macrophages are localized mainly at rupture-prone site of the plaque, whereas there is no significant difference in the prevalence of the two subpopulations in the fibrous cap. On the contrary, a prevalence of M2 macrophages has been described at the level of the avventitia [70].

3.2.3.3 Foam cells formation

A critical event in atherogenesis is the focal accumulation of lipid-laden foam cells derived from macrophages, smooth muscle cells and other vascular cells with subsequent fatty streak formation. Macrophages-derived foam cells play a central role in the atherogenic process as modulators of both lipid metabolism and the immune response [71]. The initiating effect in atherosclerosis may be the accumulation of LDL in the subendothelial matrix [62]. Accumulation is greater when levels of circulating LDL are raised, and both the transport and retention of LDL are increased in the sites of lesion formation. LDL trapped in the subendothelial matrix may also aggregate contributing to foam cell formation [50]. Modified LDLs are uptaken by macrophages and lead to generation of foam cells [72]. This uptake is mediated by a family of scavenger receptors (SRs) [73]. In detail, class A SRs (SR-AI, SR-AII, SR-AIII), class B SR (CLA-1/SR-BI, SR-BII, CD36), and the class D receptor CD68 are thought to be the most important ones during foam cell formation. In fact, they mediate the uptake of modified LDLs [74] and the engulfment of ox-

LDL itself induces the expression of SR-A and CD36 SRs [75], which may provide a positive feedback mechanism that could amplify foam cell formation.

3.2.3.4 Macrophage proliferation

The macrophages proliferation within the atherosclerotic lesion could contribute to the growth and development of the atherosclerotic plaque [76]. Ox-LDLs are able to induce cell proliferation and their effect on macrophages has been demonstrated in several in vitro studies [77-79]. Ox-LDLs play a detrimental role in the development of atherosclerotic lesions due to their active components such as lysophosphatidylcholine [80], apolipoprotein (Apo)-B and oxidized phospholipids [81] that can trigger various intracellular mechanisms associated with proliferation. Concerning this one, ox-LDLs are known to induce transient expression of mRNA encoding for GM-CSF, resulting in an increased secretion of this growth factor through a mechanism that is dependent on protein kinase C (PKC) activation [82]. The involvement of PKC in cell proliferation was demonstrated in in vitro models in which macrophages showed a reduced proliferation induced by ox-LDL after treatment with PKC-inhibitors [83].

3.2.3.5 Macrophage apoptosis

Macrophages are involved in another important process that contributes to plaque development: the apoptosis [84].

In 1992 Kerr and colleagues coined the term “apoptosis” that refers to a certain type of programmed cellular death. Apoptosis is characterized by several cell modification that include cell rounding, pseudopodia retraction, cell volume reduction, chromatin condensation, nuclear fragmentation with a minimal, if not absent, structural modification of cytoplasmic organelles. Apoptotic cell death is an important process during all atherosclerosis development. In fact, at plaque level, several cell types are involved in apoptosis: vascular cells, such as endothelial cells and smooth muscle cells, but also immune system cells such as T lymphocytes and macrophages [85]. In particular, macrophages represent approximately 40% of the apoptotic cells present within the plaque [86]. Moreover, the amount of apoptotic cells present in the atherosclerotic lesion is closely related to the evolution stage of the lesion: in general, the adaptive thickening of the intima and the fatty streak contain few apoptotic cells, while advanced lesions show real apoptotic foci [87]. Apoptotic process can be induced by numerous factors that are involved in

the atherosclerotic process. These ones include high levels of intracellular free cholesterol and ox-LDLs, pro-apoptotic cytokine production such as TNF-α, release of high amounts of free radicals of oxygen (ROS) by macrophages and hypoxia [88]. The consequences of the apoptotic process on the atherosclerotic lesions depend on the cell types involved, their location, and the lesion grade. At this regard, apoptosis of endothelial cells in contact with the bloodstream may favor plaque erosion with subsequently onset of a thrombotic event [89] as well as SMC apoptosis can contribute to destabilization of fibrous cap and can lead to plaque rupture [90]. Macrophages present within atherosclerotic plaque contain high amount of apoptotic material and cellular debris as a result of an active phagocytosis but the increase number of apoptotic cells can derive from an impairment of their clearance.

3.3 Efferocytosis

Efferocytosis is specifically refered to the phagocytosis of apoptotic cells. The difference between efferocytosis and pathogens phagocytosis is the lack of phagocytic pro-inflammatory response. Indeed, efferocytosis is an anti-inflammatory process because prevent apoptotic cells transformation into necrotic cells, with subsequent secretion of cytotoxic mediators, and reduce the release of anti-inflammatory mediators such as TGF-β and IL-10 [91]. Moreover, efferocytosis inhibits the release of pro-inflammatory cytokines like TNF-α by macrophages [92]. Hence, this process protects tissue from inflammation and immunogenic response to the post-apoptosis necrosis. The apoptosis is part of the physiological cells replacement, so a ready elimination of apoptotic cells is needed to maintain tissue homeostasis. Many cell populations are involved in this process, not only "professional phagocytes" like macrophages and dendritic cells, but also endothelial cells, SMC and fibroblasts.

During the efferocytic process, it is possible to distinguish different steps: the recruitment of phagocytes to the apoptotic cell, the recognition of apoptotic cells, the uptake of the cells and the phagocytic response. In detail, when cells undergo apoptosis, they release soluble mediators, also known as "find me" or "eat me" signal, that are able to recruit phagocytes [93]. Among the "find me" signals, fractalkine, lysophosphatidylcholine (lysoPC), sphingosine-1-phosphate (S1P) and triphosphate nucleotides (adenosine triphosphate (ATP) and uridine triphosphate (UTP)) have been included. The fractalkine is a soluble protein that is associated to cell membrane and it is released from apoptotic cells. It is recognized by CX3CL1 receptor expressed on the phagocytes surface, and this interaction promotes efferocytosis process [94]. LysoPC has been the first "find me" lipid signal identified: it is expressed on apoptotic cells due to the caspase-3 mediated activation of the calcium-independent phospholipase A2. This signal interacts with G2a receptor (a G protein coupled receptor) that induce the phagocyte migration toward apoptotic cells [95]. S1P is also a lipid molecule that origin from the phosphorylation of sphingosine by sphingosine kinase 1. It acts both as "find me" and "eat me" signal and it has both anti-inflammatory and atheroprotective functions [96]. The interaction between SP1 with his receptor S1P-R1 present on phagocytes membrane diminishes plaque inflammation though the promotion of cyclooxygenase-2 mRNA stabilization and protein expression in macrophages, a prerequisite for PGE2 formation [97]. Recently, a new class of "find me" signals has been

identified. ATP and UTP belong to this class and it has been observed that apoptotic cells release these nucleotides through caspase-3/7–activated hexameric pannexin-1 channels exposed on their surface [98]. Extracellular nucleotides ATP and UTP act as "find me" signals to promote cell clearance by stimulating recruitment of motile phagocytes expressing P2Y purinergic receptors and also by causing upregulation of phagocytic receptors [99, 100].

As regards to "eat me" signals, they translocate on membrane surface of cells that undergo to apoptosis, and promote the interactions between apoptotic cells and phagocytes. To date, many "eat me" signals have been identified and among them phosphatidylserine (PS) is the most studied.

The structure of the membrane of apoptotic cells is different from that of the integral ones: the first changes occurring during apoptosis is the PS translocation to the external surface of cells. Under physiological conditions, PS is localized on the inner side of cell membrane; conversely, in apoptotic cells, PS is transported on the external side of cell membrane through the action of a translocase ATP-dependent. There are many receptors expressed from phagocytes that are able to recognize PS on apoptotic cells and, among them, four are the best studied: brain specific angiogenesis inhibitor (BAI) 1, T-cell immunoglobulin mucin receptor (TIM), Stabilin, and CD300. The G-protein–coupled receptor BAI1 directly binds PS via a series of N-terminal thrombospondin repeats and subsequently stimulates actin polymerization and phagocytosis via recruitment and activation of the Elmo-Dock bipartite Rac-GEF [101]. The TIM family are type I cell surface glycoproteins that bind PS via N-terminal IgV domains to mediate apoptotic cell engulfment [102]. Of the seven human CD300 genes, three have been shown to bind PS and modulate efferocytosis: CD300A, CD300B, and CD300F [103]. In particular, CD300A inhibits phagocytosis of apoptotic cells. Accordingly, macrophages treated with siRNA specific for CD300A exhibit a higher efficiency in the engulfment of apoptotic cells compared with macrophages that have been treated with non-target siRNA [104]. CD300B signaling, via the adaptor protein DAP12, positively regulates efferocytosis. Finally, CD300F is required for phagocytosis of apoptotic cells via recruitment of p85α of the PI3K signaling pathway [105].

There are numerous molecules that facilitate the interaction between PS expressed on the apoptotic cell membrane and the receptors present on the phagocytes surface. Among these, the most investigated ones are the epidermal growth factor MFGE8, the growth arrest-specific gene 6 protein (Gas6) and the plasma-protein β2- glycoprotein 1 (β2-GPI). MFGE8 mediate the

binding between PS and vitronectin integrin receptors αvβ3 and αvβ5 present on macrophages [106]. Gas6 bind Tyro-3-Axl-Mer (TAM) family (that are tyrosine kinase receptor) play a crucial role in the efferocityc process. In particular, it has been demonstrated that his depletion leads to the accumulation of apoptotic cells, to the extension of necrotic core and, as consequence, to increase the size of plaque [107]. However, recently it has been demonstrated that the PS exposition on cell membrane alone is not enough for an efficient efferocytosis. Phagocytes show significant redundancy in recognition strategies and are able to use many receptors at the same time [108]. This redundancy is important in order to activate a rapid clearance of apoptotic cells. Indeed, many phagocytes receptors take part in the elimination of apoptotic cells and the modulation of their expression is very important both in physiological and pathological conditions. Among these molecules, CD36 that recognizes thrombospondin [109], low density lipoprotein receptor-related protein 1 (LRP1) that interacts with PS-binding complement factor C1q to engulf apoptotic cells in association with its co-receptor (calreticulin) [110] and CD14, are the most important receptors involved in the efferocityc process.

In particular, CD14 is a glycoprotein, initially identified as the receptor for LPS; it is a surface receptor specifically expressed from monocytes and macrophages that is found both anchored to the membrane and in soluble form into the cell cytoplasm. During the phagocytosis of pathogens, the binding between LPS and CD14 induces a pro-inflammatory response mediating by the nuclear factor NF-κB activation. In detail, CD14 recognize ICAM-3 that is greater express on the apoptotic cell membrane [111]. During the uptake of apoptotic cells, macrophages release anti-inflammatory mediators like IL-10 [112].

The presence of specific receptors on the cellular membrane allows the recognition of apoptotic cells by phagocytes and to discriminate them from non apoptotic cells. The efficiency of efferocytic process depends by the balance between the quantity and the quality of positive signal “eat me” and negative “don’t eat me” expressed on apoptotic cell membrane. Among the “don’t eat me” signals expressed by non apoptotic cells CD31 (also known as platelet endothelial cell adhesion molecule (PECAM-1)) and CD47 (also known as integrin associated protein (IAP)) are the most studied. Notably, CD47 is recognized by signal regulatory protein α (SIRPα) and their interaction inhibits the efferocytic process; when CD47 expression is diminished during apoptotic process, the cell is cleared by efferocytosis [113].

The efferocytic process involves the protrusion of pseudopodia with the consequent cytoskeleton remodeling in the phagocytic cells when they bind apoptotic cells. These cytoplasm filled projections envelope the apoptotic cell, resulting in a phagosome with membranes in close contact with the ingest cells. The cell internalization activates the guanosine tryphosphate (GTP)-ases, in particular the family of Rho GTP-ase. This family belongs to Ras superfamily that contain small proteins involved in cellular motility [114]. In particular, RhoA, Cdc42 and Rac play an important role in the efferocityc process. More in detail, RhoA inhibition induced the efferocytosis enhancement; in contrast, its activation is associated to a reducing efferocityc capability. The active form of RhoA cause an increase of the activity of Rho-associated coiled-coil-containing protein kinase (ROCK), that in turn mediates the myosin phosphorylation of light chain promoting cellular contraction [115]. As a consequence, the cell is not able to radiate pseudopodia and to promote phagosome. Conversely, the RhoA activation seems to be necessary to promote the apoptotic cell digestion through the regulation of phagosome acidification [116]. After the apoptotic cell internalization, the phagosome sequentially expresses different proteins during its maturation, ultimately leading to fusion with an acidic lysosome structure, forming the phagolysosome. Inside phagolysosome, apoptotic cell is digested in his basal components such as peptides, sterols, nucleotides and lipids [117].

Other members of Ras family are involved in efferocytic process. In particular, Rac promotes efferocytosis and regulates cell internalization process through the activation of actin related protein (Arp) 2/3 complex that acts on actin polymerization. As a consequence, the cytoskeleton rearrangement promotes the pseudopodia radiation [118].

Phagocytes can fit to this increased metabolic load by activating degradation and efflux pathways [119]. In effect, a number of recent studies have shown that engulfment of apoptotic cells itself engages multiple metabolic sensing pathways in macrophages to control phagocytosis and immune signaling [120, 121]. Among these, it has been demonstrated the role of mitochondrial uncoupling protein (UCP) 2. This protein uncouples oxidative phosphorylation and ATP synthesis, and reduces the potential of mitochondrial membrane inside the cells. It has been shown that an overexpression of this protein enhances the phagocytosis of apoptotic cells instead his downregulation inhibits this process, suggesting the role of mitochondria in the regulation of efferocytosis [122]. Furthermore, efferocytosis can modulates the cholesterol metabolism through the increase of ATP binding cassette (ABCA) 1 receptor expression. In

particular, it has been observed that cholesterol derived from apoptotic cell degradation becomes an integral part of cholesterol pool inside the phagocyte and, in response to the cholesterol loading, phagocyte potentiates the cholesterol efflux pathway [123].

3.3.1 Role of efferocytosis in atherosclerotic disease

Clearance of apoptotic cells by phagocytic cells plays a pivotal role in the resolution of inflammation. The phagocytic removal or apoptotic cells before they undergo lysis results in potent anti-inflammatory and immunosuppressive effects through the production of anti-inflammatory cytokines such as TGF-β1 and PGE2 and the suppression of release of proinflammatory mediators, including IL-8, TNF-α and thromboxane A2 from activated macrophages [124]. Emerging evidence indicates that efferocytosis is impaired during atherogenesis and despite it is not yet understood why this process is dysfunctional, several studies have evidenced a dysregulation of "eat me" signals [125]. During atherosclerosis the apoptosis process is increased and several studies suggest that, in early lesions, the phagocytic clearance of apoptotic cells appears to be efficient. Apoptotic cells are rapidly removed through the efferocytic process performed by phagocytes present in the intimal layer, mainly M2 macrophages [126]. Conversely, during atherogenesis phagocytes become less effective. In advanced lesion, phagocytosis of apoptotic cells is severely compromised: this involves accumulation of apoptotic and necrotic macrophages and SMC that inhibit inflammation resolution and promote local necrosis and plaque instability [127]. Several factors may contribute to defective phagocytic clearance of apoptotic cells, leading to a secondary necrosis of these cells and a proinflammatory response. The possible mechanisms undrelying the reduction of the clearance of apoptotic cell were firstly suggested by Steinberg and Witztum. In particular, they observed that ox-LDLs compete with apoptotic bodies in the recognition by macrophages [128]. In fact, both ox-LDLs and apoptotic bodies exhibit oxidized lipid molecules or modified protein fractions which are recognized by macrophages [129]. Ox-LDL have immunogenic properties and the presence of auto-antibodies directed toward this modified lipoproteins have been identified in the atherosclerotic plaques [130]. These antibodies can also bind to apoptotic cells resulting in the inhibition of the phagocytosis by macrophages [131].

Another factor that can contribute to the reduction of efferocytosis in the atherosclerotic plaque is the oxidative stress. PS as well as proteins or lipidic molecules present on membranes of

apoptotic cells or on macrophages are sensitive to the action of oxidizing agents. During the apoptotic process, PS may be oxidized and oxidized PS induces the secretion of pro-inflammatory proteins such as MCP-1 and IL-8, which contribute to maintaining a chronic inflammatory state [132]. In addition, the ingestion by macrophages of particles that are difficult to degrade leads to a "stiffening" of macrophage cytoskeletal, with consequent inhibition of the morphological changes needed for the pseudopodia emission and a reduction in apoptotic bodies phagocytosis [133]. Accordingly, the reduced efferocytosis may depend on the suppression or decreased expression of molecules that mediate the interaction between apoptotic and phagocytic cells such as Gas6 and MFG-E8 [134].

A reduction in clearance of apoptotic bodies promotes a number of processes that can contribute to plaque instability and the thrombus formation. Apoptotic cells that are not removed through the efferocytic process undergo a secondary necrosis that contributes to the growth of the necrotic core of the atheromasic plaque. The macrophage interaction with necrotic cells translates into an additional inflammatory response exacerbated by increased pro-inflammatory cytokine secretion such as TNF-α and IL-12, and a reduced release of anti-inflammatory proteins such as TGF- β and IL-10 [135]. All these mechanisms promote plaque development that may result in the plaque rupture. It has been observed that, in parallel with the accumulation of apoptotic cells, an increased expression and exposure of the tissue factor (TF) occur. TF is an activator of the extrinsic coagulation pathway, and its exposure, coming from the breakdown of an unstable plaque, lead to the formation of thrombi and, on consequence, to the cardiovascular event [136].

3.4 Transglutaminase 2

The transglutaminases (TGs) are widely distributed in tissue mammals and include a peculiar group of enzymes that catalyze the post-translational modification of proteins. Thus far, nine distinct TG isoenzymes have been identified including the 7 isoforms, factor XIII (protein of coagulation cascade) and band 4.2 (erythrocyte protein enzymatically inactive). TG2, a 78-kDa calcium-dependent enzyme, is the most widely distributed member of the TG family and almost all cell types in the body express TG2 to varying extents. Inside the cell, TG2 is localized mainly in the cytoplasm but it is situated also on the cellular and mitochondrial membranes, in the nucleus and in the extracellular matrix [137]. TG2 is involved in several pathology such as celiac disease [138] and in neurodegenerative disorders including Alzheimer, Parkinson and Huntington diseases [139].

TG2 catalyze the thiol- and calcium dependent transamidation reactions that results in the crosslinking of proteins by epsilon-(gamma-glutamyl)lysine isopeptide bonds. In detail, the catalytic mechanism for crosslinking involves the thiol group from a Cys residue in the active site of TG2. The thiol group attacks the carboxamide of a glutamine residue on the surface of a protein or peptide substrate, releasing ammonia and producing a thioester intermediate. The thioester intermediate can then be attacked by the surface amine of a second substrate (typically from a lysine residue). The end product of the reaction is a stable isopeptide bond between the two substrates. Alternatively, the thioester intermediate can be hydrolyzed, resulting in the conversion of the glutamine residue to glutamic acid.

Besides its classical transamidating/protein cross-linking activity, TG2 possesses several other enzymatic functions [137]. The first demonstration that TG2 can bind to and hydrolyze GTP came in 1987. In particular, the Gαh subunit of TG2 is able to activate phospholipase C (PLC)δ1 through the interaction with α1-adrenergic [140], thromboxane A2 [141] , and oxytocin receptors [142]. Biochemical studies revealed that the transamidating and GTPase activities of this protein are mutually exclusive: Ca2+-bound TG2 has no GTPase activity, whereas GTP-bound TG2 does not exhibit TG activity [143]. The protein can also hydrolyze ATP, an activity which is believed to facilitate the promineralization capacity of TG2 in osteoblasts [144]. Moreover, TG2 was found to display protein disulfide isomerase (PDI) activity in vitro [145] and in vivo [146]. More recently, and even more surprisingly, TG2 was reported to phosphorylate insulin-like growth factor-binding protein-3 (IGFBP-3) on the cell surface, and p53 tumor suppressor protein,

histones and retinoblastoma protein (Rb) in the nucleus, suggesting that it has an intrinsic serine/threonine protein kinase activity [147]. Finally, the vast array of TG2 functional activities in the cell is not limited to its enzymatic functions. TG2 was found engaged in the formation of noncovalent complexes with various cytoplasmic, cell surface, ECM, nuclear, and mitochondrial proteins [137]. This emerging adapter/scaffolding function of TG2, which is independent on its enzymatic activities, appears to regulate cell adhesion, ECM remodeling, survival, growth, migration, and differentiation due to modulation of several signaling pathways [148].

The multifunctionality of TG2 is dependent to his chemical structure. TG2 is composed by 4 domains:

- N-term domain: β-barrel structure that contains the binding site for fibronectin;
- Catalytic domain: the binding site for the substrate and the catalytic triad involved in transamination reactions;
- C-term domain: two β-barrel structures, once for GTP and adrenergic receptor α-1 binding site and the other for PLC interaction.

The functions of TG2 are regulated by calcium and GTP/GDP binding (Figure 3). Specifically, the binding with calcium induces the transaminase activity of TG2, instead, GTP binding inhibits this function. Depending on bound cofactor, TG2 takes different structural conformations that are been characterized by crystallography. In GTP bound form, the 2 C-term domains are overlapping so that block the substrate binding site inside catalytic core: in this case, TG2 is closed, compact and inactive. When TG2 binds calcium, the protein is in open conformation and the 2 C-term domains are far from active site. This is the active enzyme form since the catalytic site is accessible to the substrate [149].

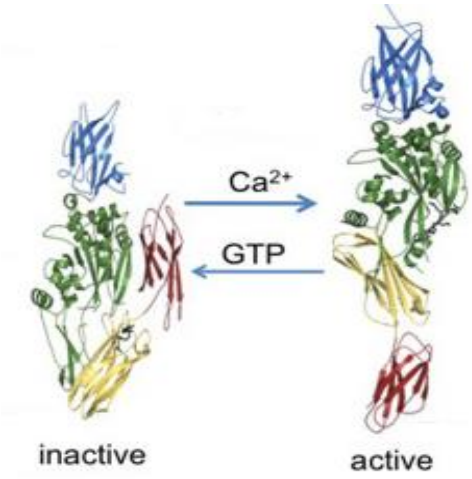

Figure 3. Inactive and active form of TG2.

In the image are represented the 4 domains: N-term in blue, catalytic site in green, the 2 C-term domain in red and yellow, respectively

3.4.1 Role of TG2 in atherosclerotic disease

Recent study have reported the involvement of TG2 in several cardiovascular diseases. In particular, it has been observed its role in glucose level regulation, platelet activity, hypertension development, atherosclerotic progression, in the modulation of vascular permeability and angiogenesis [150]. Cardiomyocytes, vascular cells and in particular macrophages express high levels of this protein [151] and recently several studies have demonstrated the role of TG2 in the macrophages efferocytic process [152, 153]. In particular, it has been demonstrated that the expression of this protein is fundamental for the formation of phagocyte portals [154]. Moreover, experiments conducted using TG2-/- mice have demonstrated that the absence of TG2 results in a significant reduction in the efferocitic capacity of macrophages and is associated with the development of splenomegaly and the production of autoantibodies. In particular, lack of protein seems to reduce in phagocyte capacity to internalize but not to bind the apoptotic cell and induces an increase in inflammatory response [155].

3.5 Tissue Factor

TF is the transmembrane receptor for factor VII/VIIa. The TF/FVIIa complex is the major cellular initiator of the blood coagulation cascade. TF is a membrane glycoprotein of 47-KDa belonging to the cytokine receptor protein superfamily and consists of three domains [156]:

- extracellular domain, composed by of two fibronectin type III modules whose hydrophobic cores merge in the domain-domain interface and serves for factor FVIIa binding;
- transmembrane domain;
- cytosolic domain of 21 amino acids length inside the cell which is involved in the signaling function of TF.

FVIIa is the main activator of the coagulation cascade since it leads to thrombin generation and, as a consequence, to fibrin deposition. In the coagulation extrinsic pathway, the formation of TF/FVIIa complex leads to the activation of factor X (FXa) that in turn promotes the formation of the complex composed by FXa and his cofactor FVa [157]. This complex is responsible for the conversion of prothrombin into thrombin, which cuts fibrinogen to form fibrin. Moreover, fibrin promote the FXIII activation that contribute to the clot stabilization through the crosslinking between fibrin molecules (Figure 4).

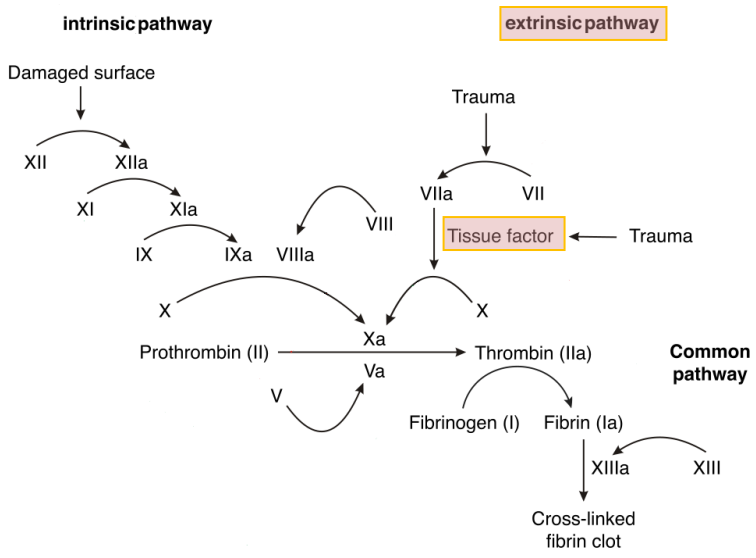

Figure 4. Coagulation cascade

Because the contact of TF with blood is sufficient to initiate coagulation, TF expression in vessels is strictly regulate to preclude activation. In fact, TF is anatomically sequestered from the blood in physiological condition, being selectively expressed at sites isolated from plasma. In physiological condition, peripheral blood cells, endothelium and SMC do not have detectable TF levels. TF associated with vessel is predominately localized on fibroblasts of adventitia, pericytes and subendothelium cells [158, 159]. Moreover, TF is expressed in several organs such as brain, lung, heart, uterus, placenta, and testis, whereas low to undetectable levels are present in skeletal muscle, joints, and liver [160].

Maintaining a nonthrombogenic vascular endothelial cell surface is achieved by the specific inhibitor for TF/VIIa, namely TF pathway inhibitor (TFPI). TFPI is synthesized by endothelium and remains bound to endothelial cells for inhibition of cell surface TF/VIIa in a Xa-dependent manner [161]. TFPI is a serin protease composed by a C-term domain, three repeated protease domains (Kunitz domains) and an N-term domain [162]. The mechanism of inhibition of the extrinsic coagulation cascade by TFPI is based on two different steps. First, TFPI binds FX through the Kunitz domain 2, inhibiting his activity. Second, the TFPI/FXa complex bind TF/FVIIa complex, forming TFPI-Xa-VIIa-TF quaternary complex so TF/FVIIa is not able to activate the coagulation cascade. The equilibrium between TF-FVIIa complex and TFPI is fundamental for maintaining haemostasis and alterations in this balance can lead to thrombosis or hemorrhagic events due to the prevalence of one or the other. In fact, it has been observed in mice embryos that the total absence of TF promote hemorrhagic death, instead TFPI lacking cause death for thrombosis [163].

TF/FVIIa complex is involved not only in the coagulation cascade but also in different biological process. These functions are related to his similarity to class II cytokine receptors [164]. In particular, the binding through FVIIa and TF induced the activation of several mitogen-activated protein (MAP) kinase family members like p38, p42/p44 and c-Jun N-terminal kinase (JNK), [165] through G protein coupled protease-activated receptors (PARs), in particular PAR-2 [166]. Hence by activating different kinases involved in signal transduction, TF/FVIIa complex regulates the transcription of several genes involved in physiological and pathological processes such as cell migration, cell growth, or apoptosis.

3.5.1 Role of TF in atherosclerosis

Many studies have demonstrated that TF in atherosclerotic plaques is the primary responsible for the thrombogenicity of the plaque and the primary cause of atherothrombosis [167]. Plaque disruption and subsequent arterial thrombosis is a sudden event in atherosclerosis resulting in acute vascular syndromes, such as myocardial infarction [168]. TF expression has been found to be correlated with the progression of human atherosclerotic lesions [169]. For instance, plaques from patients with unstable coronary syndromes and myocardial infarction showed higher TF activity in respect with those of patients with stable disease [170]. Within the plaque, not only macrophages, foam cells, and SMCs but also cell-derived micropartilces (MPs) and cellular debris derived from apoptotic foam cell in the necrotic core are TF sources [171]. TF expression is induced by several stimuli such as inflammatory cytokines (like TNF-α) and ox-LDLs. In particular, TNF-α promotes the expression of MCP-1, a chemokine involved in both the initiation and progression of atherosclerosis, that induces TF expression in both monocyte/macrophages and SMCs [172]. Moreover, ox-LDL is a potent activator of TF in monocytes [173], SMCs [174], and endothelial cells [175] through the binding to scavenger receptors and toll like receptors (TLRs), especially TRL4.

During the atherosclerosis disease, TF not only triggers clotting but also may contribute to SMC migration, and cytokine and chemokine production. Indeed, TF contributes to SMC migration in vitro and in vivo [176], through the activation of PAR-2 signaling pathway [177]. Moreover, the TF activation of the PAR-2 results in the secretion of the inflammatory cytokine IL-6 and the chemokine IL-8 [178], and further leukocyte recruitment to the atherosclerotic lesion, thus enhancing the progression of atherosclerosis [179].

3.6 Oxidative stress

Oxidative stress is caused by an imbalance between oxidant in particular ROS and antioxidant factors in favor of the oxidant ones. ROS include: free radicals, that contain one or more unpaired electrons, and non radicals species, formed when 2 free radicals shared their unpaired electrons. ROS can be classified on the basis of their origin: endogenous or exogenous. Endogenously, ROS are produced as a result of normal cell metabolism. The major ROS that are of physiological significance are superoxide anion (O_2^-), hydrogen peroxide (H_2O_2) and the hydroxyl radical (•OH). In particular, O_2^- is formed by the addition of an electron to the molecular oxygen (O_2) [180]. Many enzymatic reactions can produce ROS. In particular, nicotine adenine dinucleotide phosphate NADPH oxidase (NOX), xanthine oxidase and mitochondrial electron transport system are recognized sources of ROS in polymorphonuclear leukocytes, monocytes, and macrophages. Upon phagocytosis, these cells produce a burst of O_2^- as the bactericidal activity. O_2^- is converted into H_2O_2 by the action of superoxide dismutases (SODs). H_2O_2 is also produced by peroxisomes in metabolic reactions during consumption of O_2. The most reactive ROS, •OH is produced by the degradation of H_2O_2 through Haber–Weiss and Fenton reactions [181].

In addition to endogenous ROS, there are also exogenous sources of oxidant molecules that derive from cigarette smoke [182], ozone exposure, hyperoxia [183], ionizing radiations [184] and heavy metal ions [185].

ROS can attack organic molecules, lipids, proteins and DNA resulting in marked modifications of these compounds. DNA damage, including degradation and modification of bases, single- or doublestranded DNA breaking, mutations, deletions or translocations, and cross-linking with proteins, may modulate numerous pathways through the activation of several stress-induced transcription factors and the production of pro- and anti-inflammatory cytokines. The extent of DNA damage determines cell fate: cell cycle arrest and DNA repair or the activation of apoptoitc pathways. A single double-strend break can cause apoptosis [186], inactivate key genes, or induce serious chromosomal aberration [187]. DNA damage leads to the loss of homeostasis and it is involved in several pathologies like tumors, neurodegenerative, autoimmune and cardiovascular diseases. Furthermore, oxidant molecules can induce lipid peroxidation. In the biological system, the most favorable substrate for peroxidation is represented by polyunsaturated fatty acid (PUFA), major constituents of cellular and subcellular membranes. In

particular, lipid peroxidation, taking an electron from PUFA, leads to structural disorganization of the membrane and deterioration of pores crossing the phospholipid bilayers [188]. This process modifies membrane properties such as membrane fluidity, alters the physiological functions of cell membranes, and contributes to cell membrane damage [189]. This cellular damage can have negative consequence for the organism, as modification of proteins, activation of kinases and inhibition of nuclear transcription factors.

Moreover, ROS can promote also protein modification. The thiol group in proteins undergoes reversible and irreversible oxidation reactions, impacting on protein structure and function. In fact, oxidative stress may increase susceptibility to proteolysis by proteases degradation [190]. All together, these modifications can promote serious damage which may culminate in cell death.

3.6.1 Antioxidant response

Given the enormous range of reactivity of oxidant and given the different range of the targets, living cells can act different strategies to counteract oxidative damage. Cells activate several defense mechanisms in order to maintain tissue homeostasis, as the activation of superoxide dismutases (SOD), glutathione (GSH), catalases, paraoxonases (PON), heme-oxygenase-1, and nitric oxide (NO), which directly or indirectly counteract the oxidants. Among them GSH and nuclear factor erythroid 2–related factor 2 (Nrf2)/ heme-oxygenase-1 (HO-1) are widely studied.

3.6.1.1 GSH

γ-L-glutamyl-L-cysteinyl-glycine, chiefly known as GSH, represent the major antioxidant system in the cells [191]. It belongs to thiols family [192] and is fundamental to maintain cellular homeostasis in order to protect cells by oxidative stress. GSH is generated in vivo by the consecutive action of two ATP-dependent enzymes, from the precursor aminoacids cysteine, glutamate and glycine. The first enzyme, glutamate–cysteine ligase (GCL), is the rate-limiting enzyme, while the second one, glutathione synthase is required for de novo GSH biosynthesis. The majority of cellular GSH (almost 90%) is in the cytosol, which also represents the main place for its synthesis; from cytosol, GSH is distributed into organelles such as mitochondria, nucleus and endoplasmic reticulum [193]. In contrast to GSH synthesis, which occurs intracellularly, GSH degradation occurs exclusively in the extracellular space, and, in particular, on the surface of

cells that express the γ-glutamyltransferase (GGT) [194]. GGT hydrolyzes GSH into glutamic acid and cysteinyl-glycine that is further hydrolyzed by cell surface dipeptidases and the resulting aminoacids taken up by cells for regeneration of intracellular GSH [195]. GSH levels depend not only by de novo synthesis but also by reduction of his oxidized form (GSSG). GSSG is characterized by a disulphide bond between two molecules of GSH that is efficiently reduced back to GSH by the NADPH-dependent catalysis of the flavoenzyme GSH reductase. The intra- and extra-cellular GSH levels are determined by the balance between its production, consumption, and transportation.

Regarding its mechanism of action, it has been established that the thiol moiety of GSH is important in its antioxidant function, i.e. the direct scavenge of radical species. Indeed, the direct action of GSH towards oxidant and oxidized molecules happens thank to oxidation/reduction reaction of thiol group (-SH) of cysteine, that acts as reducing group. The redox state of GSH is due to an alternation between its reduced and oxidized form, and GSH/GSSG ratio is commonly used to define the redox state of a cellular system [196].

GSH not only reacts directly with oxidants but it also acts as cosubstrate of enzymes like glutathione peroxidases (GSH-PXs) and GSH-s-transferases (GSTs). GSH-Pxs are a selenium-dependent family of tetrameric enzymes that converts H_2O_2 into water or the peroxide lipids into water and their relative alcohols, with parallel GSH oxidation. Moreover, GSTs inactivate secondary metabolites such as unsaturated aldehydes, epoxides, and hydroperoxides. GSTs catalyze the conjugation between GSH and oxidized substrates, favoring their elimination by the organism.

3.6.1.2 Nrf2/HO-1 pathway

Nrf2 is a transcription factor sensitive to oxidative stress. It is the major regulator of the adaptative response to oxidative stress and induces the expression of several cytoprotective genes with antioxidant activities. Under basal unstressed conditions, Nrf2 is constitutively expressed and degraded directly by its cytoplasmic antagonist Kelch-like erythroid cell-derived protein with cap'n'collar homology-associated protein 1 (Keap1). Keap1 is a protein that promotes the ubiquitination and the proteosomic degradation of this transcription factor through the activation of Cil3/Rbx1 pathway. Instead, under oxidative stress stimulus, the complex Keap1/Nrf2 dissociate, and Nrf2 translocated into the nucleus. Here, associating with

antioxidant responsive element (ARE), Nrf2 promotes the transcription of proteins with antioxidant activity. Among them, HO-1 play a fundamental role in the antioxidant mechanism within the cell [197].

HO-1 is a microsomal enzyme that belong to oxidoreductases. Three isoforms of HO have been identified in mammals: HO-1, 2 and 3 [198, 199]. HO-1 is a 32 kDa protein and it is the inducible form of HO. Its expression occurs to several oxidant stimuli such as hypoxia, H_2O_2, heavy metal and pro-inflammatory cytokines like TNF-α or by heme catabolism [200, 201]. HO-2, a 36 kDa protein, is the constitutive form of HO an it is expressed in the majority of the cells and organs [202]. Finally, HO-3 (33 kDa) is the isoform lacking of catalytic activity [199]. Using O_2 and NADPH as cofactor, HO-1 catalyzes the opening of heme ring promoting the production of carbon monoxide (CO), biliverdin and ferrous iron (Fe^{2+}) [203]. Subsequently, biliverdin is reduced to bilirubin through biliverdin reductase, and iron is sequestered by ferritin [204]. These three molecules are involved in the cell protection [204]. CO has a double face: from one side, high levels of CO are lethal for the cells, in fact they can induce hypoxia; from the other side, several studies have demonstrated that low CO levels have positive effect on physiological cellular functions [205]. Bilirubin, like CO, at high level shows toxic effect, especially in babies [206], but in physiological condition have cytoprotective effects [207, 208]. Fe^{2+} is able to generate ROS [209], but his binding with ferritin neutralizes his capacity to participate in redox reactions [210].

3.6.2 Oxidative stress and antioxidant response in atherosclerosis

Among the ROS generators, NADPH oxidases (NOXs) and xanthine oxidase are the most important ones in atherosclerosis. Several NOX isoforms participate to atherosclerosis pathogenesis and development. NOX1 is upregulated in diabetes and its deletion is correlated with the reduction of atherosclerosis, similarly to what happens for NOX2 deletion. NOX5 is upregulated in diabetes, hypertension and in atherosclerotic lesions [211].

Furthermore, macrophages and SMC express xanthine oxidase. In presence of oxidative stress stimulus, xanthine oxidase increased the expression of lipoxygenase (LOX)-1 and CD36 in these cell types and lead to the activation of inflammasome and the transformation of macrophages and SMC into foam cells [212]. In addition to NOX and xanthine oxidase, myeloperoxidase is involved in atherosclerosis process. In fact, it has been observed that the levels of this enzyme are increased in patients with atherosclerotic coronary artery disease [213]. Myeloperoxidase

contribute to atherosclerosis pathogenesis through several pathways. It is known that this enzyme is responsible for the conversion of thiocyanate into hypothiocyanous acid [214] and this product can alter MAPK signaling and induce apoptosis in vascular cells. Moreover, hypothiocyanous acid promotes the oxidation of LDL, favoring the atherosclerosis process [215]. Using electronic paramagnetic resonance imaging for ROS visualization coupled to a non linear optical microscopy to study structured features it has been demonstrated that ROS are present at high concentration at lipid region of atherosclerotic plaque [216].

The cells within the plaque try to counteract the oxidative stress damage through the activation of several antioxidant systems. In particular, GSH and HO-1 have an important role during the atherosclerosis. Yang *et al.* have discovered that GSH regulates CD36 activity [217] and observed that macrophages treated with buthionine sulfoximine (BSO), a compound that inhibits GSH synthesis, show a decrease of intracellular GSH levels, had increased ROS production and CD36 increased expression.

Another mechanism of oxidative stress cellular response is represented by HO-1. Several studies have demonstrated an atheroprotective role of HO-1. In vascular cells, HO-1 is induced by ox-LDL [218]. It has been observed that in macrophages, SMC and endothelial cells HO-1 expression is greater after exposition to ox-LDL, instead his levels are reduced in the presence of native LDL [219, 220]. HO-1 plays a protective role in atherosclerotic lesions as high HO-1 levels diminish the production of pro-inflammatory mediators and contrasts the inactivation of eNOS due to the presence of ox-LDL and TNF-α [221]. Moreover, it inhibits the expression of TNF-α and IL-1β and, in parallel, increases IL-10 levels both in macrophages and in endothelial cells by the production of CO [222]. Finally, the induction of HO-1 and CO downregulates the expression of endothelin-1, PDGF and VEGF that leads to the reduction of SMC proliferation [223].

it has been shown that leukocytes from CAD patients express HO-1 and its levels are correlated with the severity of disease [224]. Moreover, it has been also observed that vulnerable plaque present higher HO-1 levels in respect to stable ones [225].

3.7 Fatty Acids

Fatty acids are the most important components of all lipid classes and they are widely diffused in all living organisms. In humans, they are present in high concentration in cell membranes, in the adipose tissue (in the form of triglycerides) and in the myelin sheath. These molecules are carboxylic acids with a aliphatic chain composed from 4 to 36 carbon atoms. They can be classified on the basis of the length of aliphatic chain into:

- short-chain fatty acids (SCFA) containing of 1 to 6 carbons;
- medium-chain fatty acids (MCFA) with aliphatic tails ranging from 6 to 14 carbons;
- long-chain fatty acids (LCFA) with aliphatic tails of 16 to 36 carbons.

Fatty acids are also classified according to the presence of double bonds in the aliphatic chains: saturated fatty acids, with no double bonds, and unsaturated fatty acids that are characterized by the presence of one (monounsaturated) or more double bonds (polyunsaturated). The main saturated fatty acids present in biological systems are palmitic acid (C16:0) and stearic acid (C18:0) (Table 1A).

The nomenclature of fatty acids is very complex and the position of double bonds can be described by indicating the number of carbon atoms starting from COOH- end (C-n notation) or –CH_3- end (ω-n notation). The double bond position in C-n notation is also indicated by Δn, where n is the number of carbon atom in which the double bond is localized. For example, in a 18 carbons fatty acid, a double bond between C-12 (or ω-7) and C-13 (or ω-6) is reported either as Δ12 if counted from the –COOH end, or as ω-6 (or omega-6) if counting from the –CH_3 end.

A

Fatty acid	**Chemical structure**	***C:D***
Lauric acid	$CH_3(CH_2)_{10}COOH$	12:0
Myristic acid	$CH_3(CH_2)_{12}COOH$	14:0
Palmitic acid	$CH_3(CH_2)_{14}COOH$	16:0
Stearic acid	$CH_3(CH_2)_{16}COOH$	18:0
Arachidic acid	$CH_3(CH_2)_{18}COOH$	20:0
Behenic acid	$CH_3(CH_2)_{20}COOH$	22:0
Lignoceric acid	$CH_3(CH_2)_{22}COOH$	24:0
Cerotic acid	$CH_3(CH_2)_{24}COOH$	26:0

B

Fatty acid	**Chemical structure**	**Δ^x**	***C:D***
Palmitoleic acid	$CH_3(CH_2)_5CH=CH(CH_2)_7COOH$	*cis*-Δ^9	16:1
Oleic acid	$CH_3(CH_2)_7CH=CH(CH_2)_7COOH$	*cis*-Δ^9	18:1
Linoleic acid	$CH_3(CH_2)_4CH=CHCH_2CH=CH(CH_2)_7COOH$	*cis*,*cis*-Δ^9,Δ^{12}	18:2
Linoelaidic acid	$CH_3(CH_2)_4CH=CHCH_2CH=CH(CH_2)_7COOH$	*trans*,*trans*-Δ^9,Δ^{12}	18:2
α-Linolenic acid	$CH_3CH_2CH=CHCH_2CH=CHCH_2CH=CH(CH_2)_7COOH$	*cis*,*cis*,*cis*-Δ^9,Δ^{12},Δ^{15}	18:3
Arachidonic acid	$CH_3(CH_2)_4CH=CHCH_2CH=CHCH_2CH=CHCH_2CH=CH(CH_2)_3COOH$	*cis*,*cis*,*cis*,*cis*-$\Delta^5\Delta^8$,Δ^{11},Δ^{14}	20:4
Eicosapentaenoic acid (EPA)	$CH_3CH_2CH=CHCH_2CH=CHCH_2CH=CHCH_2CH=CHCH_2CH=CH(CH_2)_3COOH$	*cis*,*cis*,*cis*,*cis*,*cis*-Δ^5,Δ^8,Δ^{11},Δ^{14},Δ^{17}	20:5
Erucic acid	$CH_3(CH_2)_7CH=CH(CH_2)_{11}COOH$	*cis*-Δ^{13}	22:1
Docosahexaenoic acid (DHA)	$CH_3CH_2CH=CHCH_2CH=CHCH_2CH=CHCH_2CH=CHCH_2CH=CHCH_2CH=CH(CH_2)_2COOH$	*cis*,*cis*,*cis*,*cis*,*cis*,*cis*-Δ^4,Δ^7,Δ^{10},Δ^{13},Δ^{16},Δ^{19}	22:6

Table 1. Examples of saturated (A) and unsaturated (B) fatty acids

Unsaturated fatty acids are also classified by the position of the two hydrogen atoms adjacent the double bond. In detail, when they are present on the same side of the chain, they have a *cis* configuration,which causes the chain to bend. In fact, when a chain has many *cis* bonds, it becomes quite curved. When the adjacent two hydrogen atoms lie on opposite sides of the chain there is *trans* configuration (Table x B). As a result, they do not cause the chain to bend much, and their shape is similar to straight saturated fatty acids. The differences between saturated and unsaturated fatty acids, as well in geometry between the various types of unsaturated fatty acids, play an important role in biological processes, in the construction of biological structures (such as cell membranes) and in cell functions.

3.7.1 Biosynthesis of fatty acids

Fatty acids biosynthesis occurs predominantly in the liver, adipose tissue, kidneys, brain, lungs and in the mammary glands. In detail, fatty acids are synthesized in the cytoplasm of the cells from acetyl-CoA. Acetyl-CoA is obtained in mitochondria from oxidative decarboxylation of pyruvate catalyzed by pyruvate dehydrogenase or from fatty acids β-oxidation. Acetyl CoA needs to be transported into cytosol and this cannot occur directly. To obtain cytosolic acetyl-CoA, the citrate (produced by the condensation of acetyl-CoA with oxaloacetate) is removed from the Krebs cycle and carried across the inner mitochondrial membrane into the cytosol. At this level, it is cleaved by ATP citrate lyase into acetyl-CoA and oxaloacetate. The oxaloacetate returns to the mitochondrion as malate. For each acetyl-CoA molecule that is transported in the cytosol, it is produced a molecule of nicotinamide adenine dinucleotide phosphate (NADPH), a co-factor

essential in fatty acids biosynthesis (Figure 5). The other co-factors fundamental for the process are ATP, necessary for carbon dioxide (CO_2) binding forming malonyl-CoA, manganese (Mn^{++}), biotin and bicarbonate (HCO_3^-) as a source of CO_2.

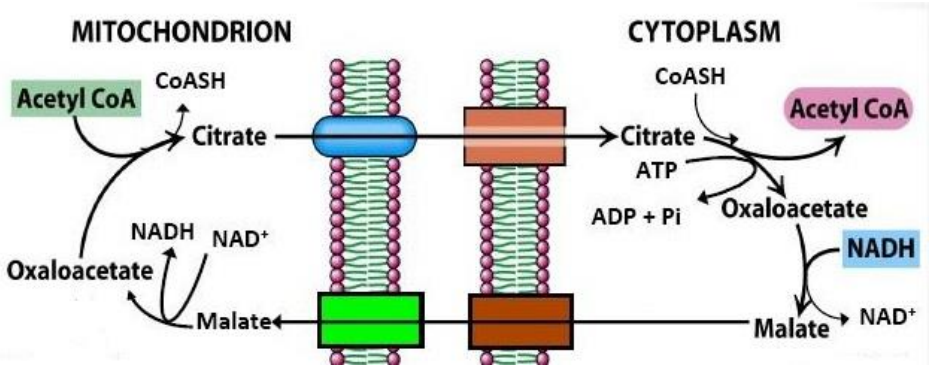

Figure 5. Scheme of the transfer of acetyl CoA from mitochondrion to cytosol

The standard way for cells to synthesize fatty acids is through the fatty acid synthesis cycle. This cycle is composed by seven reactions catalyzed by seven enzymes: acyl-CoA carboxylase (ACC), acyltransferase, ketoacyl synthase, ketoacyl reductase, hydroxyacyl dehydratase, enoyl reductase, and thioesterase (Figure 6).

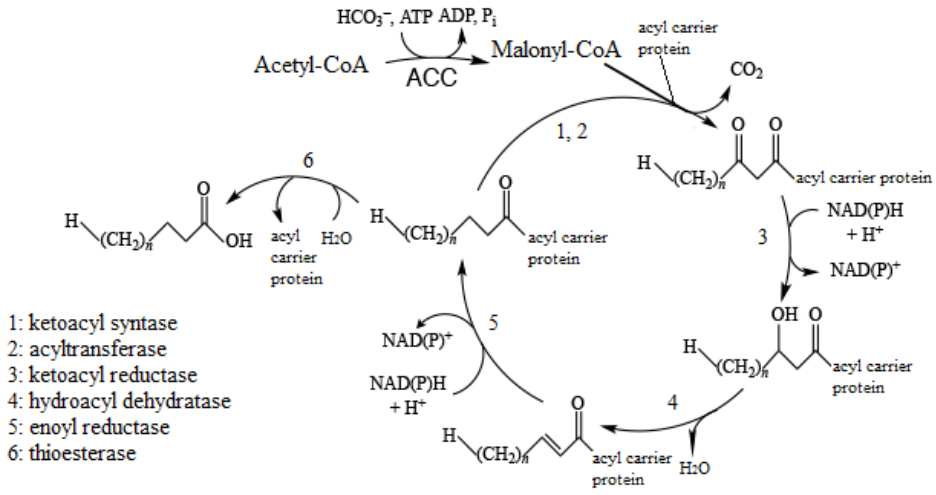

Figure 6. Fatty acids biosynthesis

ACC is a biotin dependent enzyme that controls all the biosynthetic pathway. It catalyzes carboxylation of cytosolic acetyl-CoA to produce malonyl-CoA, using ATP and HCO_3^- as co-factors. With ketoacyl synthase and acyltransferase catalysis, malonyl-CoA is added to an acyl chain,

usually activated with acyl carrier protein, making an acyl chain two methylene groups longer. Further reduction, dehydration, and reduction with ketoacyl synthase, hydroxyacyl dehydratase, and enoyl reductase catalysis, respectively, leads to a saturated and unhydroxylated acyl chain activated with acyl carrier protein. When the chain is of appropriate length, it is attacked by thioesterase to release acyl carrier protein, yielding the finished fatty acid. All these enzymes together are called elongases and have been given the designation Elovl for *elo*ngation of *v*ery *l*ong fatty acids (Elovl 1–7).

Palmitic acid (C16:0) is the longer fatty acid synthetized by the cycle and can be the precursor of LCFA. This fatty acid can be elongated to form stearic acid (C18:0) or a longer fatty acids through subsequently addition of acetylic units. This reaction is catalyzed by elongation complex present in the endoplasmic reticulum that lengthens the fatty acid chain of two carbons, donate by malonyl-CoA, leading to stearyl-CoA formation. The stearyl-CoA will be reduced, dehydratated and re-reduced to generate stearoyl-CoA, a 18 carbon atoms saturated product.

Fatty acid desaturases are enzymes that removes two hydrogen atoms from a fatty acid, creating a carbon/carbon double bond. Four desaturases occur in humans: Δ^9, Δ^6, Δ^5, and Δ^4 desaturases. Δ^9 desaturase, also known as stearoyl-CoA desaturase1 (SCD1) is a microsomal enzyme which facilitate the formation of monounsaturated fatty acids (MUFAs) from saturated fatty acid precursors. More specifically, SCD1 converts palmitoyl-CoA and stearoyl-CoA to palmitoleoyl-CoA and oleoyl-CoA, respectively [226]. Δ^6 and Δ^5 desaturases are required for the synthesis of highly unsaturated fatty acids (HUFAs) such as EPA and DHA (synthesized from α-linolenic acid), and arachidonic acid (synthesized from linoleic acid) [227]. This is a multi-stage process requiring successive actions by elongase and desaturase enzymes (Figure 7).

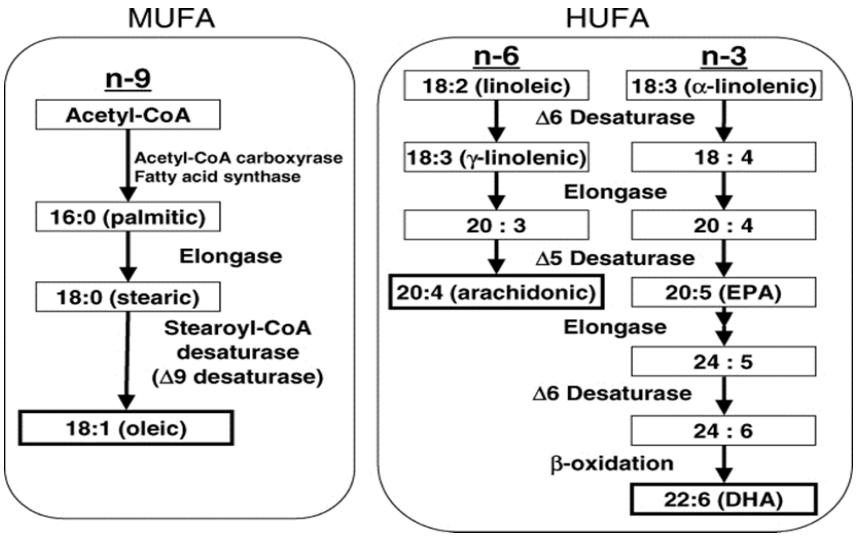

Figure 7. MUFAs and HUFA synthesis

The precursors of HUFAs, linoleic acid and α-linolenic acid are essential fatty acids as they cannot be synthesized in the body and have to be intaken with food. They are characterized by the presence of the double bond in a specific position: α-linolenic acid is a (ω-3) fatty acid; while linoleic acid is a (ω-6).

The cell membrane fatty acids composition is fundamental in both physiological and pathological state. In particular, the balance between unsaturated and saturated fatty acids play a fundamental role in several cell types such as lymphocytes, neutrophils and macrophages.

3.7.2 Macrophages fatty acid compositions

Calder and his group have observed that the main fatty acids present in the neutral lipid fraction (esters of fatty acids and alcohols, for example triacylglycerols) of macrophages were palmitate and stearate that reflected 40% and 15 % respectively of the total fatty acids. They also observed that the neutral lipid of macrophages contained approximately two fold the saturated fatty acids than the unsaturated ones. Moreover, they noticed that the principal MUFA acid was oleate and only 10% of the fatty acids were PUFA. They have also seen that in the phospholipid fraction of macrophages, the main fatty acids were palmitate and stearate and that they each comprised over 20% of the total fatty acids. Finally, they observed that the content of polyunsaturated fatty acid was higher in the phospholipid fraction compared with the neutral lipid fraction. In particular, they showed that PUFA were the 27 %, and among them, arachidonate was major portion, representing 18 % of the total fatty acids [228].

The fatty acid composition of the membrane influences membrane fluidity that in turn modify receptor function and/or the activity of signal transduction mechanisms [229]. Interactions of macrophages with the extracellular matrix and with other cells are important in several functions such as tissue repair, inflammation, immunity and atherosclerosis [19, 230]. Many of these interactions, including binding to endothelial cells, migration into tissues, interaction with T- lymphocytes, uptake of lipoproteins depend upon specific plasma membrane receptors [231]. In particular, the changing in fatty acid composition of macrophages can influence their ability to adhere to endothelium. In fact, it has been demonstrated that adhesion of macrophages that were enriched with saturated fatty acids was greater than that of those cells enriched with unsaturated fatty acids [228]. Moreover, it has been observed that the phagocytosis processes is influenced by membrane structure, in particular by the fluidity of the membrane; the latter is influenced markedly by the lipid composition [232]. In particular, an increase in membrane unsaturated fatty acids content, that is correlated to a high membrane fluidity, is associated with an increase in phagocytosis rate [233].

4. Objective

Oxidative stress and inflammation are primary drivers of the pathological changes during atherosclerosis, from the formation of lipid-laden foam cells within the intima to the necrotic lipid core of unstable plaque. In the vascular wall, many cell types have been shown to be able to produce reactive oxidant species (ROS). Among these, monocytes/macrophages are a significant source of ROS in atherosclerotic lesions. Superoxide anion ($O2^-$) participates in atherogenesis through the formation of oxidized lipids, particularly in low density lipoproteins. Moreover, it may contribute to the pathogenesis of atherosclerosis through the alteration of different cell functions, including adhesion, proliferation, and motility. High levels of oxidative stress induce also an adaptive endogenous defence mechanism that mediates the activation of antioxidant responses. Among them, nuclear factor erythroid 2–related factor 2 (Nrf2)/ heme-oxygenase-1 (HO-1) pathway is one of the most studied. In presence of oxidative stress, Nrf2 induces the transcription of HO-1 that mediates the antioxidant response. It has been shown that HO-1 protein levels correlated with plaque instability and it is expressed in macrophages of human atherosclerotic lesion.

Macrophages are hallmarked by morpho-phenotypic heterogeneity and distinct subpopulations, with pro-inflammatory or reparative characteristics, have been identified in experimental animal models and in human atherosclerotic lesions. Given the contrasting properties pro- or anti-inflammatory of macrophages, the nature of macrophage phenotype may exert harmful or beneficial functions in progression and/or destabilization of the atherosclerotic plaque. Recently, we have shown in healthy subjects that human monocytes spontaneously differentiated into macrophages (MDMs) display two dominant morphotypes co-existing in the same culture, namely round MDMs with functional traits reminiscent of a non-inflammatory and reparative phenotype, and spindle MDMs exhibiting a pro-inflammatory profile. However, no information is available concerning the behaviour of MDMs in patients with coronary artery disease (CAD).

The aim of the study was to assess the biochemical and functional profile of spontaneously differentiated MDMs obtained from CAD patients. We assessed also the oxidative stress levels and the Nrf-2/HO-1 response in MDMs of our study population. Moreover, we investigated the relationship between the characteristics observed in MDMs *in vitro* with plaque features observed *in vivo* by optical coherence tomography (OCT).

The combination between these data could provide a unique signature for identification of atherosclerotic process prone to coronary event.

5. Material and methods

5.1 Patient population

Ninety consecutive CAD patients undergoing coronary angiography, due to stable angina (SA) or acute coronary syndrome (ACS), as their first manifestation of ischemic heart disease, were included in the study between October 2014 and May 2017. Patients enrollment was performed at Centro Cardiologico Monzino, Milan, Italy. SA was defined as angina on effort with a stable pattern of symptoms for at least the last six months prior to admission; ACS diagnosis encompassed patients presenting with non-ST-elevation (NSTEMI) or ST-elevation-acute myocardial infarction (STEMI). NSTEMI was defined as chest pain at rest in the last 48 h preceding the admission associated with evidence of transient ST-segment depression on 12-lead electrocardiogram and normal (unstable angina) or elevated (NSTEMI) serum troponin I levels; while the diagnosis of STEMI was based on typical symptoms lasting more than 30 minutes and new ST-segment elevation at the J point in ≥2 contiguous leads (≥0.2 mV in V1 through V3 and ≥0.1 mV in other leads). All included NSTEMI patients underwent coronary angiography within 24 hours from admission, while all enrolled STEMI patients underwent primary percutaneous coronary intervention within 12 hours of symptom onset. In 50 out of the 90 CAD patients, OCT assessment was also performed, aiming at investigating the association between the MDMs morpho-phenotype and coronary plaque morphology. The exclusion criteria were: previous history of CAD (any previous diagnosis of stable or unstable coronary syndrome); severe chronic heart failure (NYHA class III-IV), severe heart valve disease, acute and chronic infections, liver diseases, neoplasia, evidence of immunologic disorders, use of anti-inflammatory or immunosuppressive drugs and recent (<3 months) surgical procedures or trauma. In all patients cardiovascular risk factors were examined, including family history of early CAD (first degree relative with a history of myocardial infarction <60 years), diabetes (fasting blood glucose >126 mg/dl or treated diabetes), hypercholesterolemia (total cholesterol >200 mg/dl or treated hypercholesterolemia), smoking, and hypertension (systolic blood pressure >140mmHg and/or diastolic blood pressure >90mmHg or treated hypertension). Body Mass Index (BMI) and laboratory data, including hemochrome, serum glucose, serum creatinine, lipid profile, and high-sensitivity (hs)-CRP were recorded. Medications taken on admission were also recorded. Twenty-five healthy volunteers, with neither history of CAD, nor cardiovascular risk factors, nor inflammatory disorders, and specifically not taking any cardiovascular therapy, served as control group. All patients gave their written informed consent for participation in the

study; all volunteers provided written informed consent at the time of enrollment, as well. The ethics committee approved the study protocol, and the study was performed according to the Declaration of Helsinki.

5.2 Blood collection

All patients underwent venous blood sampling for biological measurements within 12 hours following coronary angiography. Venous blood samples were drawn from the antecubital vein of healthy subjects and CAD patients into tubes containing EDTA (9.3 mM; Vacutainer Systems, Becton Dickinson, Franklin Lakes, NJ, USA). The laboratory data were available for all enrolled subjects.

5.3 Methodologies

5.3.1 Monocyte isolation and culture

Monocytes were isolated from venous blood of all enrolled subjects. Mononuclear cells were isolated by Ficoll-Paque Plus (GE Healthcare, Milan, Italy) density centrifugation at 450 g for 20 min at room temperature (RT). To remove platelet contamination, lymphocyte/monocyte-rich layer was washed with PBS containing 5mM ethylenediaminetetraacetic acid (EDTA) and suspended in RPMI 1640 (Lonza Milano S.r.l, Bergamo, Italy) supplemented with 2mM L-glutamine (Lonza), 100 U/ml penicillin, 100 µg/ml streptomycin (Lonza), and 10% autologous serum freshly obtained from blood clotted for 2 h at 37°C. Mononuclear cells were then plated ($2x10^6$/ml) in 35mm well plates (PrimariaTM, Falcon, Sacco S.r.l, Como, Italy) and kept at 37°C (5% CO_2). After 90 min, non-adherent cells were removed and those adherent were cultured over 7 days at 37°C (5% CO_2) in Medium 199 (Lonza) supplemented with 2mM L-glutamine, 100 U/ml penicillin, 100 µg/ml streptomycin, and 10% autologous serum. Medium was not replaced throughout the culture period. The endotoxin levels of all culture materials and reagents used was measured by the Limulus amoebocyte lysate assay (Lonza). To avoid MDM activation, only preparations free of endotoxin or containing <30 pg/ml were used. MDM morphology was examined by phase contrast microscopy (AxioVert 200M, Zeiss, Milan, Italy) at 20× or 40× magnification. MDM were defined spindle/elongated when a length >70µm and a width <30µm were detected; while round MDMs were defined when width and length >35-40µm were found.

Cells, whose morphology and dimension did not satisfy the above criteria, were defined as undefined MDMs. Both MDM morphotypes, round and spindle, stained positively for the pan-leukocyte antigen CD45 and for the specific macrophage marker CD68.

5.3.2 Western Blot

Cells were washed twice with PBS and lysated in a buffer (Tris 20 mM, SDS 4% and glycerol 20%) containing protease inhibitors (ortovanadate 1mM, NaF 1mM, leupeptin 1µg/mL, benzamidine 1mM, EDTA 1mM, trypsin inhibitors 10 µg/mL, pefabloc 0.5 mM, DTT 0.5 mM) . Protein concentration was determined by the micro-BCA assay (Thermo Fisher, San Jose, CA, USA). Equal amounts of lysates (40 µg of protein) were subjected to SDS–polyacrylamide gel electrophoresis on 7% gels running over night and were transferred onto nitrocellulose membrane by a semidry transfer unit (Hoefer Scientific Instruments) for 2 hours at room temperature. The membrane was saturated in a solution of T-TBS containing 5% of BSA. After washing, the blots were incubated with the appropriate primary antibodies. After wash with T-TBS, horseradish peroxidase-conjugated anti-mouse or anti-rabbit secondary antibody (Jackson ImmunoResearch Labs Inc., Li StarFISH, Milan, Italy) was used at 1:5000 dilution and incubate for 1 hour and 30 minute at RT. β-Actin (1:10000) was used as internal standard for control of protein load.

5.3.3 Immunofluorescence

Adhered MDMs were washed twice with PBS and fixed with 2% para-formaldehyde (PFA) (Merck & Co., USA) for 15 min at RT. Plates, washed twice with PBS, were air dried. After, was added 5% bovine serum albumin (BSA) (Sigma-Aldrich, Milan, Italy) solution containing 0.1% saponin (Carlo Erba, Milan, Italy) for 30 min at RT due to blocked non-specific reactive sites. MDMs were incubated overnight at 4°C with the appropriate primary antibody. Detection was performed with appropriate Alexa Fluor 488 (green emission) (10 µg/ml, 60 min, RT) (Life Technologies Italia, Monza, Italy). Nuclei were visualized by Hoechst 33258 (Sigma-Aldrich) 1:10000. Negative control experiments were performed by omitting the primary antibodies.

5.3.3.1 Quantitative image analysis

Fluorescent images were captured on an AxioObserver.Z1 microscope connected to a digital camera using the image processor AxioVision 4.7 (Zeiss, Milan, Italy). Fluorescence intensity

(densitometric sum of gray) was quantified, as an index of the amount of the protein investigated. Data are expressed as mean±S.D. of fluorescence intensity/μm^2 for each MDM morphotype, subtracted of the negative control value obtained in the absence of primary antibody. Multiple fields of view (at least three fields, 400× magnification) were captured for each culture.

5.3.4 Apoptosis of Jurkat-T cells

Jurkat T-cell line, clone E6-1 (ATCC), was purchased from LGC Standards S.r.l., Milan, Italy, and cultured in RPMI 1640 supplemented with 10% fetal calf serum (Lonza) and 26mM HEPES. Early and late apoptotic Jurkat cells were obtained upon incubation ($4x10^6$ cells/ml) in serum-free RPMI 1640 with 10 µM etoposide (Sigma–Aldrich) for 2 h. The extent of apoptosis was evaluated by flow cytometry using annexin V PE (BD Biosciences, Oxford, UK), according to the manufacturer's instructions. A total of 20000/sample events were acquired. Apoptosis was also assessed in PFA-fixed Jurkat T-cells by the evaluation of chromatin condensation (Hoechst 33258 stain, Sigma–Aldrich).

5.3.5 Efferocytosis assay

Jurkat T-cells were stained with 5µM carboxyfluorescein diacetate succinimidyl ester (CFSE, Life Technologies) for 30 min at 37°C before the induction of apoptosis. CSFE-labeled apoptotic cells ($1x10^6$ cells/ml) were co-cultured with MDMs (2:1 ratio) for 30 min. Non-ingested cells were removed. Adherent MDMs were detached with trypsin, incubated with 10 µl of APC-conjugated monoclonal mouse anti-human CD14 antibody (BD Biosciences), or 10 µl of isotype-matched irrelevant antibody, for 15 min at RT, and analyzed by flow cytometry. MDMs were gated on the basis of forward and side scatter properties. 10000 events were acquired, and the data were analyzed using CellQuest software (BD Biosciences).

5.3.6 Thrombin generation measurement

Adherent MDMs were lysed with 15 mM octyl-β-D-glycopiranoside (Sigma Aldrich). 1 µg cell lysed (20 µl) were mixed with 10 µl of HEPES buffered- Saline and 20 µl of platelet-poor plasma. Thrombin generation was triggered by the addition of fluorogenic substrate Z-Gly-Gly-Arg-AMC (Stago Italia S.R.L. Unipersonale, Milan, Italy) in the presence of $CaCl_2$ and measured for 60 min

using the Calibrated Automated Thrombogram® assay (Thrombinoscope BV, Maastricht, the Netherlands). The lag-time, peak of thrombin generation, endogenous thrombin potential (ETP), and velocity index of propagation phase (VelIndex) were calculated using Thrombinoscope software (Thrombinoscope BV).

5.3.7 Enzyme activity assay

Adherent MDMs were washed twice with PBS and 1 ml of fresh RPMI 1640 medium (Lonza) containing 0.2% fatty acid free albumin (Sigma-Aldrich) was added. After overnight incubation supernatant was collected, centrifuged at 200 g for 5 min at 4°C and the activity of matrix metalloproteinase (MMP)-9 secreted by MDMs was evaluated using colorimetric analysis using BiotrakTM activity assay system (Amersham, GE Healthcare, Milan, Italy). In brief, standards and samples (100 µl) were incubated in microtitre wells precoated with anti-MMP-9 antibody over night at 4°C. The wells were washed 4 times with wash buffer (Amersham, GE Healthcare, Milan, Italy), and 50 µl of p-Aminophenylmercuric Acetate (APMA) (Amersham, GE Healthcare) was added. The plate was incubated for 1.5 hours at 37 °C. At the end of incubation, 50 µl of detection reagent (Amersham, GE Healthcare) was added. The plate was shaked for 20 second and it was read at 405 nm in a microplate spectrophotometer Mithras LB 940 (Berthold Italia, Milano, Italy). The concentration of active MMP-9 in a sample was determined by interpolation from a standard curve.

5.3.8 Mass spectrometry analysis

5.3.8.1 GSH/GSSG determination

The determination of GSH and GSSG was performed using a LC-MS/MS method [234]. In detail, macrophages were washed twice with PBS and detached from plate using a cell scarper. The cells were collected into a tube and centrifuge at 100 g for 10 min. After centrifugation, the supernatant was discarded and the pellet was suspended in a solution of PBS containing 0.1µg of leupeptin, 0.2 M benzamidine and 1µg of trypsin inhibitor (Sigma-Aldrich) and mixed with 10% trichloroacetic acid (TCA) containing 1 mM EDTA solution in a 1:1 (v/v) ratio. After centrifugation at 13100 g for 10 min at RT, the supernatant was diluted 1:20 with 0.1% formic acid. Liquid chromatography was performed using an Accela HPLC pump system (Thermo Fisher Scientific). The separation of analytes was conducted on a Luna analytical PFP column (100x2.0 mm, particle

size 3 µm) maintained at 35°C. The mobile phase was composed by two solvents: solvent A (ammonium formate 0.75 mM adjusted to pH 3.5 with formic acid) and solvent B (methanol). Separation was performed under isocratic conditions with 99% mobile phase A at flow rate of 200 µl/min for a total run time of 10 min per sample. Mass spectrometric analysis was performed using a TSQ Quantum Access (Thermo Fisher) triple quadrupole mass spectrometer coupled with electrospray ionization (ESI) operated in positive mode. The selected reaction-monitoring (SRM) was performed by monitoring the transitions *m/z* 308.1→ *m/z* 76.2 + 84.2 + 161.9 (GSH) and *m/z* 613.2 → *m/z* 230.5 + 234.6 + 354.8 (GSSG). The operating conditions for MS analysis were as follows: spray voltage, 2500 V; capillary temperature and voltage, 280 °C and 35 V, respectively; sheat gas and auxiliary gas flow, 30 and 5 arbitrary units, respectively; tube lens offset, 84 V for GSH and 115 V for GSSG. The mass spectrometer was employed in MS/MS mode using argon as collision gas. The method validation was based on U.S. Food and Drug Administration [235]. Data acquisition and analysis were performed with Xcalibur®software, version 2.0 (Thermo Fisher).

5.3.8.2 Total and free fatty acid composition assessment

The determination of the total and free fatty acid composition was performed using a LC-MS method [236]. In detail, macrophages were washed twice with PBS and detached from plate using a cell scarper. The cells were collected into a tube and centrifuge at 100 g for 10 min. After centrifugation, the supernatant was discard and the pellet was conserved at -80°C until the analysis. For the analysis, pellets were suspended with 25µl of standard mix, composed by linoleic acid- $^{13}C_{18}$ (Sigma-Aldrich) 2 ng/µl and palmitic acid- $^{13}C_{16}$ (Sigma-Aldrich) 2 ng/µl in methanol, and with a 1 ml of methanol/acetonitrile (50:50 v/v). After centrifugation at 13100 g for 5 min at 4°, the supernatant was divided into two aliquots for the analysis of total and free fatty acid composition, respectively.

For total fatty acid quantification, in each sample were added 2.5 ml of methanol/ chloroform (50:50 v/v), 1.25 ml of chloride acid 1M and 1.25 ml of methanol. The samples were kept in agitation for 1 hour and 30 minutes and after that, 1.25 ml of water and 1.25 ml of chloroform were added. Samples were shaken vigorously; the organic phase was collected and dried under nitrogen flow. Dry pellets were suspended in 200 µl of methanol/water (50:50 v/v) and 100 µl were transferred into a 96 well plate and placed in an auto-sampler for LC-MS analysis.

For free fatty acid quantification, the supernatants were dried under nitrogen flow and suspended in 200 µl of methanol/water (50:50 v/v). 100 µl of these suspensions were transferred into a 96 well plate and placed in an auto-sampler for LC–MS analysis.

Liquid chromatography was performed using Agilent 1200 binary Pump (Agilent Technologies, USA). The separation of analytes was conduct on a Hypersil GOLD C8 column (100x3.0 mm, particle size 3 µm) maintained at 40 °C. The mobile phase was composed by two solvents: solvent A (isopropylethylamine10 mM and acetic acid15 mM) and solvent B (methanol). Separation was performed under gradient condition as follows: T 0: 20% A, T 20: 1% A, T 25: 1% A, T 25.1: 20% A, T 30: 20% A at a flow rate 500 µl/min for a total run time of 30 min per sample.

Mass spectrometric analysis was performed using an API 4000 (AB Sciex, USA) triple quadrupole mass spectrometer coupled with electrospray ionization (ESI) operated in negative ion mode. The selected ion-monitoring (SIM) was performed by monitoring the ion *m/z* 279.23 (linoleic acid), *m/z* 277.22 (g-linolenic acid), *m/z* 303.23 (arachidonic acid), *m/z* 327.23 (docosahexaenoic acid), *m/z* 283.26 (stearic acid), *m/z* 311.30 (arachic acid), *m/z* 339.33 (behenic acid), *m/z* 281.25 (oleic acid), *m/z* 255.23 (palmitic acid), *m/z* 253.22 (palmitoleic acid), *m/z* 301.22 (eicosapentaenoic acid), *m/z* 365.34 (nevronic acid), *m/z* 337.31 (erucic acid), *m/z* 367.36 (lignoceric acid), *m/z* 269.25 (megaric acid), *m/z* 297.30 (linoleic acid- $^{13}C_{18}$) and *m/z* 256.41 (palmitic acid- $^{13}C_{16}$).

The operating condition for MS analysis were as follow: IonSpray voltage (IS), 4500 V; temperature (TEM), 500 °C; Ion Source Gas 1 (GS1) and Ion Source Gas 2 (GS2), 50 and 55 arbitrary units, respectively; Curtain Gas (CUR), 40 L/min; Collision Gas (CUR), 3 L/min.

Data acquisition and analysis were performed with MultiQuant™ software, version 3.0 (AB Sciex).

5.3.9 OCT analysis

5.3.9.1 OCT image analysis

Culprit lesion in acute myocardial infarct (AMI) patients was identified by means of angiography, electrocardiographic T-wave or ST-segment alterations, and/or regional wall motion abnormalities on echocardiographic assessment. In SA patients, OCT analysis was performed at the minimal lumen area (MLA) site. Frequency domain OCT (FD-OCT) images were acquired by a commercially available system (C7 System, LightLab Imaging Inc/ St Jude Medical, Westford, MA)

connected to an OCT catheter (C7 Dragonfly; LightLab Imaging Inc/ St Jude Medical), which was advanced to the culprit lesion. All images were recorded digitally and every single frame (0.2 mm) was analyzed by two expert and independent investigators who were blinded to clinical and laboratory values (Institute of Cardiology, Catholic University of the Sacred Heart, Policlinico Gemelli, Rome, Italy). At the MLA site or at culprit lesion, respectively in SA and AMI patients, the analysis was targeted on plaque characterization (calcified, fibrous, or lipid plaques), presence of plaque rupture, measurement of fibrous cap thickness, presence of intracoronary thrombus and intra-plaque micro channels. When a plaque contained two or more lipid-containing quadrants, it was considered a lipid-rich plaque, and the lipid arc and the cap thickness were measured. Thin-cap fibroatheroma (TCFA) was defined as a lipid-rich plaque with a fibrous cap thickness of ≤65 μm.

5.3.9.2 OCT macrophage analysis

We assessed the presence of macrophage infiltration (MØI) in the analyzed lesions by OCT. Macrophages were qualitatively identified according to International Working Group for Intravascular Optical Coherence Tomography (IWG-IVOCT) Consensus standards [237]. In particular, macrophages have been visualized by OCT imaging as signal-rich, distinct, or confluent punctate regions that exceed the intensity of background speckle noise and generate a backward shadowing. For caps having a thickness <125 μm^2, the depth of the region of interest (ROI) was matched to the cap thickness. Median filtering was performed with a 3x3 square kernel to remove speckle noise. In plaques with MØI, quantitative evaluation of macrophage content was obtained by measuring the normalized standard deviation (NSD) known to have a high degree of positive correlation with histological measurements of macrophage content, by using dedicated software provided by S. Jude medical. In particular, NSD was measured for each pixel within each cap using a 125 μm^2 window centered at the pixel location: NSD (x,y) = [σ (x,y)125 μm^2/(Smax-Smin)] x 100. Where NSD (x,y) is the normalized standard deviation of the OCT signal at pixel location (x,y), Smax is the maximum OCT image value, and Smin is the minimum OCT image value. Pixels within the (125 x 125) μm^2 window that did not overlap with the segmented cap were excluded.

5.4 Biochemical signatures

The biochemical profile of MDMs obtained from our study population was assessed by western blot and immunofluorescence methodologies. In particular we assessed transglutaminase (TG)2 and tissue factor (TF) levels in MDMs population through western blot using primary antibody directed against TG2 (Cell signaling, Euroclone, Milano, Italy) (1:1000) and TF (America Diagnostica, Sekisui Diagnostics, Cabru, Milan, Italy) (1:500), respectively. To evaluate the levels of this protein in both morphotypes we used immunofluorescence technique with primary antibody directed against TG2 (Cell signaling) (1:100) and TF (1:200), respectively.

Moreover, we analysed the activity of mediators releasing by our cells population. In particular, the activity of matrix metalloproteinase (MMP)-9 secreted by MDMs was evaluated using BiotrakTM activity assay system (Amersham, GE Healthcare, Milan, Italy).

Finally, we assessed the total and free fatty acid composition of MDMs obtained from our study population through mass spectrometry analysis.

5.5 Functional analyses

The functional profile of MDMs obtained from healthy subjects and CAD patients was assessed by the evaluation of efferocytic capability using the efferocytic assay and the thrombin production by thrombin generation assay.

5.6 Oxidative stress evaluation

We also evaluated the oxidative stress of MDMs obtained from our study population by:

- the assessment of GSH/GSSG using mass spectrometry.
- the determination of Nuclear-realetd factor 2 (Nrf2) and heme-oxigenase 1 (HO-1) pathway using western blot and immunofluorescence techniques. In detail, for assessment of Nrf2 and HO-1 levels through western blot we used primary antibody direct against Nrf2 (Santa Cruz Biotechnology, DBA Italia, Milano, Italy) (1:500) and HO-1 (Abcam, Prodotti Giann S.p.A., Milano, Italy) (1:250), respectively. For immunofluorescence determination we used primary antibody against Nrf2 (Cell signaling) (1:200) and HO-1 (Abcam) (1:100), respectively.

5.7 Statistical analysis

The distribution of continuous variables was assessed by visual inspection of frequency histograms and with the use of the Shapiro–Wilk test. Continuous variables were expressed as mean±SD or median with interquartile range, if they followed a normal or non-normal distribution, respectively. Continuous variables were compared with unpaired t-test or Mann–Whitney U-test, whereas categorical variables were compared using the Chi square test or Fisher's exact test, as appropriate. Paired-group comparison was performed using the paired t-test or Wilcoxon test, as appropriate. Unpaired t-test or Mann-Whitney U-test were used for the comparison of continuous variables between groups; continuous variables among groups were compared with ANOVA or Kruskal-Wallis test, and Bonferroni's correction for multiple comparison was applied and a Bonferroni-adjusted (Ba)-p-value was reported. Analysis of trends, according to the severity of the disease, was performed by Spearman's rank test. Correlations between variables were performed using the Pearson test or the Spearman's rank test, as appropriate. Intra-observer and inter-observer variability in the analysis of MØI in the fibrous cap were assessed by Kappa measure of agreement. Regarding the evaluation of MØI, Kappa measures of agreement for intra-observer and inter-observer variability were 0.89 ($p<0.0001$) and 0.94 ($p<0.001$), respectively. Of note, all performed analyses have been adjusted for age and sex. All tests were two-sided. A p value <0.05 was considered to indicate statistical significance. All calculations were computed with the aid of the SAS software package (Version 9.2; SAS Institute Inc., Cary, NC).

6. Results

6.1 Study population

The principal demographic, clinical and laboratory characteristics of the patient groups and of healthy subjects analysed in this study are depicted in Table 2.

		CAD group				
Variables	**Healthy subjects n=25**	**SA n=41**	**NSTEMI n=28**	**STEMI n=21**	**ANOVA all subjects**	**ANOVA CAD patients only**
Demographics						
Age (years)	49±15	68±9	65±13	60±13	0.0001	0.034
Male sex, n (%)	10 (40)	33 (81)	20 (74)	18 (82)	0.002	0.765
BMI (kg/m²)	24.5±1.8	28.6±3.3	28.3±2.9	30.3±5.0	0.0001	0.125
Clinical characteristics						
Current smoking, n (%)	-	26 (63)	16 (59)	14 (64)		0.933
Diabetes mellitus, n (%)	-	11 (27)	12 (44)	11 (50)		0.138
Dyslipidemia, n (%)	-	21 (51)	15 (56)	11 (50)		0.916
Hypertension, n (%)	-	24 (58)	13 (48)	14 (64)		0.533
Family history of CAD, n (%)	-	19 (46)	19 (70)	8 (36)		0.043
LVEF (%)	-	55±7	51±7	52±6		0.578
Laboratory data						
WBC ($\times10^9$/l)	7.25±2.91	9.21±3.60	8.80±3.41	8.72±2.59	0.148	0.820
RBC ($\times10^{12}$/l)	4.57±0.69	4.62±0.70	5.70±4.36	5.13±2.39	0.262	0.274
Neutrophil count ($\times10^9$/l)	4.63±2.50	6.41±3.21	5.90±3.29	6.03±2.19	0.122	0.769
Lymphocyte count ($\times10^9$/l)	1.98±0.98	2.03±0.83	1.87±0.70	2.05±0.95	0.853	0.668
Eosinophil count ($\times10^9$/l)	0.14±0.12	0.37±1.14	0.21±0.25	0.54±1.60	0.502	0.599
Monocyte count ($\times10^9$/l)	0.49±0.20	0.63±0.23	0.58±0.27	0.62±0.23	0.094	0.698
Basophil count ($\times10^9$/l)	0.02±0.02	0.01±0.03	0.01±0.02	0.01±0.02	0.028	0.935
Platelets ($\times10^9$/l)	244±61	220±74	238±83	214±60	0.40	0.472
hs-CRP (mg/l)	1.9 (1.4-2.6)	2.10 (1.40-3.20)	7.80 (3.35-16.95)	21.35 (10.43-30.25)	0.001	0.0001*
Creatinine (mg/dl)	1.03±0.15	1.02±0.37	0.93±0.28	1.01±0.35	0.301	0.487
Glycaemia (mg/dl)	105±29	124±27	123±32	141±39	0.0001	0.084
Total cholesterol (mg/dl)	168±32	170±35	192±45	222±40	0.0001	0.0001

LDL (mg/dl)	113±26	97±26	119±45	141±34	0.0001	0.0001
HDL (mg/dl)	44±12	50±15	43±10	43±10	0.017	0.033
Triglycerides (mg/dl)	119±24	122±55	163±68	163±59	0.006	0.007
Peak TnI (µg/dl)	-	0.001 (0.001-0.002)	1.70 (0.75-7.00)	30.85 (17.10-73.75)		0.0001*
Peak CK-MB (µg/dl)	-	2.10 (1.60-3.42)	19.00 (9.45-42.65)	231.50 (114.25-297.75)		0.0001*
Angiographic data						
Culprit or treated vessel, n (%)						
LAD	-	16 (39)	22 (81)	11 (50)		
LCX	-	7 (17)	2 (7)	3 (14)		
RCA	-	18 (44)	3 (11)	8 (30)		
Multivessel disease, n (%)	-	28 (68)	15 (56)	8 (36)		0.051
Admission therapy						
ASA, n (%)	-	14 (34)	12 (44)	8 (36)		0.692
Beta-Blockers, n (%)	-	12 (29)	11 (41)	3 (14)		0.116
ACE-inhibitors, n (%)	-	21 (51)	9 (33)	2 (9)		0.003
Statins, n (%)	-	17 (41)	6 (22)	8 (36)		0.264

Table 2: Baseline clinical, laboratory and angiographic characteristics of healthy subject and coronary artery disease patients according to their clinical presentation

Data are expressed as mean ± SD or median and interquartile range. p value: ANOVA t test, *Kruskal-Wallis test.

SA, stable angina; AMI, acute myocardial infarction; CAD, coronary artery disease; BMI, body-mass index; LVEF, left ventricular ejection fraction; WBC, white blood cells; RBC, red blood cells; LDL, low-density lipoprotein; HDL, high-density lipoprotein; hs-CRP, high-sensitive C-reactive protein; TnI, troponin-I; CK-MB, Creatine phosphokinase-MB; LAD, left anterior descending; LCX, left circumflex; RCA, right coronary artery; ASA, aspirin; ACE-inhibitors, angiotensin-converting enzyme-inhibitors.

The study groups differ for age and sex that were considered as confounders for group comparisons. CAD patients had a significant higher BMI and received cardiovascular therapy. The risk factor were absent in healthy subjects, as stated in exclusion criteria. Regarding CAD group, acute patients (NSTEMI and STEMI) had more frequently a family history of CAD compared to SA. In addition, acute patients showed high levels of hs-CPR.

6.2 Morphological characterization of MDMs

MDMs spontaneously differentiated from monocytes of healthy subjects showed two dominant and distinct morphotypes, spindle and round, that coexist in the same culture with a 1:1 ratio. MDMs of CAD patients also had two prevalent and different morphotypes, but the number of round MDMs was greater compared to spindle or to undefined macrophages (Figure 8A). Further, when analyzing the different clinical presentation groups (SA, NSTEMI and STEMI), the prevalence of round MDMs in STEMI patients was significantly greater than NSTEMI and SA, and in parallel a significant decrease in spindle MDMs was observed in this clinical conditions (Figure 8B).

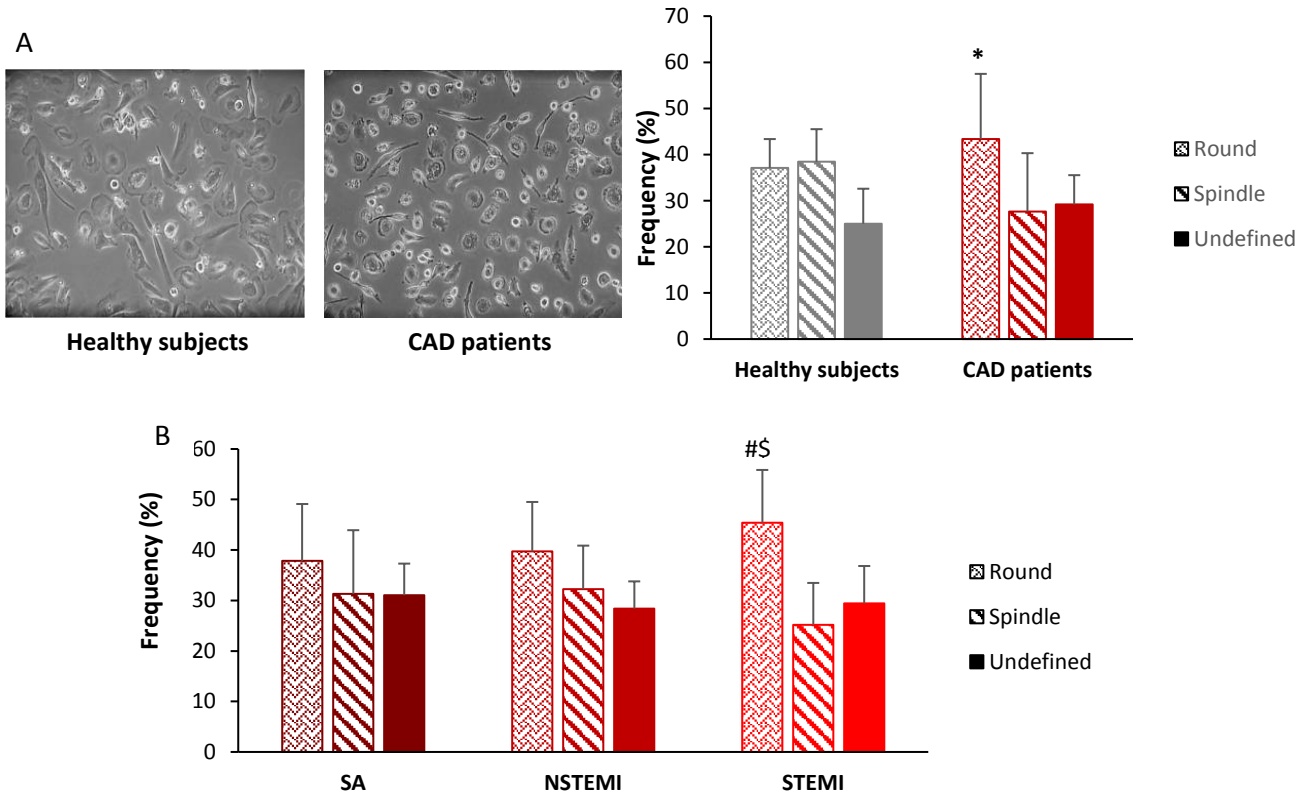

Figure 8: A) Monocyte-derived macrophage morphology in healthy subjects and CAD patients. B) Monocyte-derived macrophage morphology in SA patients compared to NSTEMI and STEMI patients. Data are expressed as the mean ± SD and derived from independent cultures obtained from 25 healthy subjects and 50 CAD patients (SA (n=19), NSTEMI (n=20) and STEMI (n=11)). *p<0.05 vs. healthy subjects; $ p<0.05 vs. SA; #p<0.05 as spindle and undefined MDM in STEMI patients.

6.3 Biochemical and functional profile assessment

6.3.1 Efferocytosis of MDMs

We assessed the efferocytosis of MDMs in our study groups. We found that the efferocytotic capacity of MDMs obtained from CAD patients (SA, NSTEMI and STEMI) was significantly lower compared to healthy subjects, while it was similar in SA or acute patients (Figure 9).

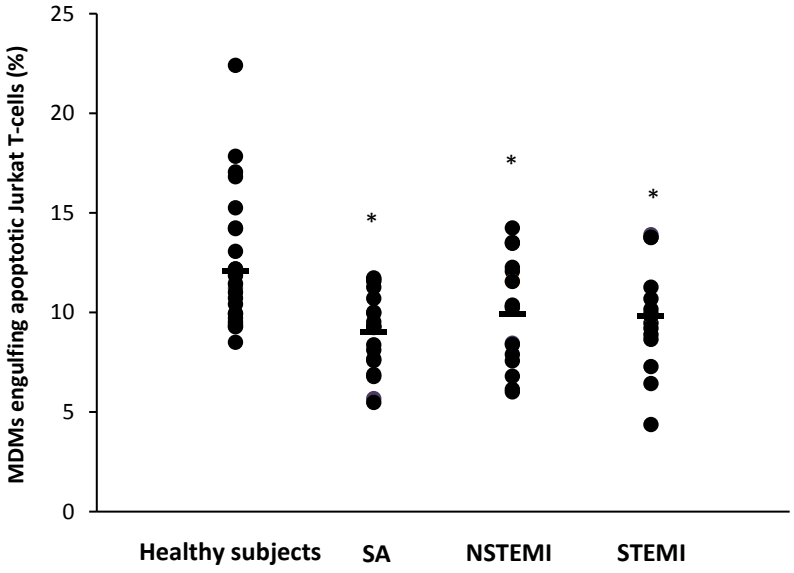

Figure 9: Efferocytic capacity of MDMs obtained from healthy subjects and CAD patients. Data are expressed as percentage of MDMs that have engulfed carboxyfluorescein diacetate succinimidyl ester (CSFE)-stained apoptotic cells and derive from independent cultures obtained from 25 healthy subjects and 50 CAD patients (SA (n=19), NSTEMI (n=16), STEMI (n=15)). * $p<0.05$ vs. healthy subjects

6.3.2 Evaluation of TG2 levels

In order to verify the potential involvement of TG2, protein involved in phagosomal formation, in the efferocytosis of MDMs we assessed the expression of TG2. MDMs obtained from CAD patients showed lower levels of TG2 compared to healthy subjects (Figure 10A). Immunofluorescence analysis evidenced that while in healthy subjects TG2 was more abundant in round than spindle MDMs, in SA, NSTEMI and STEMI patients TG2 levels were similar in both round and spindle MDM morphotypes. In Figure 10B, representative images were shown. Moreover, we observed significantly lower TG2 levels in round MDMs of CAD patients (SA, NSTEMI and STEMI) in comparison to healthy subject round MDMs (Figure 10C).

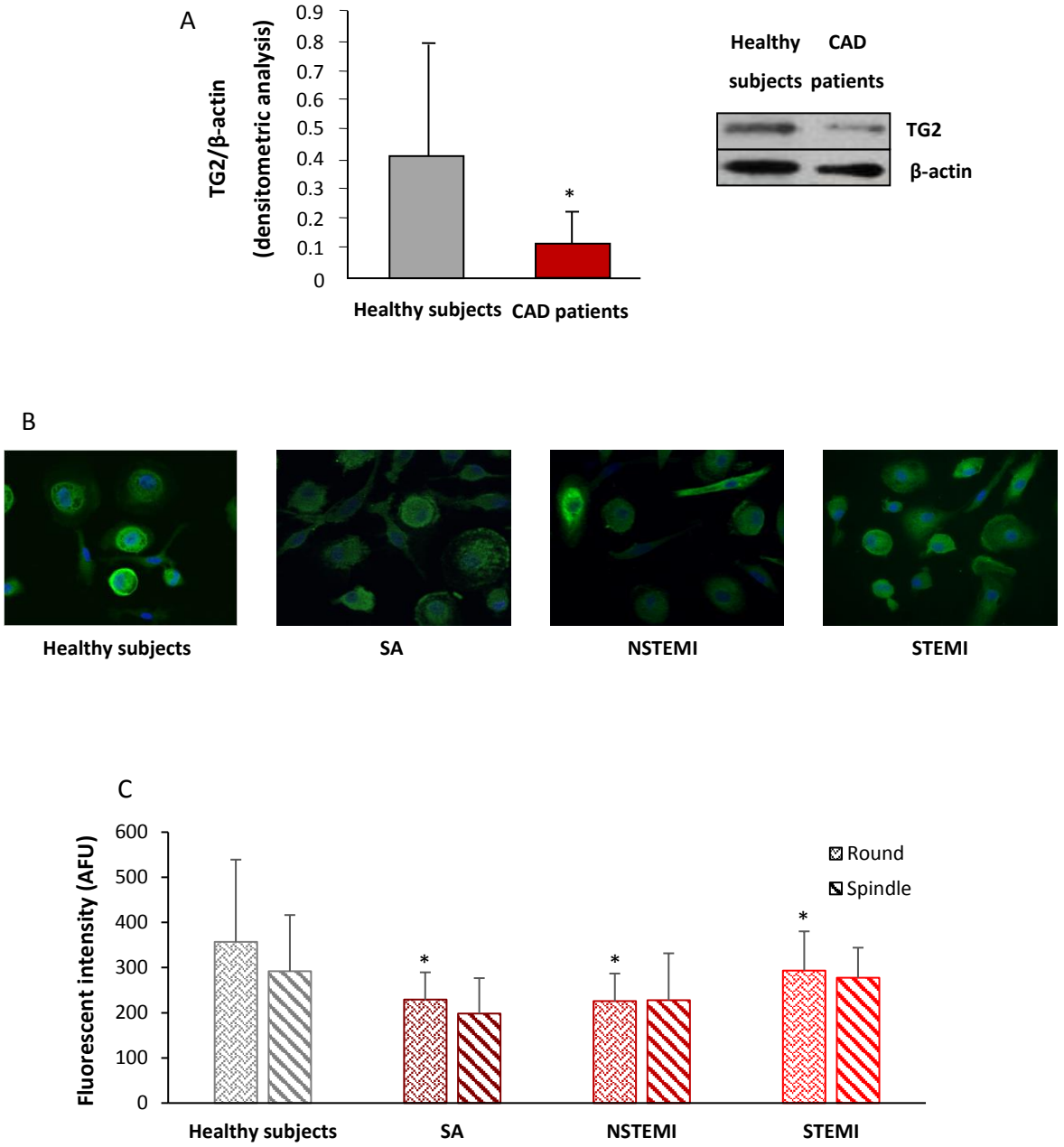

Figure 10: TG2 levels. A) TG2 was detected by western blot analysis in MDMs obtained from CAD patients and healthy subjects. β-actin was used as a control of protein loading. Densitometry is shown in the bar graph. Data are expressed as the mean ± SD and derive from MDMs obtained from 5 healthy subjects and 10 CAD patients. B) Representative images of TG2 in round and spindle MDMs obtained from healthy subjects and CAD patients (400× original magnification), nuclei were visualized by Hoechst 33258. C) Quantitative analysis of TG2 in round and spindle MDMs. Data are expressed as the mean ± SD of fluorescence intensity/µm2 (at least 3 fields, 400× magnification, were analysed) and derive from independent cultures obtained from 10 healthy subjects and 30 CAD patients (SA (n=10), NSTEMI (n=10) and STEMI (n=10)). *p<0.05 vs. healthy subjects.

6.3.3 Evaluation of TF levels

We assessed TF levels in MDMs obtained from our study population by western blot analysis. We observed that, MDMs of CAD patients had significantly higher TF levels in relation with healthy subjects (Figure 11A). The immunofluorescence analysis shows an equally distribution of this protein in both spindle and round MDMs morphotypes in healthy as well as in patients. However, a significant increase in TF fluorescence intensity was detected in both MDM morphotypes of CAD patients in respect to their counterparts in healthy subjects (Figure 11B). In particular, a trend of MDM TF levels both in round and spindle morphotypes (p_{trend}=0.004 and p_{trend}=0.001, respectively) according to the severity of the disease from healthy subjects to SA, NSTEMI, and STEMI patients, was observed. The highest TF expression was found in both round and spindle MDMs of STEMI patients (Figure 11C).

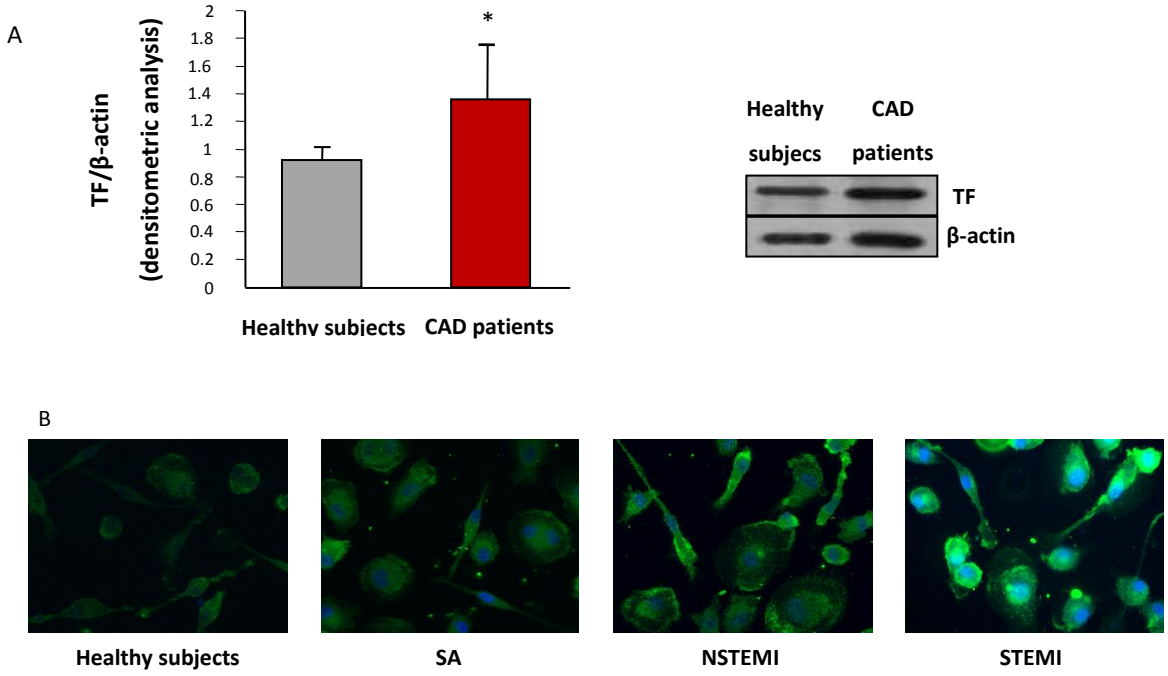

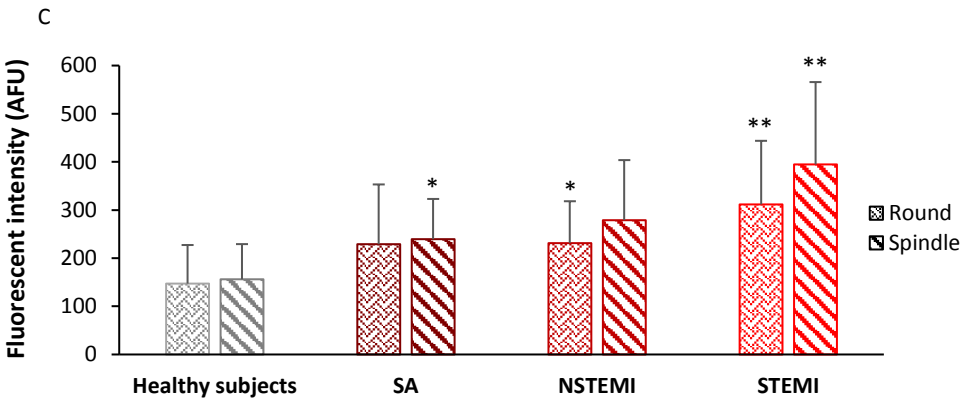

Figure 11: TF levels in CAD patients and healthy subjects. A) TF was detected by western blot analysis. β-actin was used as a control of protein loading. Densitometry is shown in the bar graph. Data are expressed as the mean ± SD and derive from MDMs obtained from 8 healthy subjects and 15 CAD patients. B) Representative images TF in round and spindle MDMs obtained from healthy subjects and CAD patients (400× original magnification), nuclei were visualized by Hoechst 33258. C) Quantitative analysis of TF in round and spindle MDMs. Data are expressed as the mean ± SD of fluorescence intensity/µm2 (at least 3 fields, 400× magnification, were analyzed) and data derive from independent cultures obtained from 10 healthy subjects and 30 CAD patients (SA (n=10), NSTEMI (n=10) and STEMI (n=10)). * $p<0.05$, ** $p<0.01$, vs. healthy subjects.

6.3.4 Thrombin generation

Enhanced antigenic expression of TF in MDMs of CAD patients displayed a functional consequence in thrombin generation. In fact, CAD patients showed a reduction in the lag time and in the time to peak with respect to healthy subjects with no change on the peak of thrombin generation or endogenous thrombin potential (ETP) (Table 3).

Parameters	Healthy subjects	CAD	P value
Lag Time (min)	14.51 ± 4.12	12.8 5± 3.73	0.04
ETP (nM min)	1167.42 ± 287.03	1216.30 ± 256.92	0.59
Peak (nM)	149.63 ± 63.67	178.11 ± 59.82	0.17
ttPeak (min)	18.17 ± 4.90	14.93 ± 4.21	0.04
VelIndex (nM/min)	49.51 ± 35.31	68.12 ± 38.37	0.14

Table 3: Thrombin generation evaluated using Thrombinoscope in healthy subjects (n=16) compared to CAD patients (n=20). Time to peak (ttPeak), endogenous thrombin potential (ETP), and velocity index of propagation phase (VelIndex)

6.4 Matrix Metalloproteinase-9 Activity

We analyzed the MMP-9 activity in MDMs obtained from healthy subjects and CAD patients. We observed that MMP-9 activity in MDMs was higher in CAD patients than in healthy subjects. In particular, when we analyzing the different clinical presentation (SA, NSTEMI and STEMI), we observed a progressive increase in MMP-9 activity from SA to acute patients reaching a maximum in STEMI patients (p_{trend}=0.004) (Figure 12).

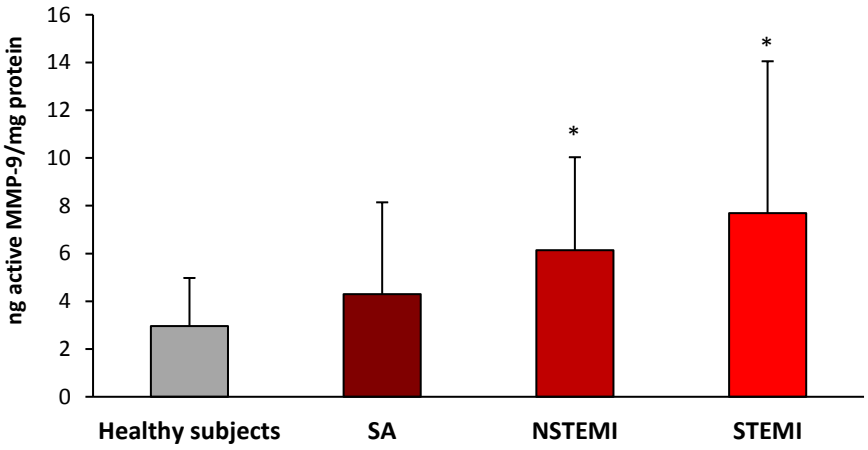

Figure 12: MMP-9 activity in SA, NSTEMI and STEMI patients and healthy subjects. Data are expressed as the mean ± SD derived from independent cultures obtained from 10 healthy subjects and 30 CAD patients (SA (n=10), NSTEMI (n=10) and STEMI (n=10)). * p<0.05 vs. healthy subjects.

6.4.1 Evaluation of GSH/GSSG ratio

In order to evaluate the oxidative stress status in the study population, we measured in MDMs the levels of the reduced and the oxidized form of glutathione, whose ratio is a recognized index of oxidative stress. The results are showed in Figure 13. The GSH/GSSG ratio was decreased in CAD patient respect to healthy subjects. When analyzing the different clinical presentation groups (SA, NSTEMI and STEMI) the GSH/GSSG ratio was lower in MDMs of STEMI patients in respect to healthy subject, SA and NSTEMI patients (p_{trend}=0.022).

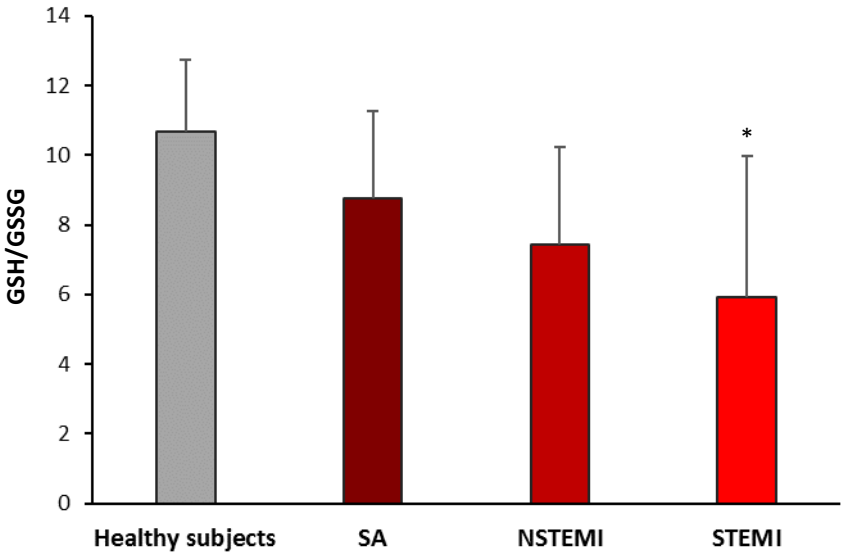

Figure 13: GSH/GSSG evaluation in SA, NSTEMI and STEMI patients and healthy subjects. Data are expressed as the mean ± SD derived from independent cultures obtained from 5 healthy subjects and 15 CAD patients (SA (n=5), NSTEMI (n=5) and STEMI (n=5)). * p<0.05 vs. healthy subjects.

6.4.2 Evaluation of Nrf2 and HO-1 levels

In order to evaluate the response of MDMs to oxidative stress, we evaluated the activation of Nrf2/HO-1 pathway. We observed that Nrf2 was higher in MDMs of CAD patients with respect to those of healthy subjects (Figure 14A). These data are confirming by immunofluorescence (Figure 14B). In detail, when we analyzed the distribution of this transcription factor in different clinical presentation (SA, NSTEMI and STEMI), an increasing Nrf2 (p_{trend} round=0.035, p_{trend} spindle=0.121) in NSTEMI and STEMI was observed (Figure 14C). This behavior was mirrored by Nrf2 target protein. HO-1 was higher in CAD patients (Figure 15A and 15B) and a trend according to the severity of clinical presentation was detected (p_{trend} round<0.001, p_{trend} spindle=0.003).

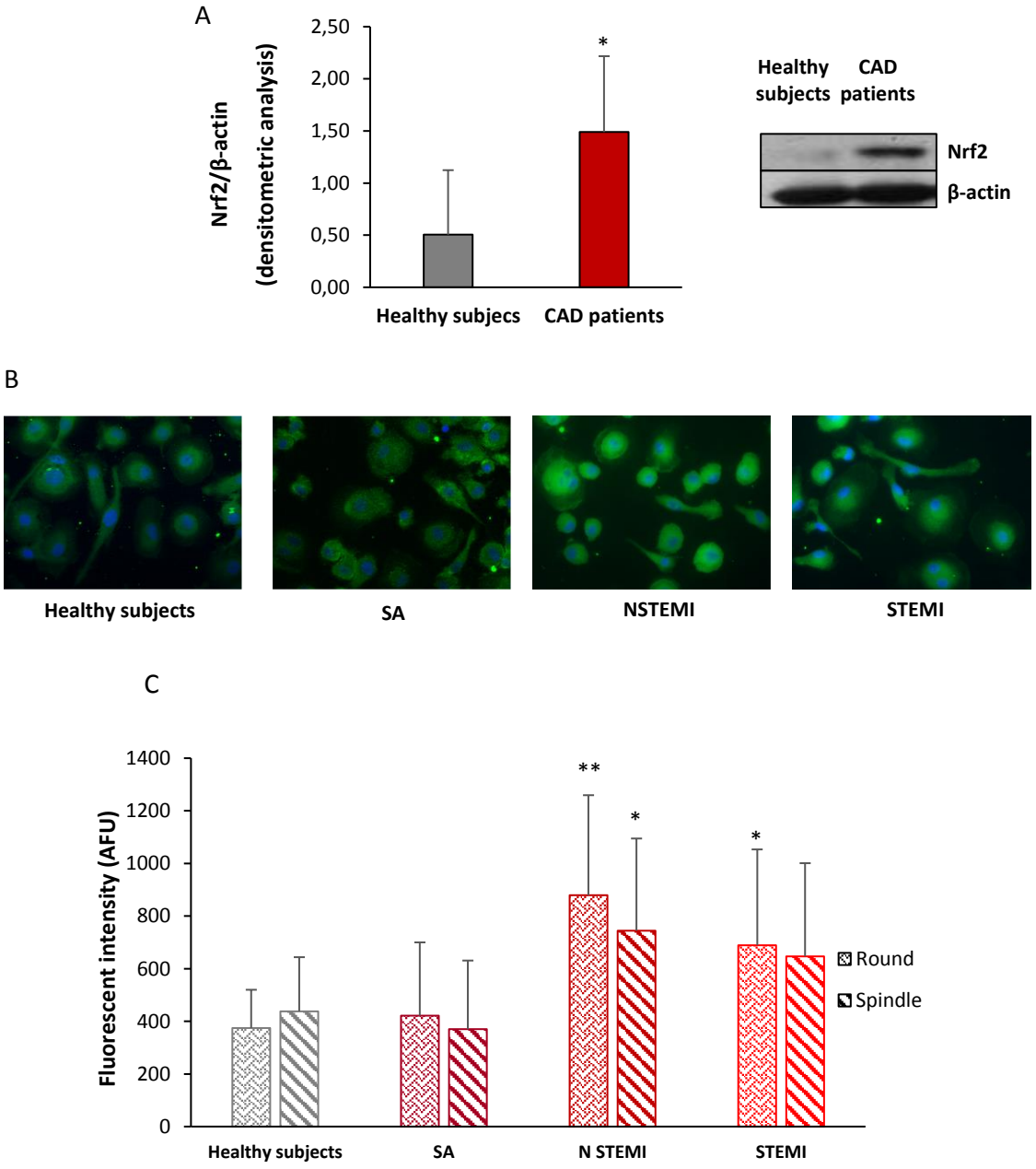

Figure 14: Nrf2 levels in CAD patients and healthy subjects. (A) Nrf2 was detected by western blot analysis. β-actin was used as a control of protein loading. Densitometry is shown in the bar graph. Data are expressed as the mean ± SD and derive from MDMs obtained from 11 healthy subjects and 17 CAD patients. (B) Representative images of Nrf2 in round and spindle MDMs obtained from healthy subjects and CAD patients (400× original magnification), nuclei were visualized by Hoechst 33258. C) Quantitative analysis of Nrf2 in round and spindle MDMs. Data are expressed as the mean ± SD of fluorescence intensity/µm2 (at least 3 fields, 400× magnification, were analyzed) and data derive from independent cultures obtained from 10 healthy subjects and 30 CAD patients (SA (n=10), NSTEMI (n=10) and STEMI (n=10)).
* $p<0.05$, ** $p<0.01$, vs. healthy subjects

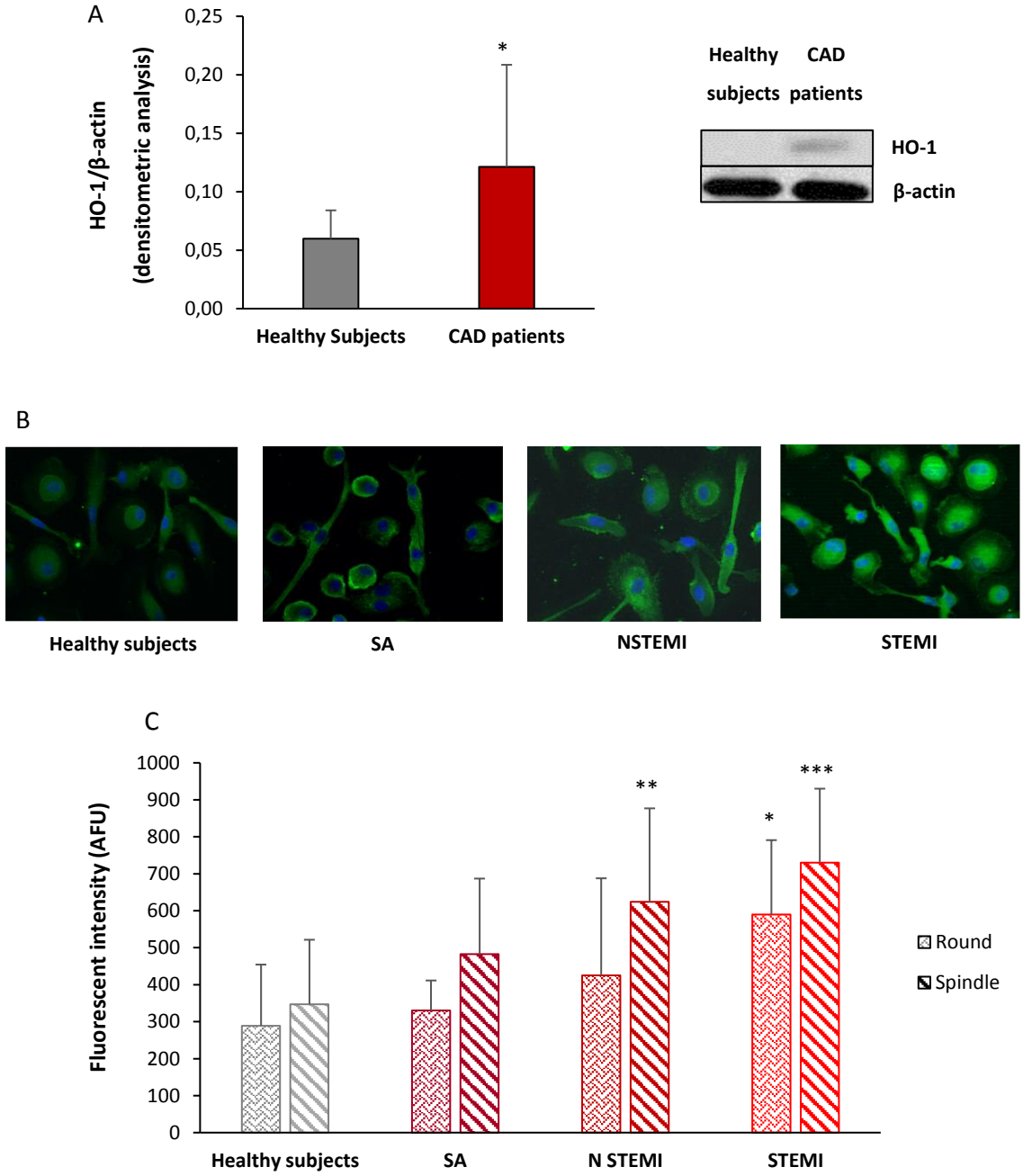

Figure 15: HO-1 levels in CAD patients and healthy subjects. (A) HO-1 was detected by western blot analysis. β-actin was used as a control of protein loading. Densitometry is shown in the bar graph. Data are expressed as the mean ± SD and derive from MDMs obtained from 11 healthy subjects and 17 CAD patients. (B) Representative images of HO-1 in round and spindle MDMs obtained from healthy subjects and CAD patients (400× original magnification), nuclei were visualized by Hoechst 33258. C) Quantitative analysis of HO-1 in round and spindle MDMs. Data are expressed as the mean ± SD of fluorescence intensity/µm2 (at least 3 fields, 400× magnification, were analyzed) and data derive from independent cultures obtained from 10 healthy subjects and 30 CAD patients (SA (n=10), NSTEMI (n=10) and STEMI (n=10)). * p<0.05, ** p<0.01, *** p<0.001 vs. healthy subjects.

6.5 Fatty acid composition

In order to evaluate if the lipid content of MDMs could influence the oxidative stress status and the efferocytic capacity of these cells, we evaluated the total fatty acid composition of MDMs obtained from healthy subjects and CAD patients. As show in Figure16 no differences in fatty acids composition (Figure 16A and B), desaturation index (Figure 16C) and membrane fluidity index (MFI) (Figure 16D) between the study groups were present.

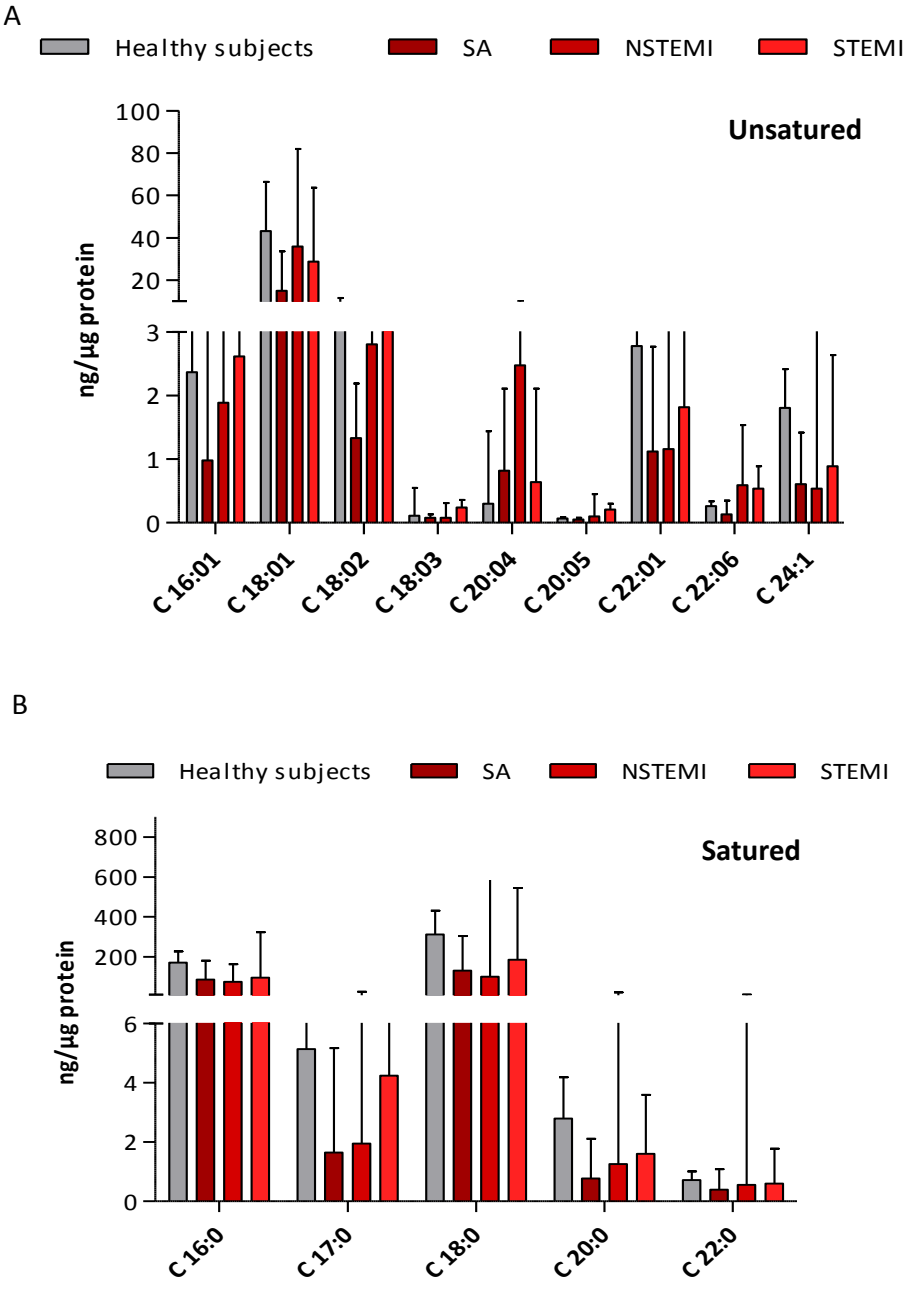

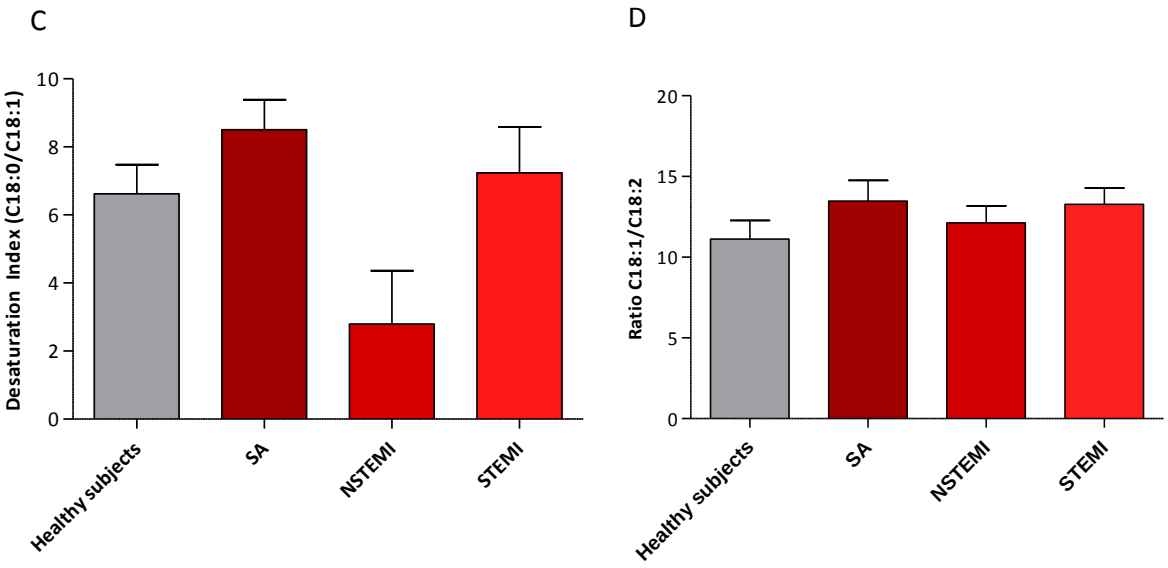

Figure 16: Fatty acids profile of MDMs obtained from healthy subjects (n=10), SA (n=11), NSTEMI (n=11) and STEMI (n=10) patients. Unsatured (A) and Satured (B) fatty acids of MDMs purified from the four experimental groups. C) Desaturation index as ratio of C18:0 (stearic acid)/C18:1 (oleic acid). D) MFI as ratio of C18:1 (oleic acid)/C18:2 (linoleic acid). Data are expressed as the median ± E.S.

Nevertheless, if we grouped patients, we observed a positive correlation between GSH/GSSG ratio and the membrane fluidity index (MFI) in both healthy subjects and CAD patients, indicating the existence of a relationship between oxidative stress and lipid composition (Figure 17A e B, $p<0.0001$ and $p=0.0003$, respectively).

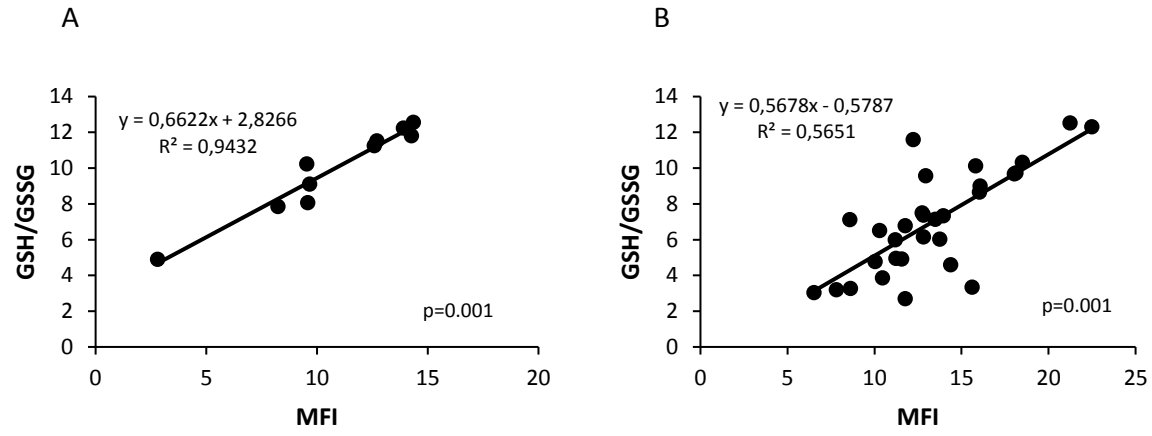

Figure 17: Correlation between GSH/GSSG ratio and MFI (stearic acid/oleic acid) in healthy subjects (n=10) (A) and CAD patients (n=32) (B)

MFI positively correlate also with efferocytosis in both study groups, underlying the importance of lipid composition in this process (Figure 18A e B).

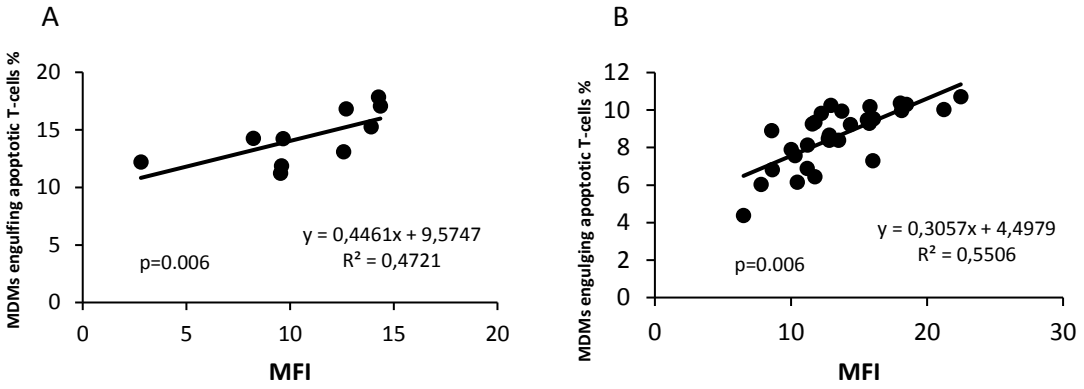

Figure18: Correlation between efferocytosis and MFI (stearic acid/oleic acid) in healthy subjects (n=10) (A) and in CAD patients (n=32) (B)

6.6 MDMs: biochemical and morphological characteristics and OCT plaque features

Representative OCT images of *in vivo* coronary atherosclerotic plaques are showed in Figure 19.

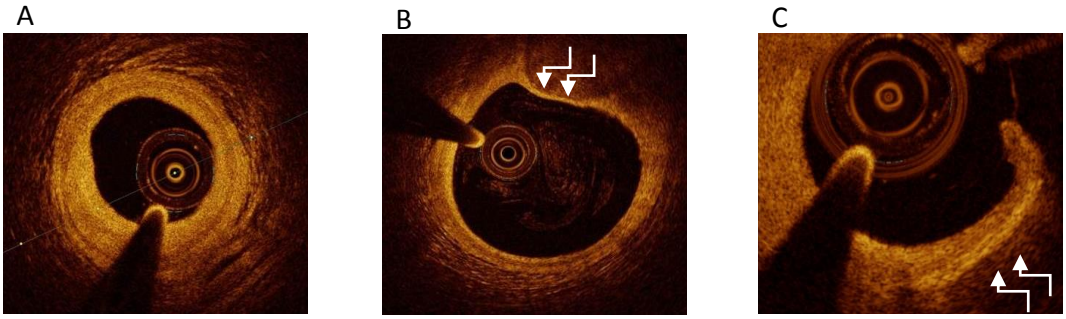

Figure 19: Representative OCT images of coronary atherosclerotic plaque. (A) Stable fibrous coronary plaque. (B) High-risk thin-cap fibroatheroma (white arrows). (C) Coronary rupture plaque with macrophage infiltration (white arrows).

At OCT analysis, acute patients present more frequently a lipid plaque, a ruptured plaque, a thin cap fibroatheroma and the presence of thrombus (white and red) with respect to SA patients. Moreover, acute patients present plaque with grater lipid content compared to those of SA, evidenced by higher number of lipid quadrant and lipid arc degree. Furthermore, these patients showed higher numbers of microchannels and higher macrophage content respect to SA patients. On contrary, SA patients present more frequently a fibrous and calcific plaque in respect to acute patients (Table 4).

Variables	SA (N=26)	AMI (N=24)	p VALUE
Lipid plaque, n (%)	15 (57)	22 (92)	0.01
Fibrous plaque, n (%)	9 (35)	2 (8)	0.04*
Calcific plaque, n (%)	7 (27)	2 (8)	0.14*
Plaque rupture, n (%)	6 (23)	18 (75)	0.01
MLA, mm^2	1.59 (0.71-3.85)	1.54 (0.70-3.75)	0.99
TCFA, n (%)	8 (31)	19 (79)	0.001
Thrombus, n (%)	2 (8)	20 (83)	0.0001*
White, n (%)	1 (4)	18 (75)	0.0001*
Red, n (%)	1 (4)	7 (29)	0.02*
Lipid quadrants, n	2.1±1.0	3.1±1.6	0.0001
Lipid arc degree °	135 (87-265)	269 (161-280)	0.0001
Presence of microchannels, n (%)	4 (15)	15 (63)	0.0006*
Macrophage infiltration detection, n (%)	14 (54)	22 (92)	0.001
Macrophage NSD	3.45±1.01	6.19±1.95	0.001

Table 4. Optical coherence tomography features of coronary artery disease patients according to the clinical presentation
Data are expressed as mean ± SD or median and interquartile range. p value: Wilcoxon testfor quantitative variables; *Fisher test.
MLA, minimal lumen area; TCFA, thin-cap fibroatheroma; NSD, normalized standard deviation.

6.6.1 MDMs morphology

We wanted to evaluate if there were some associations between the frequency of MDM morphotypes observed *in vitro* in CAD patients and plaque features *in vivo* assessed by OCT.
We observed that the prevalence of round MDMs was significantly higher in patients presenting a thin cap fibroatheroma (TCFA), a lipid plaque, a ruptured plaque, and a presence of thrombus (Figures 20A-20D). Moreover, the identification of high number of intra-plaque macrophages was associated with a high prevalence of round MDMs (Figure 20E) and the latter positively correlated with macrophage content which was represented by NSD parameter (Figure 20F).

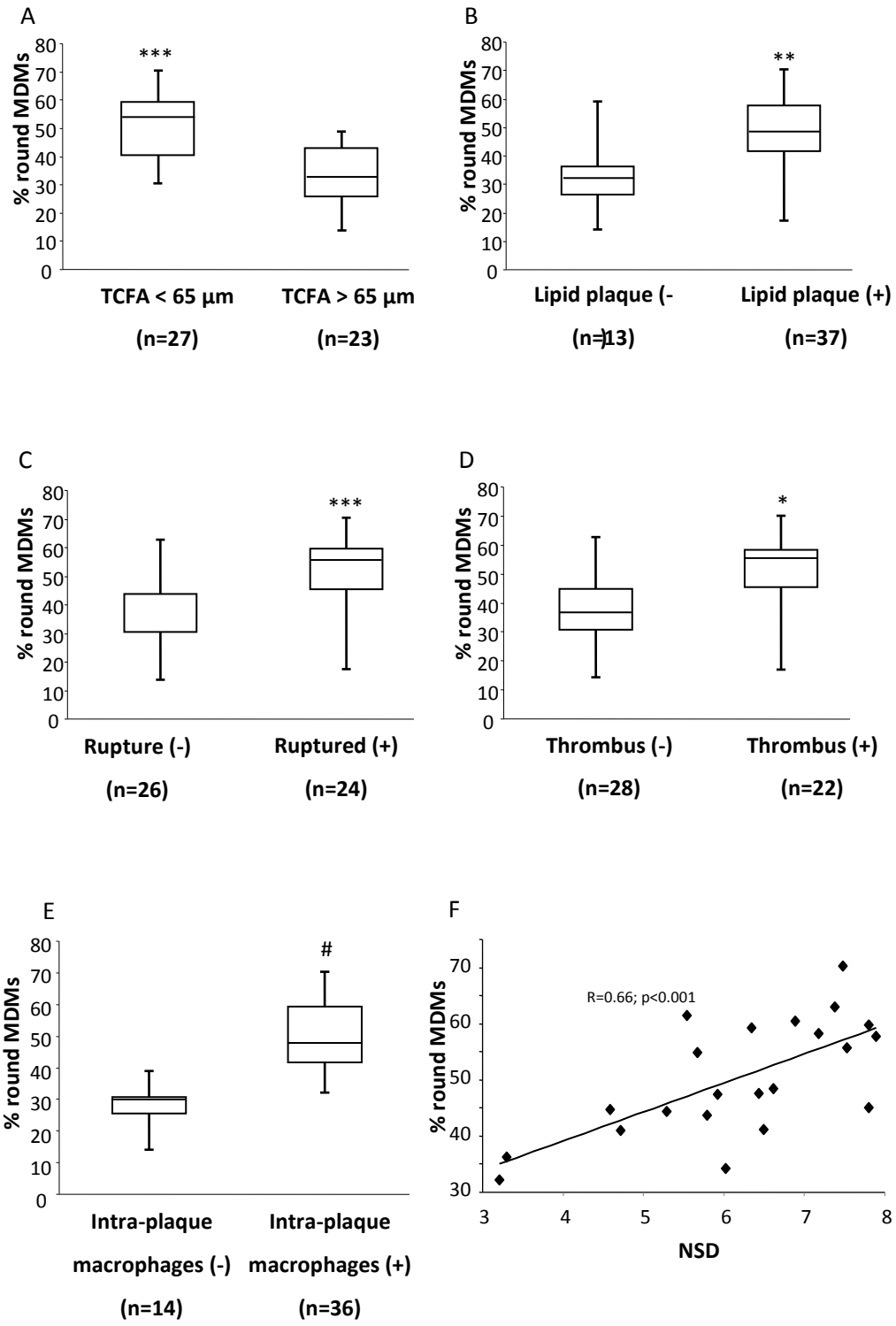

Figure 20: OCT plaque features and frequency of round MDM morphotype. Association between round MDM morphotype and thin-cap fibroatheroma, TCFA(A), plaque lipid content(B), fibrous cap integrity(C), presence of thrombus(D), presence of intra-plaque macrophages (E), and correlation between macrophage content (normalized standard deviation (NSD)) (F) detected by means OCT in in vivo plaque. *p<0.02; **p<0.002; ***p<0.0005; #p<0.0001.

6.6.2 MDMs TF levels

High TF levels observed in in round and spindle MDMs of CAD patients are associated with the presence of a ruptured plaque (Figure 21A), of thrombus (B) and of intra-plaque macrophages (C) analyzed by OCT.

A

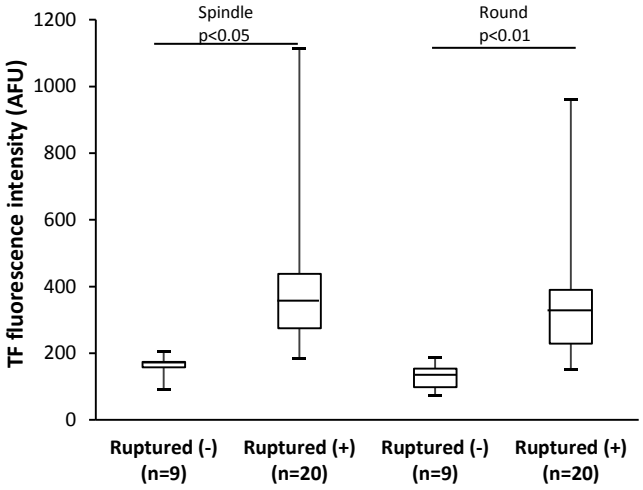

B

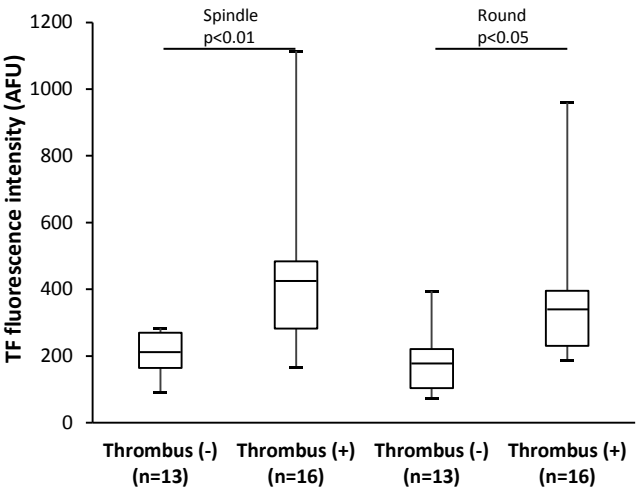

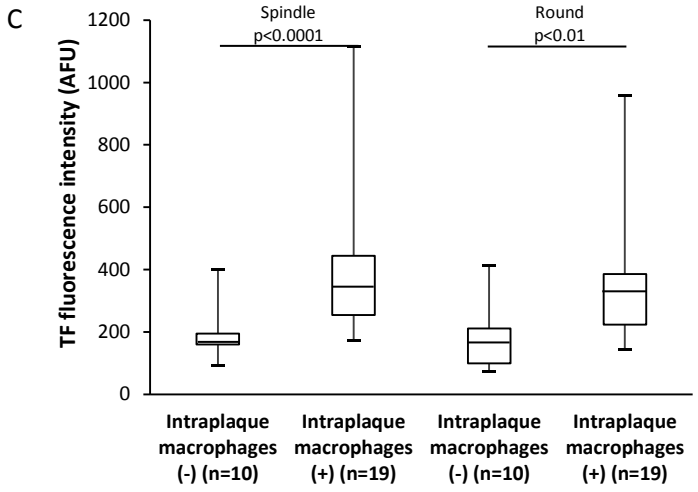

Figure 21: Correlation between TF levels in round and spindle MDMs and ruptured plaque (A), presence of thrombus (B) and intraplaque macrophages content (C).

6.6.3 MDM oxidative stress profile and plaque features analyzed by OCT

In order to highlight if existed some relationships between high oxidative stress levels observed in MDMs obtained *in vitro* and coronary plaque features detected in vivo by OCT, we analyzed possible association between these parameters. We observed that there was an association between GSH/GSSG and the presence of ruptured plaque (Figure 22A). Moreover, we showed that patients with high levels of HO-1 more frequently displayed a ruptured plaque (Figure 22B), a reduction in TCFA (Figure 22C) and presence of thrombus (Figure 22D). In addition, we observed a correlation between HO-1 levels in both MDM morphotypes with macrophage content (NSD) (Figure 22E) and max lipid arc (Figure 22F).

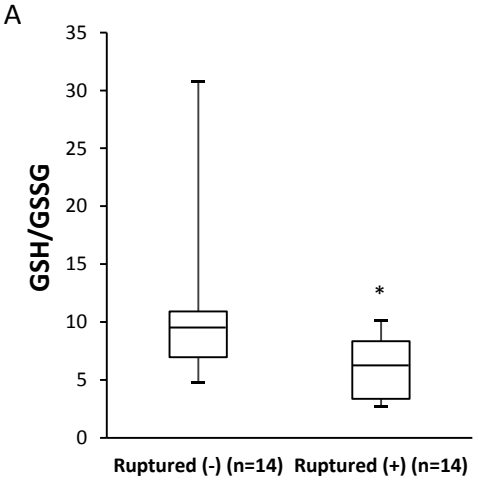

B

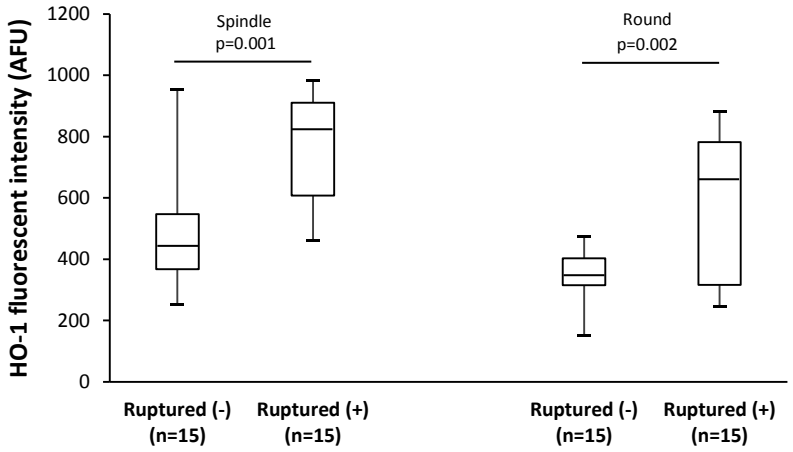
HO-1 fluorescent intensity (AFU)
1200
1000
800
600
400
200
0
Spindle
p=0.001
Round
p=0.002
Ruptured (-) (n=15)
Ruptured (+) (n=15)
Ruptured (-) (n=15)
Ruptured (+) (n=15)

C

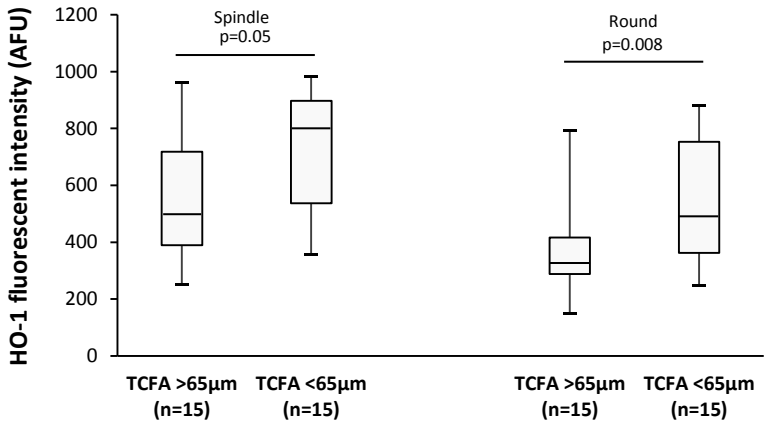
HO-1 fluorescent intensity (AFU)
1200
1000
800
600
400
200
0
Spindle
p=0.05
Round
p=0.008
TCFA >65µm (n=15)
TCFA <65µm (n=15)
TCFA >65µm (n=15)
TCFA <65µm (n=15)

D

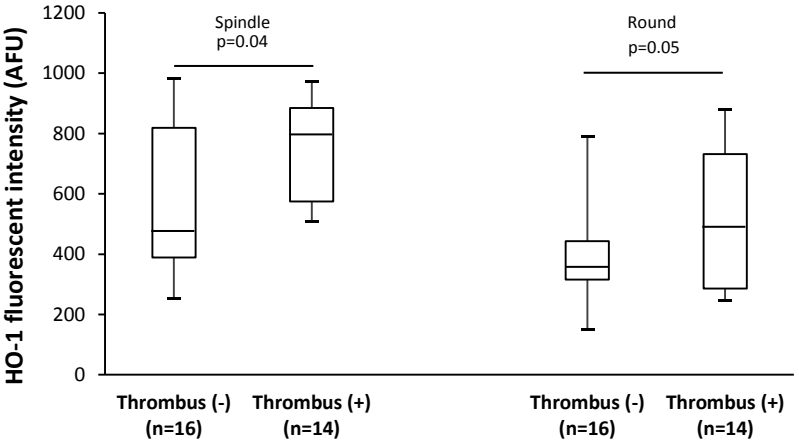
HO-1 fluorescent intensity (AFU)
1200
1000
800
600
400
200
0
Spindle
p=0.04
Round
p=0.05
Thrombus (-) (n=16)
Thrombus (+) (n=14)
Thrombus (-) (n=16)
Thrombus (+) (n=14)

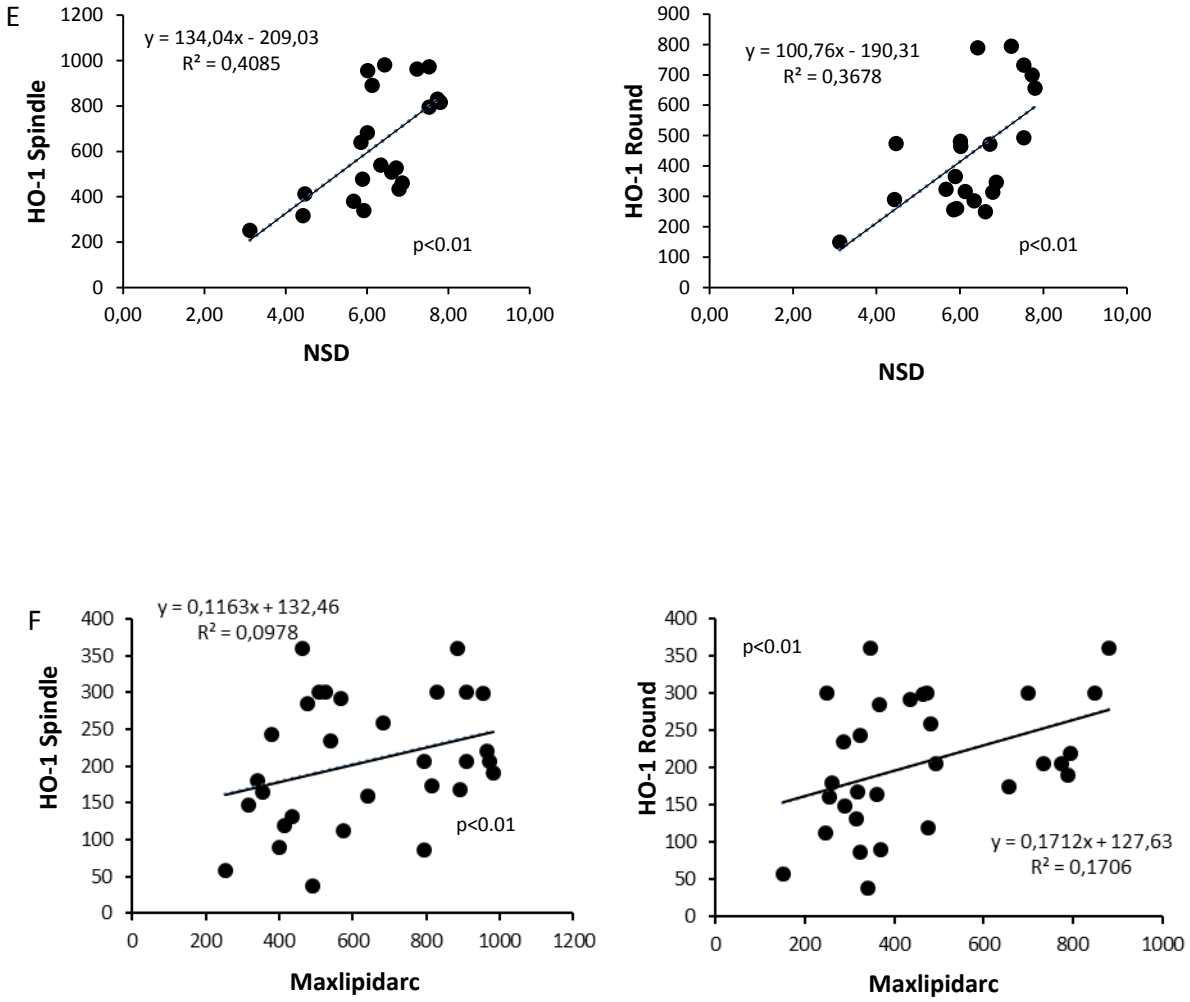

Figure 22: OCT plaque features and oxidative stress. Association between GSH/GSSG ratio and presence of ruptured plaque (* p<0.05) (A); association between HO-1 level and fibrous cap integrity (B), thin cap fibroatheroma (TCFA) (C), presence of thrombus (D); correlation between HO-1 levels in round and spindle MDM and macrophage content (E) and max lipid arc (F) detected by means OCT in *in vivo* plaque.

7. Discussion

Macrophages are instrumental to the atherogenic process and contribute to its initiation, progression and symptomatology. They comprise heterogeneous populations with several subtype having different, even opposite functions. This heterogeneity has been detected also in atherosclerotic plaque where the prevalence of a specific macrophage phenotype may have either harmful or beneficial function in the progression or stabilization of the plaque [238, 239]. Studies on tissue-resident macrophages are very challenging for the difficulties in macrophage isolation without affecting their viability. In addition, human coronary atherosclerotic plaque is a compartment not easy to obtain. Various *in vitro* models currently used to obtain macrophages as monocytic cell line exposed to differentiating agents do not, however, adequately reflect the heterogeneity and the plasticity of primary tissue macrophages [240], thus questioning whether deductions drawn by these approaches may be appropriate for tissue macrophages. Macrophages obtained from a spontaneous differentiation of monocytes isolated from peripheral blood are commonly accepted as a good surrogate of macrophages infiltrating tissue. On these bases, we have cultured monocytes for 7 days in a medium containing 10% of autologous serum to preserve the individual trait of each donor. A previous study from our group have demonstrated in MDMs obtained from healthy subjects, the presence of two dominant subsets different in morphology (spindle- or round-shaped) and in function [241]. Notably, these phenotypes exhibit a number of features that resemble M1 and M2 profile, with round MDMs showing functional traits reminiscent of the non-inflammatory and reparative M2 phenotype, whereas spindle MDMs exhibiting a pro-inflammatory profile and expressing genes driving lymphocyte activation. Based on this model, in the present study, we have characterized MDM morphotypes (round and spindle) in consecutive CAD patients, in order to delineate a biochemical and functional profile of different MDM morphotypes and their contribute in plaque instability.

In contrast to that observed in healthy subjects, who are characterized by a similar frequency of the two dominant morphotypes, spindle and round cells, MDMs obtained from CAD patients showed a prevalence of round ones.

Interestingly, the prevalence of round MDMs in CAD patients was grater, their efferocytic ability was reduced. Since in a previous study we have demonstrated that in healthy subjects round MDMs are better efferocytes than spindle [241], this observation suggests that CAD condition is

associated with a particular round phenotype exhibiting reduced anti-inflammatory properties compared to round MDMs of healthy subjects.

Atherosclerotic lesion is a complex, debris-rich microenvironment in which apoptosis rates are very high and engulfment mechanisms are continuously solicited. Therefore, blockage of efferocytosis has strong effects with a worsening of inflammation and increased atherosclerosis. It was demonstrated that the invalidation of only one pathway involved in efferocytic process leaded to a marked accumulation of apoptotic cells, even in early lesions, with the consequent increase of necrotic core and plaque growth [107, 242-244].

It is well known that, at atherosclerotic plaque level, efferocytosis is impaired and the efferocytic rate is related to atherosclerotic lesion stage [88]. In advanced atherosclerotic lesions the presence of inefficient mechanism for the removal of apoptotic cells by macrophages were documented by the occurrence of apoptotic debris in the extracellular compartment and the high numbers of free apoptotic cells [245]. Several factors may impaired the phagocytosis of apoptotic cells by macrophages in atherosclerotic plaque, including the cytoplasmic overload of apoptotic cells, the oxidative stress, the competitive inhibition by oxidized LDL for the same receptors on the macrophages [125].

Based on *in vivo* study on animal model, an additional mechanism mediated by TG2 was described [154, 246, 247]. TG2 is a protein-cross-linking enzyme expressed in endothelial cells and MDMs and its activity is needed for the formation of an efficient phagocyte during efferocytosis [106]. Accordingly, TG2 fundamentally impairs efferocytosis in macrophages, in part through the activation of latent TGF-β, which in turn facilitates efferocytosis [154, 248]. In addition, in the absence of TG2, the integrin β3 das not recognize correctly the apoptotic cell, the formation of “phagocyte portal” is less efficient and the portals that are formed take up the apoptotic cells at a slower rate [154]. Moreover, in a recent paper, we have demonstrated that the inhibition of TG2 in MDMs reduces the efferocytosis via mechanisms involving CD14 and SR-AI, receptors involved in the tether and uptake of apoptotic cell, respectively [153]. This observation suggests that a mechanism of cross-talk among efferocytic pathways exists and that the deletion of critical players impact the phagocytosis also via other receptors [249]. In the present study we found that TG2 was more expressed in round than spindle MDMs of healthy subjects, supporting the notion that round MDMs are mainly involved in efferocytosis, as previously described [241]. In CAD patients, a marked reduction of TG2 levels respect to healthy

subjects is observed, indicating that the lower efferocytosis observed in CAD may be in part related to TG2 expression. Numerous regulators of efferocytosis pathways have been shown to exert strong effects on atherosclerosis progression [250] and the current knowledge on the several molecular mechanisms involved in efferocytosis, the different efferocyte subsets and their relationship with the immune system, require further investigation in order to highlight the determinants of plaque progression and plaque instability.

It is known that the accumulation of macrophage and apoptotic cells in atherosclerotic plaque favor rupture of fibrous cap, due to secretion of pro-inflammatory cytokines and proteolytic enzymes, and thrombus formation due to release of TF [251, 252]. High levels of TF are expressed in atherosclerotic plaque associated with both cellular and acellular regions [171, 253-256]. TF is the key element in the activation of the extrinsic pathway of the coagulation cascade and plays a critical role in atherosclerotic plaque thrombogenicity, as TF is needed for thrombin generation and subsequent thrombus formation. In line with these observations, unstable lesions contain more TF than stable lesions, mostly in macrophage-rich regions close to the necrotic core [171]. Moreover, Lee *et al.* have shown that TF was markedly expressed at the site of rupture in ACS patients, with a co-localization of TF with CD68 positive cells, suggesting that macrophages are the major source of TF in ruptured plaque [257]. However, TF was also expressed in SMC and extracellular space, indicating that it can be derived from other sources [171]. Furthermore, has been reported that TF expression in lipid-rich plaque was more than threefold compared with fibrous plaque and its activity in the acellular lipid core was mainly associated with apoptotic microparticles of monocytic and lymphocytic origin, suggesting a link between inflammation, apoptosis and thrombogenicity [258]. In addition, previous studies have shown that not only TF expressing monocytes but also TF plasma levels are higher in ACS than in SA patients [259-261]. It has been suggested that circulating TF may potentiate and propagate the thrombogenic stimulus represented by vessel wall-associated TF, resulting in the formation of larger and more stable thrombus, and it may bind cellular receptors, upregulating the inflammatory response [262, 263]. In our study, we show that MDMs obtained from CAD expressed higher TF levels compared to MDMs of healthy subjects and, as evidenced by immunocytochemical experiments, this protein is equally distributed between round and spindle cells in healthy subjects as well as in CAD patients. A progressive increase going from healthy subjects to SA and ACS patients was observed in TF expression with a peak in STEMI patients.

These findings indicate that TF expression may contribute to the severity of coronary syndrome triggering atherothrombosis. This enhanced antigenic expression of TF displayed a functional consequence in thrombin generation. Indeed, CAD patients showed a reduction in the lag time and in the time to peak with respect to healthy subjects with no change on the peak of thrombin generation or endogenous thrombin potential. The difference observed between patients and healthy subjects, suggests a potential greater contribution to thrombus formation in this patient setting. Taken together, these findings indicate that TF expression may contribute to the severity of coronary syndrome triggering atherothrombosis.

An increasing body of evidence have suggested that oxidative stress is closely associated with atherosclerotic progression and plaque instability [264, 265]. Oxidative stress is considered a major mechanism involved in endothelial dysfunction and ROS production is associated to the cardiovascular risk factors such as hypertension, diabetes, smoking, and dyslipidemia [266]. In artery wall ROS generation promotes and activates several pathological pathways involved in atherosclerosis, including lipids oxidation, expression of adhesion molecules, stimulation of SMC proliferation and migration, cell apoptosis, activation of metalloproteinase [267-270]. Accumulation of ROS in the cell induces irreversible damage of cellular component, as proteins, lipids, and DNA, generally leads to necrosis. To limit the impact of oxidative stress and to protect vital cellular components, cells activate several antioxidant systems and among them GSH is the most important endogenous antioxidant involved in the maintenance of intracellular redox balance. GSH depletion is a feature of many disease and several studies have evidenced an imbalance between GSH and GSSG in cardiovascular disease both in human [271] and in animal models [272]. Moreover, macrophages GSH levels are inversely related to oxidation of LDL [273]. In addition to the contribute of GSH depletion in atherosclerotic process, there is also evidence of GSH reduction in platelet in condition associated with increased risk of thrombosis [274]. The ratio between GSH/GSSG is commonly used as an indicator of oxidative status [275] and in accordance with the demonstration of a decrease of this ratio in whole blood of CAD patients [276] we have detected a progressive decrease of this oxidative stress marker in MDMs obtain from SA, NSTEMI and STEMI patients, respectively. Increase of oxidative stress activates several redox-sensitive signaling molecules pathways converging in the regulation of transcription factors including Nrf2, AP-1, NF-kB, HIF-1, which induce the expression of gene involved in the detoxification of oxidizing molecules to maintain cellular homeostasis. Nrf2 is a pleiotropic

transcription factor that regulate the expression of a numerous antioxidant proteins to induce cytoprotective responses to oxidative and electrophilic stress [277, 278]. Increasing evidence strengthens the antiatherogenic role of Nrf2 to preserve the vascular integrity and endothelial function, for example, sustaining the release of NO and protecting from apoptosis [279-285]. Moreover, the activation of Nrf2 protects the human coronary artery endothelial cells against oxidative challenge [286]. In macrophages has been demonstrated that the exposure to ox-LDL increase Nrf2 expression which indirectly safeguards the cells from ox-LDL-mediated injury via antioxidants and phase 2 enzyme induction [287]. The evidence that the absence of Nrf2 in mice high fat diet myeloid-derived macrophages increase foam cell formation and atherosclerosis progression, further support the protective role of Nrf2 in atherogenesis [288, 289]. Although substantial evidence sustains the antiatherogenic role of Nrf2-mediated signaling pathways, some authors have reported that Nrf2 deficiency in mice leads to decreased atherosclerotic lesion in Apo E null mice, suggesting its expression may play a pro-atherogenic role [290-292]. This effect could be related to increased levels of plasma non-HDL cholesterol, likely via enhanced lipogenesis [291, 293], upregulation of CD36 scavenger receptor with increase of lipid uptake and foam cells formation [291, 294], increased expression of IL-1α in macrophage which may induce monocyte migration to the lesion [292, 295]. The signaling pathways Nrf2-mediated are very complex and the specific conditions in which Nrf2 attenuates or stimulates atherosclerosis are unclear. It appears that the level of regulation upon these responses is important indeed the deletion of antioxidant genes as HO-1 results in exacerbation of atherosclerosis; in contrast, the deletion of Nrf2 transcription factor, reduces atherosclerosis progression [296]. In the present study, we have evidenced augmented levels of Nrf2 in MDMs of CAD patients respect to healthy subjects, with a significant increase in NSTEMI and STEMI patient. In healthy subjects, the levels of this transcription factor are very low and feeble fluorescence is detected in the cytosol of the cells. This is in line with its cytosolic localization in basal condition, where Nrf2 is associated to Keap-1protein, which induces its ubiquitination and proteasomal degradation. Activation of Nrf2 in response to stress signals implicates the dissociation from Keap-1 and the translocation into nucleus to explicate its transcriptional activity [297]. In addition, activation of Nrf2 in response to stress signals is dependent on mechanism that increase its stability, leading to its accumulation in the cells [298, 299]. In CAD patients, a marked increase of fluorescence intensity, localized predominantly into the nucleus

of MDMs, was detected, suggesting an increase in Nrf2 activity in patients in respect to healthy subjects. The increase in Nrf2 expression in CAD patients goes in parallel with the expression of HO-1. Among the Nrf2 target genes HO-1 is significantly expressed in all main cell types present in atherosclerotic plaque, as macrophages, endothelial cells, SMC [300, 301]. The important protective role of HO-1 against human atherosclerotic lesions has been emphatized in population genetic studies, which have evidenced that a polymorphism in the promoter region of human HO-1 gene is associated to susceptibility for atherosclerosis [302-304]. HO-1 deficiency is very rare in humans, but the autopsy case report of HO-1 deficient boy who exhibited hyperlipidemia, foam cells in the liver, fatty streak and fibrous plaque in the aorta, suggests the role of HO-1 against atherogenesis [305, 306]. It has been evidenced that HO-1 deficiency lead to high levels of circulating heme with damage to vascular endothelium [307], however, it is unclear if these effects can be only attributable to HO-1 deficiency.

In animal studies, HO-1 induction prevent vulnerable plaque formation reducing the necrotic core and the lipid content, and increasing SMC accumulation in the intima and the fibrous cap thickness [225]. Moreover, immunohistological studies on human atherosclerotic lesions showed that HO-1 is mainly expressed by macrophages/foam cells residing in the neointima. Also in our experimental conditions, macrophages express appreciable levels of this protein, which is present in both morphotypes, with higher levels in spindle cells in respect to round.

It is known that membrane lipid composition profoundly affects many cell functions and several studies have reported the numerous immunological effects of fatty acids [308]. In particular, in macrophages has been demonstrated that fatty acids modulates all the known defense mechanisms of these cells, including phagocytosis, cytokine production and antigen presentation [233, 309, 310]. Changes in fatty acid composition of cellular membranes may induce modification of the physical properties such as membrane fluidity that results in effects on cell signaling pathways and gene expression [308]. In particular, the degree of fatty acids insaturation in cell membrane modulates the membrane fluidity, which may influence phagocytosis in macrophages [311, 312]. The exposure to either linoleic acid or α-linolenic acid increased phagocytosis of E. coli by macrophage cell line and this increase has been linked to an augmentation in plasma membrane PUFA content [313]. In our study we have detected a reduction of efferocytosis in MDMs of CAD patients respect to healthy subjects and a positive correlation with MFI has been reported. However, no significant difference in fatty acids

composition was evidenced between CAD patients and healthy subjects. This discrepancy might be due to the exiguous number of patients analyzed, the influence of dietary regimens and the ongoing pharmacological treatments. It is known that diet is one of the major factor that influence the fatty acids composition of the cells, as well as the statin treatment can modulate the MFI and the DI [314]. Therefore, a positive correlation between GSH/GSSG ratio and MFI has been observed, suggesting that a condition of oxidative stress may alter the membrane fluidity with consequences in activation or deactivation of signaling pathways resulting in a reduced efferocytosis.

The identification of unstable plaque is a crucial point in risk stratifying patients for acute coronary event. OCT is an imaging modality that permits to identify high risk plaque *in vivo*. In fact, OCT allows high resolution imaging of coronary atherosclerotic plaque morphology and composition giving important information to recognize the vulnerable plaques at high risk of rupture, which could cause acute coronary events and sudden death. OCT is able to detect the sites of plaque vulnerability and distinguish the differences in plaque composition with high degree of sensibility and specificity compared to histopathology [315, 316]. In particular, through OCT it is possible visualize and quantify macrophage (NSD) [317] and lipids content [316], fibrous cap thickness [318] and the presence of ruptured plaques and intraluminal thrombi [319]. From autopsy studies, it is well known that the vulnerable plaque has certain peculiar characteristics including: thin fibrous cap (<65 µm) [320] large lipid pool and inflammatory contest with activated macrophages near the fibrous cap. Indeed, the majority (about 80%) of plaques that cause acute coronary syndromes have a point of rupture at the level of an inflamed thin fibrous cap [321, 322].

Several *in vivo* studies have demonstrated the relationship between plaque morphology analyzed by OCT and patient outcome. In particular, it was observed that acute CAD patient present more frequently a lipid plaque [323], a ruptured plaque [324], a TCFA [324] and presence of thrombi [323]. Moreover, Tearney also observed that acute CAD patients presented atherosclerotic plaques with higher macrophage density compared to the plaques of SA patients. On contrary, fibrous and calcific plaques were more frequently in SA in respect to acute CAD patients [324]. According to these observations, in our study we found that acute patients present more frequently a lipid plaque with a thin cap fibroatheroma, a ruptured plaque, and the presence of thrombus with respect to SA patients. Moreover, acute patients present plaques

with grater lipid and higher macrophage contents compared to those of SA. On contrary, SA patients present more frequently a fibrous and calcific plaque in respect to acute patients.

As previously mentioned, inside atherosclerotic plaque macrophages are an heterogeneous population in term of morphology and function [238] and the prevalence of a specific morphotype could influence the progression and/or regression of the disease [239]. In our study, we found that the prevalence of round morphotype in MDMs obtained from CAD patients is associated with the presence of vulnerable plaque analyzed by OCT. In particular, the prevalence of round morphotype is associated with the presence of TCFA, lipid plaque, high presence of intra-plaque macrophages, ruptured plaque, and presence of thrombus. In addition, a positive correlation between NSD and round MDMs was found. The extended lipid core of vulnerable plaque is highly thrombogenic for the presence of cells as macrophages, monocytes, SMC, that upon activation, express high levels of TF. It has been reported that TF expression in lipid-rich plaque was more than threefold compared with fibrous plaque and its activity in the acellular lipid core was mainly associated with apoptotic microparticles of monocytic and lymphocytic origin, suggesting a link between inflammation, apoptosis and thrombogenicity [258]. Moreover, unstable lesions contain more TF than stable lesions, mostly in macrophage-rich regions close to the necrotic core [258]. Furthermore, it was observed that macrophage-derived foam cells in atherosclerotic plaque expressed TF and his expression was increased in lipid-rich plaque compared with fibrous plaque [258, 325]. Accordingly, we found that the high TF levels in round and spindle MDMs of CAD patients are associate with high intra-plaque macrophages content, presence of ruptured plaque, and thrombus formation at OCT investigation. This is in line with the observation that TF levels are higher in atheroma from patients with unstable angina than with SA [257]. TF is constitutively expressed by cells surrounding the vessel wall, including SMC and fibroblasts, but also in monocytes and macrophages in which a condition of oxidative stress may induce the expression of TF via NF-κB activation, an oxidative-stress sensitive transcription factor [326]. It is known that oxidative stress contribute to plaque vulnerability through the activation of several pathways as lipid oxidation, induction of MMP, expression of adhesion molecules and SMC proliferation and migration [267-270, 327]. According to this knowledge, we observed that patients that presented MDMs with high oxidative stress level, more frequently showed a ruptured plaque. It is also known that antioxidant molecules, such as HO-1 are expressed into atherosclerotic plaque, trying to avoid the oxidative damages. In fact, Cheng e*t al.*

have demonstrated that, in human carotid plaques, HO-1 is more present inside vulnerable plaque in respect to stable ones [225]. On this basis, it is proposed that the high expression of HO-1 detected in vulnerable plaque represent a compensatory atheroprotective response, in which HO-1 try prevent plaque instability by reducing lipid deposition and necrotic core expansion and by prolonging SMC survival in the fibrous cap [225]. Moreover, a previous paper has demonstrated that the HO-1 protein levels expressed on lymphocytes and monocytes isolated from patients at different CAD stages reflected the severity of the pathology angiographically detected, with a significant increase from SA to unstable and acute myocardial infarction [224, 328]. Accordingly, patients with highest levels of HO-1 in MDMs, more frequently show a vulnerable plaque characterized by a thin fibrous cap fibroatheroma, and increase in macrophage and lipid content. In addition, higher levels of HO-1 are detected in MDMs of patient with rupture plaque and with the presence of thrombus in respect to patients with non-ruptured plaque and without thrombus formation.

In summary, our study shows that MDMs of CAD patients have a peculiar morpho-phenotype profile, which is characterized by a predominance of round cells. MDMs of CAD patients showed differences in biochemical and functional signature compared to healthy subjects. In detail, they exhibit a reduced anti-inflammatory property evidenced by a less efferocytic capacity going in parallel with the decreased expression of TG2. Furthermore, MDMs of CAD patients display high propensity for thrombogenicity, characterized by the increase of TF levels resulting in a higher capacity to generate thrombin (Scheme 1).

Finally, we have demonstrated that CAD condition is characterized by an oxidative stress status not only at systemic levels but also in MDMs. In this cellular compartment, oxidative stress can modify some physicochemical properties of the lipid membrane with an alteration of its fluidity, feature important for an efficient phagocytosis process. Indeed, a positive correlation between membrane fluidity, expressed as MFI, and oxidative stress status, as well as MFI and capacity to engulf apoptotic cells, was found. This specific cellular profile detected in in vitro obtained MDMs is associated with the detection of high-risk and rupture-prone coronary plaques, at OCT investigation (Scheme 1).

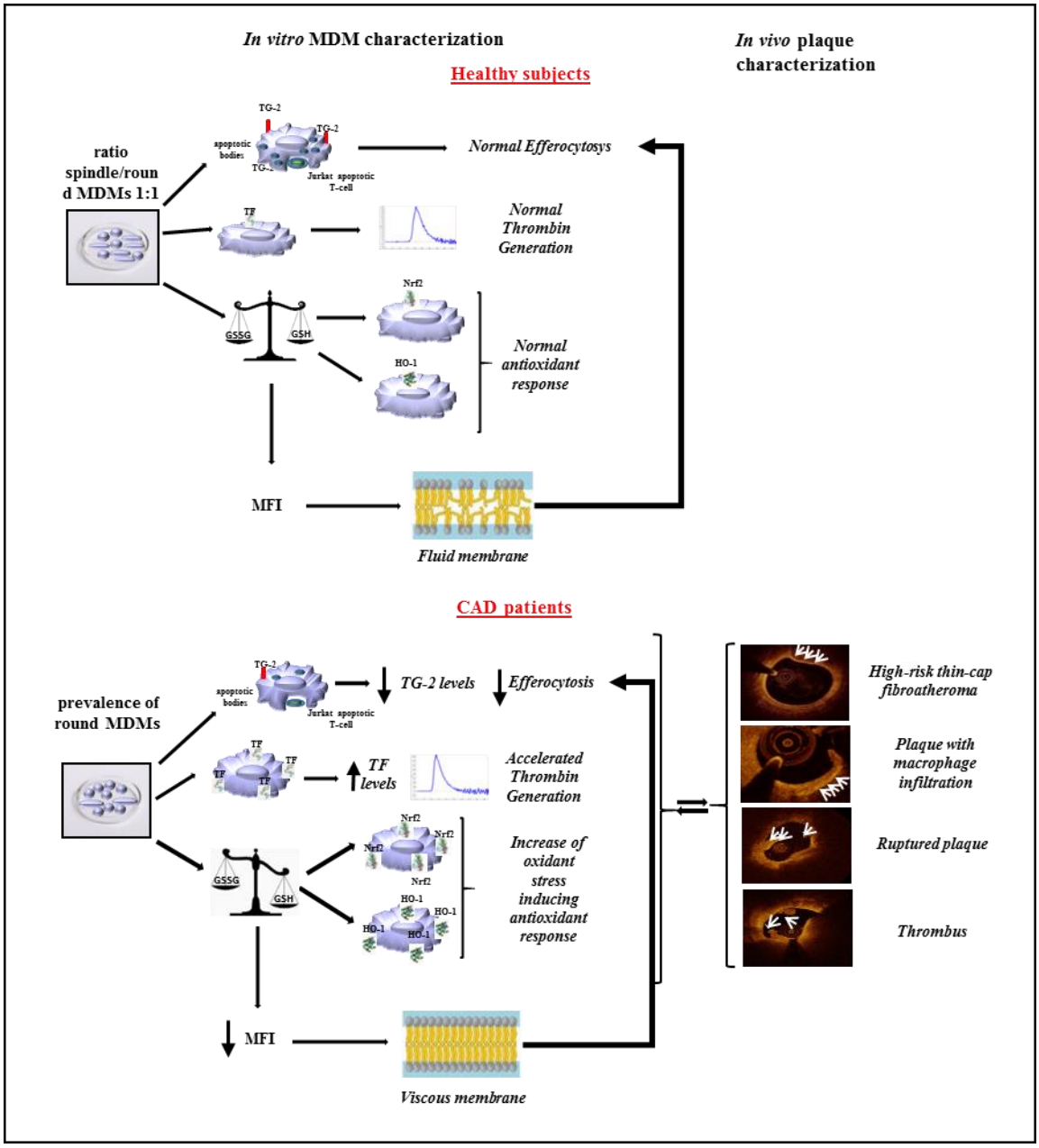

Scheme 1. MDMs biochemical and functional characteristics and OCT plaque features. TG2: transglutaminase 2; TF: tissue factor; GSSG: oxidized form of glutathione; GSH: reduced form of glutathione; Nrf2: nuclear factor erythroid 2–related factor 2; HO-1: heme oxygenase-1; MFI: membrane fluidity index.

Revealing the functional characteristics of individual macrophage phenotypes may lead to a better understanding of their contribution to coronary atherosclerosis. Different MDM phenotypes might be novel diagnostic and therapeutic target for a possible pharmacological treatment able to counteract the progression of atherosclerosis.

8. Future perspectives

Our study evidenced that macrophages obtained from spontaneous differentiation of monocytes isolated from peripheral blood of healthy subjects and patients with coronary disease (stable and instable) showed different biochemical and functional profiles. In particular, macrophages obtained from CAD patients presented reduced anti-inflammatory and increased pro-thrombotic proprieties in respect to those of healthy subjects. Moreover, this specific cellular profile detected in *in vitro* model was associated with high-risk and rupture-prone coronary plaques, at OCT investigation. These differences may derived from the characteristics of the environment in which they differentiate into macrophages, such as serum composition (i.e. cytokines and chemokines levels) or from a priming that monocytes receive into the blood stream that direct them to differentiate toward a pro-atherogenic phenotype. It is known that *in vivo* circulating monocytes are exposed to the systemic environment, including metabolic factors, such as dyslipidemia, and inflammatory molecules produced by other organs and tissues, and may thus be programmed to sustain the chronic inflammation related to atherosclerosis. So we will focus our attention on circulating monocytes in order to verify if they are able to mirror the profile of monocyte-derived macrophages and in this way to contribute to the progression of coronary atherosclerosis.

Circulating monocytes are a compartment easily obtainable and could represent a diagnostics and predictive marker and a therapeutic target for atherosclerotic disease. Therefore, a characterization of monocytes isolated from peripheral blood of healthy subjects and patients with stable angina or acute coronary syndrome may lead to better understanding their contribution to coronary disease. Hence, we will assess the genomic, proteomic, metabolomics and functional profile of these cells in relation to the clinic characteristics of enrolled population, the MDMs profile, the plaque morphology and the macrophage content of atherosclerotic lesion evaluated by OCT.

The monocytes signature may allow the better risk stratification and may permit the early prognosis. In addition, these results may help to identify monocyte markers able to predict the progression of the disease.

8. References

1. Hansson, G.K., *Inflammation, atherosclerosis, and coronary artery disease.* N Engl J Med, 2005. **352**(16): p. 1685-95.
2. Lakatta, E.G. and D. Levy, *Arterial and cardiac aging: major shareholders in cardiovascular disease enterprises: Part I: aging arteries: a "set up" for vascular disease.* Circulation, 2003. **107**(1): p. 139-46.
3. Mozaffarian, D., et al., *Heart Disease and Stroke Statistics-2016 Update: A Report From the American Heart Association.* Circulation, 2016. **133**(4): p. e38-360.
4. Perez-Lopez, F.R., et al., *Cardiovascular risk in menopausal women and prevalent related co-morbid conditions: facing the post-Women's Health Initiative era.* Fertil Steril, 2009. **92**(4): p. 1171-86.
5. Seshadri, S., et al., *Parental occurrence of stroke and risk of stroke in their children: the Framingham study.* Circulation, 2010. **121**(11): p. 1304-12.
6. Joseph, P., et al., *Reducing the Global Burden of Cardiovascular Disease, Part 1: The Epidemiology and Risk Factors.* Circ Res, 2017. **121**(6): p. 677-694.
7. Massaro, M., et al., *Nutraceuticals and prevention of atherosclerosis: focus on omega-3 polyunsaturated fatty acids and Mediterranean diet polyphenols.* Cardiovasc Ther, 2010. **28**(4): p. e13-9.
8. Zarate, A., et al., *Hypercholesterolemia As a Risk Factor for Cardiovascular Disease: Current Controversial Therapeutic Management.* Arch Med Res, 2016. **47**(7): p. 491-495.
9. van Rooy, M.J. and E. Pretorius, *Obesity, hypertension and hypercholesterolemia as risk factors for atherosclerosis leading to ischemic events.* Curr Med Chem, 2014. **21**(19): p. 2121-9.
10. Machii, R. and K. Saika, *Mortality attributable to tobacco by region based on the WHO Global Report.* Jpn J Clin Oncol, 2012. **42**(5): p. 464-5.
11. Messner, B. and D. Bernhard, *Smoking and cardiovascular disease: mechanisms of endothelial dysfunction and early atherogenesis.* Arterioscler Thromb Vasc Biol, 2014. **34**(3): p. 509-15.
12. Schmidt, A.M., et al., *Activation of receptor for advanced glycation end products: a mechanism for chronic vascular dysfunction in diabetic vasculopathy and atherosclerosis.* Circ Res, 1999. **84**(5): p. 489-97.
13. Keller, P.F., D. Carballo, and M. Roffi, *Diabetes and acute coronary syndrome.* Minerva Med, 2010. **101**(2): p. 81-104.
14. Tousoulis, D., et al., *Endothelial dysfunction: potential clinical implications.* Minerva Med, 2010. **101**(4): p. 271-84.
15. Zhang, D.X. and D.D. Gutterman, *Mitochondrial reactive oxygen species-mediated signaling in endothelial cells.* Am J Physiol Heart Circ Physiol, 2007. **292**(5): p. H2023-31.
16. Alp, N.J. and K.M. Channon, *Regulation of endothelial nitric oxide synthase by tetrahydrobiopterin in vascular disease.* Arterioscler Thromb Vasc Biol, 2004. **24**(3): p. 413-20.
17. Cooke, J.P., *Does ADMA cause endothelial dysfunction?* Arterioscler Thromb Vasc Biol, 2000. **20**(9): p. 2032-7.
18. Libby, P., *Inflammation in atherosclerosis.* Arterioscler Thromb Vasc Biol, 2012. **32**(9): p. 2045-51.
19. Moore, K.J. and I. Tabas, *Macrophages in the pathogenesis of atherosclerosis.* Cell, 2011. **145**(3): p. 341-55.
20. Libby, P., P.M. Ridker, and G.K. Hansson, *Progress and challenges in translating the biology of atherosclerosis.* Nature, 2011. **473**(7347): p. 317-25.
21. Johnson, J.L. and A.C. Newby, *Macrophage heterogeneity in atherosclerotic plaques.* Curr Opin Lipidol, 2009. **20**(5): p. 370-8.

22. Bobryshev, Y.V., *Monocyte recruitment and foam cell formation in atherosclerosis.* Micron, 2006. **37**(3): p. 208-22.
23. Hansson, G.K. and A. Hermansson, *The immune system in atherosclerosis.* Nat Immunol, 2011. **12**(3): p. 204-12.
24. Bentzon, J.F., et al., *Mechanisms of plaque formation and rupture.* Circ Res, 2014. **114**(12): p. 1852-66.
25. Stary, H.C., et al., *A definition of advanced types of atherosclerotic lesions and a histological classification of atherosclerosis. A report from the Committee on Vascular Lesions of the Council on Arteriosclerosis, American Heart Association.* Arterioscler Thromb Vasc Biol, 1995. **15**(9): p. 1512-31.
26. Townsend, N., et al., *Cardiovascular disease in Europe 2015: epidemiological update.* Eur Heart J, 2015. **36**(40): p. 2673-4.
27. Wong, N.D., *Epidemiological studies of CHD and the evolution of preventive cardiology.* Nat Rev Cardiol, 2014. **11**(5): p. 276-89.
28. Anderson, J.L., et al., *ACC/AHA 2007 guidelines for the management of patients with unstable angina/non-ST-Elevation myocardial infarction: a report of the American College of Cardiology/American Heart Association Task Force on Practice Guidelines (Writing Committee to Revise the 2002 Guidelines for the Management of Patients With Unstable Angina/Non-ST-Elevation Myocardial Infarction) developed in collaboration with the American College of Emergency Physicians, the Society for Cardiovascular Angiography and Interventions, and the Society of Thoracic Surgeons endorsed by the American Association of Cardiovascular and Pulmonary Rehabilitation and the Society for Academic Emergency Medicine.* J Am Coll Cardiol, 2007. **50**(7): p. e1-e157.
29. Kushner, F.G., et al., *2009 focused updates: ACC/AHA guidelines for the management of patients with ST-elevation myocardial infarction (updating the 2004 guideline and 2007 focused update) and ACC/AHA/SCAI guidelines on percutaneous coronary intervention (updating the 2005 guideline and 2007 focused update) a report of the American College of Cardiology Foundation/American Heart Association Task Force on Practice Guidelines.* J Am Coll Cardiol, 2009. **54**(23): p. 2205-41.
30. Wynn, T.A., A. Chawla, and J.W. Pollard, *Macrophage biology in development, homeostasis and disease.* Nature, 2013. **496**(7446): p. 445-55.
31. van Furth, R. and Z.A. Cohn, *The origin and kinetics of mononuclear phagocytes.* J Exp Med, 1968. **128**(3): p. 415-35.
32. Gentek, R., K. Molawi, and M.H. Sieweke, *Tissue macrophage identity and self-renewal.* Immunol Rev, 2014. **262**(1): p. 56-73.
33. Nerlov, C. and T. Graf, *PU.1 induces myeloid lineage commitment in multipotent hematopoietic progenitors.* Genes Dev, 1998. **12**(15): p. 2403-12.
34. Mossadegh-Keller, N., et al., *M-CSF instructs myeloid lineage fate in single haematopoietic stem cells.* Nature, 2013. **497**(7448): p. 239-43.
35. Varol, C., et al., *Monocytes give rise to mucosal, but not splenic, conventional dendritic cells.* J Exp Med, 2007. **204**(1): p. 171-80.
36. Passlick, B., D. Flieger, and H.W. Ziegler-Heitbrock, *Identification and characterization of a novel monocyte subpopulation in human peripheral blood.* Blood, 1989. **74**(7): p. 2527-34.
37. Ziegler-Heitbrock, L., et al., *Nomenclature of monocytes and dendritic cells in blood.* Blood, 2010. **116**(16): p. e74-80.
38. Kawanaka, N., et al., *CD14+,CD16+ blood monocytes and joint inflammation in rheumatoid arthritis.* Arthritis Rheum, 2002. **46**(10): p. 2578-86.

39. Poitou, C., et al., *CD14dimCD16+ and CD14+CD16+ monocytes in obesity and during weight loss: relationships with fat mass and subclinical atherosclerosis.* Arterioscler Thromb Vasc Biol, 2011. **31**(10): p. 2322-30.
40. Rothe, G., et al., *Peripheral blood mononuclear phagocyte subpopulations as cellular markers in hypercholesterolemia.* Arterioscler Thromb Vasc Biol, 1996. **16**(12): p. 1437-47.
41. Zeng, S., et al., *Monocyte subsets and monocyte-platelet aggregates in patients with unstable angina.* J Thromb Thrombolysis, 2014. **38**(4): p. 439-46.
42. Parihar, A., T.D. Eubank, and A.I. Doseff, *Monocytes and macrophages regulate immunity through dynamic networks of survival and cell death.* J Innate Immun, 2010. **2**(3): p. 204-15.
43. Ariel, A., et al., *Macrophages in inflammation and its resolution.* Front Immunol, 2012. **3**: p. 324.
44. Boyle, W.J., W.S. Simonet, and D.L. Lacey, *Osteoclast differentiation and activation.* Nature, 2003. **423**(6937): p. 337-42.
45. Hussell, T. and T.J. Bell, *Alveolar macrophages: plasticity in a tissue-specific context.* Nat Rev Immunol, 2014. **14**(2): p. 81-93.
46. Parkhurst, C.N., et al., *Microglia promote learning-dependent synapse formation through brain-derived neurotrophic factor.* Cell, 2013. **155**(7): p. 1596-609.
47. Eckert, C., et al., *The complex myeloid network of the liver with diverse functional capacity at steady state and in inflammation.* Front Immunol, 2015. **6**: p. 179.
48. Collin, M. and P. Milne, *Langerhans cell origin and regulation.* Curr Opin Hematol, 2016. **23**(1): p. 28-35.
49. Kurotaki, D., T. Uede, and T. Tamura, *Functions and development of red pulp macrophages.* Microbiol Immunol, 2015. **59**(2): p. 55-62.
50. Aichele, P., et al., *Macrophages of the splenic marginal zone are essential for trapping of blood-borne particulate antigen but dispensable for induction of specific T cell responses.* J Immunol, 2003. **171**(3): p. 1148-55.
51. Chow, A., et al., *Bone marrow CD169+ macrophages promote the retention of hematopoietic stem and progenitor cells in the mesenchymal stem cell niche.* J Exp Med, 2011. **208**(2): p. 261-71.
52. Muller, P.A., et al., *Crosstalk between Muscularis Macrophages and Enteric Neurons Regulates Gastrointestinal Motility.* Cell, 2014. **158**(5): p. 1210.
53. Martinez, F.O. and S. Gordon, *The M1 and M2 paradigm of macrophage activation: time for reassessment.* F1000Prime Rep, 2014. **6**: p. 13.
54. Sica, A. and A. Mantovani, *Macrophage plasticity and polarization: in vivo veritas.* J Clin Invest, 2012. **122**(3): p. 787-95.
55. Benoit, M., B. Desnues, and J.L. Mege, *Macrophage polarization in bacterial infections.* J Immunol, 2008. **181**(6): p. 3733-9.
56. Gordon, S., *Alternative activation of macrophages.* Nat Rev Immunol, 2003. **3**(1): p. 23-35.
57. Novak, M.L. and T.J. Koh, *Macrophage phenotypes during tissue repair.* J Leukoc Biol, 2013. **93**(6): p. 875-81.
58. Martinez, F.O., et al., *Macrophage activation and polarization.* Front Biosci, 2008. **13**: p. 453-61.
59. Zizzo, G., et al., *Efficient clearance of early apoptotic cells by human macrophages requires M2c polarization and MerTK induction.* J Immunol, 2012. **189**(7): p. 3508-20.
60. Pinhal-Enfield, G., et al., *An angiogenic switch in macrophages involving synergy between Toll-like receptors 2, 4, 7, and 9 and adenosine A(2A) receptors.* Am J Pathol, 2003. **163**(2): p. 711-21.
61. Galkina, E. and K. Ley, *Leukocyte influx in atherosclerosis.* Curr Drug Targets, 2007. **8**(12): p. 1239-48.

62. Lusis, A.J., *Atherosclerosis.* Nature, 2000. **407**(6801): p. 233-41.
63. Cybulsky, M.I., et al., *A major role for VCAM-1, but not ICAM-1, in early atherosclerosis.* J Clin Invest, 2001. **107**(10): p. 1255-62.
64. Huo, Y., A. Hafezi-Moghadam, and K. Ley, *Role of vascular cell adhesion molecule-1 and fibronectin connecting segment-1 in monocyte rolling and adhesion on early atherosclerotic lesions.* Circ Res, 2000. **87**(2): p. 153-9.
65. Gerszten, R.E., et al., *MCP-1 and IL-8 trigger firm adhesion of monocytes to vascular endothelium under flow conditions.* Nature, 1999. **398**(6729): p. 718-23.
66. Simionescu, M., *Cellular dysfunction in inflammatory-related vascular disorders' review series. The inflammatory process: a new dimension of a 19 century old story.* J Cell Mol Med, 2009. **13**(11-12): p. 4291-2.
67. Butcher, M.J. and E.V. Galkina, *Phenotypic and functional heterogeneity of macrophages and dendritic cell subsets in the healthy and atherosclerosis-prone aorta.* Front Physiol, 2012. **3**: p. 44.
68. Mosser, D.M. and J.P. Edwards, *Exploring the full spectrum of macrophage activation.* Nat Rev Immunol, 2008. **8**(12): p. 958-69.
69. Khallou-Laschet, J., et al., *Macrophage plasticity in experimental atherosclerosis.* PLoS One, 2010. **5**(1): p. e8852.
70. Stoger, J.L., et al., *Distribution of macrophage polarization markers in human atherosclerosis.* Atherosclerosis, 2012. **225**(2): p. 461-8.
71. Takahashi, K., M. Takeya, and N. Sakashita, *Multifunctional roles of macrophages in the development and progression of atherosclerosis in humans and experimental animals.* Med Electron Microsc, 2002. **35**(4): p. 179-203.
72. Goldstein, J.L., et al., *Binding site on macrophages that mediates uptake and degradation of acetylated low density lipoprotein, producing massive cholesterol deposition.* Proc Natl Acad Sci U S A, 1979. **76**(1): p. 333-7.
73. de Villiers, W.J. and E.J. Smart, *Macrophage scavenger receptors and foam cell formation.* J Leukoc Biol, 1999. **66**(5): p. 740-6.
74. Van Berkel, T.J., et al., *Scavenger receptor classes A and B. Their roles in atherogenesis and the metabolism of modified LDL and HDL.* Ann N Y Acad Sci, 2000. **902**: p. 113-26; discussion 126-7.
75. Kita, T., et al., *Role of oxidized LDL in atherosclerosis.* Ann N Y Acad Sci, 2001. **947**: p. 199-205; discussion 205-6.
76. Jenkins, S.J., et al., *Local macrophage proliferation, rather than recruitment from the blood, is a signature of TH2 inflammation.* Science, 2011. **332**(6035): p. 1284-8.
77. Yui, S., et al., *Induction of murine macrophage growth by modified LDLs.* Arterioscler Thromb, 1993. **13**(3): p. 331-7.
78. Hamilton, J.A., et al., *Oxidized LDL can induce macrophage survival, DNA synthesis, and enhanced proliferative response to CSF-1 and GM-CSF.* Arterioscler Thromb Vasc Biol, 1999. **19**(1): p. 98-105.
79. Hamilton, J.A., G. Whitty, and W. Jessup, *Oxidized LDL can promote human monocyte survival.* Arterioscler Thromb Vasc Biol, 2000. **20**(10): p. 2329-31.
80. Sakai, M., et al., *Lysophosphatidylcholine plays an essential role in the mitogenic effect of oxidized low density lipoprotein on murine macrophages.* J Biol Chem, 1994. **269**(50): p. 31430-5.
81. Martens, J.S., et al., *A modification of apolipoprotein B accounts for most of the induction of macrophage growth by oxidized low density lipoprotein.* J Biol Chem, 1999. **274**(16): p. 10903-10.

82. Matsumura, T., et al., *Two intracellular signaling pathways for activation of protein kinase C are involved in oxidized low-density lipoprotein-induced macrophage growth.* Arterioscler Thromb Vasc Biol, 1997. **17**(11): p. 3013-20.
83. Rajavashisth, T.B., et al., *Induction of endothelial cell expression of granulocyte and macrophage colony-stimulating factors by modified low-density lipoproteins.* Nature, 1990. **344**(6263): p. 254-7.
84. Andres, V., O.M. Pello, and C. Silvestre-Roig, *Macrophage proliferation and apoptosis in atherosclerosis.* Curr Opin Lipidol, 2012. **23**(5): p. 429-38.
85. Bjorkerud, S. and B. Bjorkerud, *Apoptosis is abundant in human atherosclerotic lesions, especially in inflammatory cells (macrophages and T cells), and may contribute to the accumulation of gruel and plaque instability.* Am J Pathol, 1996. **149**(2): p. 367-80.
86. Kolodgie, F.D., et al., *Localization of apoptotic macrophages at the site of plaque rupture in sudden coronary death.* Am J Pathol, 2000. **157**(4): p. 1259-68.
87. Mallat, Z. and A. Tedgui, *Apoptosis in the vasculature: mechanisms and functional importance.* Br J Pharmacol, 2000. **130**(5): p. 947-62.
88. Tabas, I., *Consequences and therapeutic implications of macrophage apoptosis in atherosclerosis: the importance of lesion stage and phagocytic efficiency.* Arterioscler Thromb Vasc Biol, 2005. **25**(11): p. 2255-64.
89. Tricot, O., et al., *Relation between endothelial cell apoptosis and blood flow direction in human atherosclerotic plaques.* Circulation, 2000. **101**(21): p. 2450-3.
90. Clarke, M.C., et al., *Apoptosis of vascular smooth muscle cells induces features of plaque vulnerability in atherosclerosis.* Nat Med, 2006. **12**(9): p. 1075-80.
91. Szondy, Z., et al., *Anti-inflammatory Mechanisms Triggered by Apoptotic Cells during Their Clearance.* Front Immunol, 2017. **8**: p. 909.
92. Michlewska, S., et al., *Macrophage phagocytosis of apoptotic neutrophils is critically regulated by the opposing actions of pro-inflammatory and anti-inflammatory agents: key role for TNF-alpha.* FASEB J, 2009. **23**(3): p. 844-54.
93. Medina, C.B. and K.S. Ravichandran, *Do not let death do us part: 'find-me' signals in communication between dying cells and the phagocytes.* Cell Death Differ, 2016. **23**(6): p. 979-89.
94. Truman, L.A., et al., *CX3CL1/fractalkine is released from apoptotic lymphocytes to stimulate macrophage chemotaxis.* Blood, 2008. **112**(13): p. 5026-36.
95. Lauber, K., et al., *Apoptotic cells induce migration of phagocytes via caspase-3-mediated release of a lipid attraction signal.* Cell, 2003. **113**(6): p. 717-30.
96. Gude, D.R., et al., *Apoptosis induces expression of sphingosine kinase 1 to release sphingosine-1-phosphate as a "come-and-get-me" signal.* FASEB J, 2008. **22**(8): p. 2629-38.
97. Johann, A.M., et al., *Apoptotic cell-derived sphingosine-1-phosphate promotes HuR-dependent cyclooxygenase-2 mRNA stabilization and protein expression.* J Immunol, 2008. **180**(2): p. 1239-48.
98. Chekeni, F.B., et al., *Pannexin 1 channels mediate 'find-me' signal release and membrane permeability during apoptosis.* Nature, 2010. **467**(7317): p. 863-7.
99. Elliott, M.R., et al., *Nucleotides released by apoptotic cells act as a find-me signal to promote phagocytic clearance.* Nature, 2009. **461**(7261): p. 282-6.
100. Marques-da-Silva, C., et al., *Purinergic receptor agonists modulate phagocytosis and clearance of apoptotic cells in macrophages.* Immunobiology, 2011. **216**(1-2): p. 1-11.
101. Park, D., et al., *BAI1 is an engulfment receptor for apoptotic cells upstream of the ELMO/Dock180/Rac module.* Nature, 2007. **450**(7168): p. 430-4.
102. Freeman, G.J., et al., *TIM genes: a family of cell surface phosphatidylserine receptors that regulate innate and adaptive immunity.* Immunol Rev, 2010. **235**(1): p. 172-89.

103. Voss, O.H., et al., *Emerging role of CD300 receptors in regulating myeloid cell efferocytosis.* Mol Cell Oncol, 2015. **2**(4): p. e964625.
104. Simhadri, V.R., et al., *Human CD300a binds to phosphatidylethanolamine and phosphatidylserine, and modulates the phagocytosis of dead cells.* Blood, 2012. **119**(12): p. 2799-809.
105. Tian, L., et al., *p85alpha recruitment by the CD300f phosphatidylserine receptor mediates apoptotic cell clearance required for autoimmunity suppression.* Nat Commun, 2014. **5**: p. 3146.
106. Hanayama, R., et al., *Identification of a factor that links apoptotic cells to phagocytes.* Nature, 2002. **417**(6885): p. 182-7.
107. Ait-Oufella, H., et al., *Defective mer receptor tyrosine kinase signaling in bone marrow cells promotes apoptotic cell accumulation and accelerates atherosclerosis.* Arterioscler Thromb Vasc Biol, 2008. **28**(8): p. 1429-31.
108. Henson, P.M., D.L. Bratton, and V.A. Fadok, *Apoptotic cell removal.* Curr Biol, 2001. **11**(19): p. R795-805.
109. Febbraio, M., D.P. Hajjar, and R.L. Silverstein, *CD36: a class B scavenger receptor involved in angiogenesis, atherosclerosis, inflammation, and lipid metabolism.* J Clin Invest, 2001. **108**(6): p. 785-91.
110. Orr, A.W., et al., *Low density lipoprotein receptor-related protein is a calreticulin coreceptor that signals focal adhesion disassembly.* J Cell Biol, 2003. **161**(6): p. 1179-89.
111. Moffatt, O.D., et al., *Macrophage recognition of ICAM-3 on apoptotic leukocytes.* J Immunol, 1999. **162**(11): p. 6800-10.
112. Devitt, A., et al., *Human CD14 mediates recognition and phagocytosis of apoptotic cells.* Nature, 1998. **392**(6675): p. 505-9.
113. Kojima, Y., et al., *CD47-blocking antibodies restore phagocytosis and prevent atherosclerosis.* Nature, 2016. **536**(7614): p. 86-90.
114. Ridley, A.J., *Rho family proteins: coordinating cell responses.* Trends Cell Biol, 2001. **11**(12): p. 471-7.
115. Tosello-Trampont, A.C., K. Nakada-Tsukui, and K.S. Ravichandran, *Engulfment of apoptotic cells is negatively regulated by Rho-mediated signaling.* J Biol Chem, 2003. **278**(50): p. 49911-9.
116. Erwig, L.P., et al., *Differential regulation of phagosome maturation in macrophages and dendritic cells mediated by Rho GTPases and ezrin-radixin-moesin (ERM) proteins.* Proc Natl Acad Sci U S A, 2006. **103**(34): p. 12825-30.
117. Kinchen, J.M. and K.S. Ravichandran, *Phagosome maturation: going through the acid test.* Nat Rev Mol Cell Biol, 2008. **9**(10): p. 781-95.
118. Nakaya, M., et al., *Opposite effects of rho family GTPases on engulfment of apoptotic cells by macrophages.* J Biol Chem, 2006. **281**(13): p. 8836-42.
119. Han, C.Z. and K.S. Ravichandran, *Metabolic connections during apoptotic cell engulfment.* Cell, 2011. **147**(7): p. 1442-5.
120. Kiss, R.S., et al., *Apoptotic cells induce a phosphatidylserine-dependent homeostatic response from phagocytes.* Curr Biol, 2006. **16**(22): p. 2252-8.
121. Hsu, C.L., et al., *Equilibrative nucleoside transporter 3 deficiency perturbs lysosome function and macrophage homeostasis.* Science, 2012. **335**(6064): p. 89-92.
122. Park, D., et al., *Continued clearance of apoptotic cells critically depends on the phagocyte Ucp2 protein.* Nature, 2011. **477**(7363): p. 220-4.
123. Fond, A.M., et al., *Apoptotic cells trigger a membrane-initiated pathway to increase ABCA1.* J Clin Invest, 2015. **125**(7): p. 2748-58.

124. Maderna, P. and C. Godson, *Phagocytosis of apoptotic cells and the resolution of inflammation.* Biochim Biophys Acta, 2003. **1639**(3): p. 141-51.
125. Schrijvers, D.M., et al., *Phagocytosis of apoptotic cells by macrophages is impaired in atherosclerosis.* Arterioscler Thromb Vasc Biol, 2005. **25**(6): p. 1256-61.
126. Tabas, I., *Apoptosis and efferocytosis in mouse models of atherosclerosis.* Curr Drug Targets, 2007. **8**(12): p. 1288-96.
127. Tabas, I., *Macrophage apoptosis in atherosclerosis: consequences on plaque progression and the role of endoplasmic reticulum stress.* Antioxid Redox Signal, 2009. **11**(9): p. 2333-9.
128. Bird, D.A., et al., *Receptors for oxidized low-density lipoprotein on elicited mouse peritoneal macrophages can recognize both the modified lipid moieties and the modified protein moieties: implications with respect to macrophage recognition of apoptotic cells.* Proc Natl Acad Sci U S A, 1999. **96**(11): p. 6347-52.
129. Chang, M.K., et al., *Monoclonal antibodies against oxidized low-density lipoprotein bind to apoptotic cells and inhibit their phagocytosis by elicited macrophages: evidence that oxidation-specific epitopes mediate macrophage recognition.* Proc Natl Acad Sci U S A, 1999. **96**(11): p. 6353-8.
130. Palinski, W., et al., *Increased autoantibody titers against epitopes of oxidized LDL in LDL receptor-deficient mice with increased atherosclerosis.* Arterioscler Thromb Vasc Biol, 1995. **15**(10): p. 1569-76.
131. Shaw, P.X., et al., *Human-derived anti-oxidized LDL autoantibody blocks uptake of oxidized LDL by macrophages and localizes to atherosclerotic lesions in vivo.* Arterioscler Thromb Vasc Biol, 2001. **21**(8): p. 1333-9.
132. Kadl, A., et al., *Apoptotic cells as sources for biologically active oxidized phospholipids.* Antioxid Redox Signal, 2004. **6**(2): p. 311-20.
133. Moller, W., et al., *Ultrafine particles cause cytoskeletal dysfunctions in macrophages.* Toxicol Appl Pharmacol, 2002. **182**(3): p. 197-207.
134. Ishimoto, Y., et al., *Promotion of the uptake of PS liposomes and apoptotic cells by a product of growth arrest-specific gene, gas6.* J Biochem, 2000. **127**(3): p. 411-7.
135. Roos, A., et al., *Mini-review: A pivotal role for innate immunity in the clearance of apoptotic cells.* Eur J Immunol, 2004. **34**(4): p. 921-9.
136. Mallat, Z., et al., *Shed membrane microparticles with procoagulant potential in human atherosclerotic plaques: a role for apoptosis in plaque thrombogenicity.* Circulation, 1999. **99**(3): p. 348-53.
137. Park, D., S.S. Choi, and K.S. Ha, *Transglutaminase 2: a multi-functional protein in multiple subcellular compartments.* Amino Acids, 2010. **39**(3): p. 619-31.
138. Klock, C., T.R. Diraimondo, and C. Khosla, *Role of transglutaminase 2 in celiac disease pathogenesis.* Semin Immunopathol, 2012. **34**(4): p. 513-22.
139. Martin, A., et al., *Possible involvement of transglutaminase-catalyzed reactions in the physiopathology of neurodegenerative diseases.* Amino Acids, 2013. **44**(1): p. 111-8.
140. Nakaoka, H., et al., *Gh: a GTP-binding protein with transglutaminase activity and receptor signaling function.* Science, 1994. **264**(5165): p. 1593-6.
141. Vezza, R., A. Habib, and G.A. FitzGerald, *Differential signaling by the thromboxane receptor isoforms via the novel GTP-binding protein, Gh.* J Biol Chem, 1999. **274**(18): p. 12774-9.
142. Baek, K.J., et al., *Oxytocin receptor couples to the 80 kDa Gh alpha family protein in human myometrium.* Biochem J, 1996. **315 (Pt 3)**: p. 739-44.
143. Feng, J.F., et al., *Calreticulin down-regulates both GTP binding and transglutaminase activities of transglutaminase II.* Biochemistry, 1999. **38**(33): p. 10743-9.

144. Nakano, Y., J. Forsprecher, and M.T. Kaartinen, *Regulation of ATPase activity of transglutaminase 2 by MT1-MMP: implications for mineralization of MC3T3-E1 osteoblast cultures.* J Cell Physiol, 2010. **223**(1): p. 260-9.
145. Hasegawa, G., et al., *A novel function of tissue-type transglutaminase: protein disulphide isomerase.* Biochem J, 2003. **373**(Pt 3): p. 793-803.
146. Malorni, W., et al., *The adenine nucleotide translocator 1 acts as a type 2 transglutaminase substrate: implications for mitochondrial-dependent apoptosis.* Cell Death Differ, 2009. **16**(11): p. 1480-92.
147. Mishra, S. and L.J. Murphy, *Tissue transglutaminase has intrinsic kinase activity: identification of transglutaminase 2 as an insulin-like growth factor-binding protein-3 kinase.* J Biol Chem, 2004. **279**(23): p. 23863-8.
148. Wang, Z. and M. Griffin, *TG2, a novel extracellular protein with multiple functions.* Amino Acids, 2012. **42**(2-3): p. 939-49.
149. Pinkas, D.M., et al., *Transglutaminase 2 undergoes a large conformational change upon activation.* PLoS Biol, 2007. **5**(12): p. e327.
150. Sane, D.C., J.L. Kontos, and C.S. Greenberg, *Roles of transglutaminases in cardiac and vascular diseases.* Front Biosci, 2007. **12**: p. 2530-45.
151. Greenberg, C.S., P.J. Birckbichler, and R.H. Rice, *Transglutaminases: multifunctional cross-linking enzymes that stabilize tissues.* FASEB J, 1991. **5**(15): p. 3071-7.
152. Rebe, C., et al., *Induction of transglutaminase 2 by a liver X receptor/retinoic acid receptor alpha pathway increases the clearance of apoptotic cells by human macrophages.* Circ Res, 2009. **105**(4): p. 393-401.
153. Eligini, S., et al., *Inhibition of transglutaminase 2 reduces efferocytosis in human macrophages: Role of CD14 and SR-AI receptors.* Nutr Metab Cardiovasc Dis, 2016. **26**(10): p. 922-30.
154. Toth, B., et al., *Transglutaminase 2 is needed for the formation of an efficient phagocyte portal in macrophages engulfing apoptotic cells.* J Immunol, 2009. **182**(4): p. 2084-92.
155. Falasca, L., et al., *Transglutaminase type II is a key element in the regulation of the anti-inflammatory response elicited by apoptotic cell engulfment.* J Immunol, 2005. **174**(11): p. 7330-40.
156. Muller, Y.A., M.H. Ultsch, and A.M. de Vos, *The crystal structure of the extracellular domain of human tissue factor refined to 1.7 A resolution.* J Mol Biol, 1996. **256**(1): p. 144-59.
157. Carson, S.D. and J.P. Brozna, *The role of tissue factor in the production of thrombin.* Blood Coagul Fibrinolysis, 1993. **4**(2): p. 281-92.
158. Drake, T.A., J.H. Morrissey, and T.S. Edgington, *Selective cellular expression of tissue factor in human tissues. Implications for disorders of hemostasis and thrombosis.* Am J Pathol, 1989. **134**(5): p. 1087-97.
159. Mackman, N., et al., *Murine tissue factor gene expression in vivo. Tissue and cell specificity and regulation by lipopolysaccharide.* Am J Pathol, 1993. **143**(1): p. 76-84.
160. Fleck, R.A., et al., *Localization of human tissue factor antigen by immunostaining with monospecific, polyclonal anti-human tissue factor antibody.* Thromb Res, 1990. **59**(2): p. 421-37.
161. Wood, J.P., et al., *Tissue factor pathway inhibitor-alpha inhibits prothrombinase during the initiation of blood coagulation.* Proc Natl Acad Sci U S A, 2013. **110**(44): p. 17838-43.
162. Broze, G.J., Jr., T.J. Girard, and W.F. Novotny, *Regulation of coagulation by a multivalent Kunitz-type inhibitor.* Biochemistry, 1990. **29**(33): p. 7539-46.
163. Bugge, T.H., et al., *Fatal embryonic bleeding events in mice lacking tissue factor, the cell-associated initiator of blood coagulation.* Proc Natl Acad Sci U S A, 1996. **93**(13): p. 6258-63.

164. Bazan, J.F., *Structural design and molecular evolution of a cytokine receptor superfamily.* Proc Natl Acad Sci U S A, 1990. **87**(18): p. 6934-8.
165. Camerer, E., et al., *Coagulation factors VIIa and Xa induce cell signaling leading to up-regulation of the egr-1 gene.* J Biol Chem, 1999. **274**(45): p. 32225-33.
166. Riewald, M. and W. Ruf, *Orchestration of coagulation protease signaling by tissue factor.* Trends Cardiovasc Med, 2002. **12**(4): p. 149-54.
167. Owens, A.P., 3rd and N. Mackman, *Sources of tissue factor that contribute to thrombosis after rupture of an atherosclerotic plaque.* Thromb Res, 2012. **129 Suppl 2**: p. S30-3.
168. Mackman, N., *Triggers, targets and treatments for thrombosis.* Nature, 2008. **451**(7181): p. 914-8.
169. Hatakeyama, K., et al., *Localization and activity of tissue factor in human aortic atherosclerotic lesions.* Atherosclerosis, 1997. **133**(2): p. 213-9.
170. Ardissino, D., et al., *Tissue-factor antigen and activity in human coronary atherosclerotic plaques.* Lancet, 1997. **349**(9054): p. 769-71.
171. Moreno, P.R., et al., *Macrophages, smooth muscle cells, and tissue factor in unstable angina. Implications for cell-mediated thrombogenicity in acute coronary syndromes.* Circulation, 1996. **94**(12): p. 3090-7.
172. Schecter, A.D., et al., *Tissue factor is induced by monocyte chemoattractant protein-1 in human aortic smooth muscle and THP-1 cells.* J Biol Chem, 1997. **272**(45): p. 28568-73.
173. Schuff-Werner, P., et al., *Enhanced procoagulatory activity (PCA) of human monocytes/macrophages after in vitro stimulation with chemically modified LDL.* Atherosclerosis, 1989. **78**(2-3): p. 109-12.
174. Cui, M.Z., M.S. Penn, and G.M. Chisolm, *Native and oxidized low density lipoprotein induction of tissue factor gene expression in smooth muscle cells is mediated by both Egr-1 and Sp1.* J Biol Chem, 1999. **274**(46): p. 32795-802.
175. Bochkov, V.N., et al., *Oxidized phospholipids stimulate tissue factor expression in human endothelial cells via activation of ERK/EGR-1 and Ca(++)/NFAT.* Blood, 2002. **99**(1): p. 199-206.
176. Pyo, R.T., et al., *Mice deficient in tissue factor demonstrate attenuated intimal hyperplasia in response to vascular injury and decreased smooth muscle cell migration.* Thromb Haemost, 2004. **92**(3): p. 451-8.
177. Marutsuka, K., et al., *Protease-activated receptor 2 (PAR2) mediates vascular smooth muscle cell migration induced by tissue factor/factor VIIa complex.* Thromb Res, 2002. **107**(5): p. 271-6.
178. Demetz, G., et al., *Tissue Factor-Factor VIIa complex induces cytokine expression in coronary artery smooth muscle cells.* Atherosclerosis, 2010. **212**(2): p. 466-71.
179. Tremoli, E., et al., *Tissue factor in atherosclerosis.* Atherosclerosis, 1999. **144**(2): p. 273-83.
180. Miller, D.M., G.R. Buettner, and S.D. Aust, *Transition metals as catalysts of "autoxidation" reactions.* Free Radic Biol Med, 1990. **8**(1): p. 95-108.
181. Haber, F., Weiss, J.J., *The catalytic decomposition of hydrogen peroxide by iron salts.* Proc R Soc Lond Ser A, 1934. **147**: p. 332-351.
182. Church, D.F. and W.A. Pryor, *Free-radical chemistry of cigarette smoke and its toxicological implications.* Environ Health Perspect, 1985. **64**: p. 111-26.
183. Matthay, M.A., et al., *Oxidant-mediated lung injury in the acute respiratory distress syndrome.* Crit Care Med, 1999. **27**(9): p. 2028-30.
184. Biaglow, J.E., J.B. Mitchell, and K. Held, *The importance of peroxide and superoxide in the X-ray response.* Int J Radiat Oncol Biol Phys, 1992. **22**(4): p. 665-9.
185. Stohs, S.J. and D. Bagchi, *Oxidative mechanisms in the toxicity of metal ions.* Free Radic Biol Med, 1995. **18**(2): p. 321-36.

186. Rich, T., R.L. Allen, and A.H. Wyllie, *Defying death after DNA damage.* Nature, 2000. **407**(6805): p. 777-83.
187. van Gent, D.C., J.H. Hoeijmakers, and R. Kanaar, *Chromosomal stability and the DNA double-stranded break connection.* Nat Rev Genet, 2001. **2**(3): p. 196-206.
188. Borza, C., Muntean, D., et al., Oxidative Stress and Lipid Peroxidation – A Lipid Metabolism Dysfunction.
189. Catala, A., *Lipid peroxidation modifies the picture of membranes from the "Fluid Mosaic Model" to the "Lipid Whisker Model".* Biochimie, 2012. **94**(1): p. 101-9.
190. Kelly, F.J. and I.S. Mudway, *Protein oxidation at the air-lung interface.* Amino Acids, 2003. **25**(3-4): p. 375-96.
191. Townsend, D.M., K.D. Tew, and H. Tapiero, *The importance of glutathione in human disease.* Biomed Pharmacother, 2003. **57**(3-4): p. 145-55.
192. Anderson, M.E., *Glutathione: an overview of biosynthesis and modulation.* Chem Biol Interact, 1998. **111-112**: p. 1-14.
193. Lu, S.C., *Glutathione synthesis.* Biochim Biophys Acta, 2013. **1830**(5): p. 3143-53.
194. Baudouin-Cornu, P., et al., *Glutathione degradation is a key determinant of glutathione homeostasis.* J Biol Chem, 2012. **287**(7): p. 4552-61.
195. Pompella, A., et al., *Gamma-glutamyltransferase, redox regulation and cancer drug resistance.* Curr Opin Pharmacol, 2007. **7**(4): p. 360-6.
196. Schafer, F.Q. and G.R. Buettner, *Redox environment of the cell as viewed through the redox state of the glutathione disulfide/glutathione couple.* Free Radic Biol Med, 2001. **30**(11): p. 1191-212.
197. Chen, B., et al., *The role of Nrf2 in oxidative stress-induced endothelial injuries.* J Endocrinol, 2015. **225**(3): p. R83-99.
198. Shibahara, S., et al., *Functional analysis of cDNAs for two types of human heme oxygenase and evidence for their separate regulation.* J Biochem, 1993. **113**(2): p. 214-8.
199. McCoubrey, W.K., Jr., T.J. Huang, and M.D. Maines, *Isolation and characterization of a cDNA from the rat brain that encodes hemoprotein heme oxygenase-3.* Eur J Biochem, 1997. **247**(2): p. 725-32.
200. Keyse, S.M. and R.M. Tyrrell, *Both near ultraviolet radiation and the oxidizing agent hydrogen peroxide induce a 32-kDa stress protein in normal human skin fibroblasts.* J Biol Chem, 1987. **262**(30): p. 14821-5.
201. Platt, J.L. and K.A. Nath, *Heme oxygenase: protective gene or Trojan horse.* Nat Med, 1998. **4**(12): p. 1364-5.
202. McCoubrey, W.K., Jr. and M.D. Maines, *The structure, organization and differential expression of the gene encoding rat heme oxygenase-2.* Gene, 1994. **139**(2): p. 155-61.
203. Maines, M.D., *The heme oxygenase system: a regulator of second messenger gases.* Annu Rev Pharmacol Toxicol, 1997. **37**: p. 517-54.
204. Otterbein, L.E. and A.M. Choi, *Heme oxygenase: colors of defense against cellular stress.* Am J Physiol Lung Cell Mol Physiol, 2000. **279**(6): p. L1029-37.
205. Motterlini, R., et al., *Heme oxygenase-1-derived carbon monoxide contributes to the suppression of acute hypertensive responses in vivo.* Circ Res, 1998. **83**(5): p. 568-77.
206. Mireles, L.C., M.A. Lum, and P.A. Dennery, *Antioxidant and cytotoxic effects of bilirubin on neonatal erythrocytes.* Pediatr Res, 1999. **45**(3): p. 355-62.
207. Dore, S., et al., *Bilirubin, formed by activation of heme oxygenase-2, protects neurons against oxidative stress injury.* Proc Natl Acad Sci U S A, 1999. **96**(5): p. 2445-50.
208. Clark, J.E., et al., *Heme oxygenase-1-derived bilirubin ameliorates postischemic myocardial dysfunction.* Am J Physiol Heart Circ Physiol, 2000. **278**(2): p. H643-51.

209. Balla, G., et al., *Exposure of endothelial cells to free heme potentiates damage mediated by granulocytes and toxic oxygen species.* Lab Invest, 1991. **64**(5): p. 648-55.
210. Balla, G., et al., *Ferritin: a cytoprotective antioxidant strategem of endothelium.* J Biol Chem, 1992. **267**(25): p. 18148-53.
211. Guzik, T.J., et al., *Calcium-dependent NOX5 nicotinamide adenine dinucleotide phosphate oxidase contributes to vascular oxidative stress in human coronary artery disease.* J Am Coll Cardiol, 2008. **52**(22): p. 1803-9.
212. Dai, Y., et al., *Xanthine Oxidase Induces Foam Cell Formation through LOX-1 and NLRP3 Activation.* Cardiovasc Drugs Ther, 2017. **31**(1): p. 19-27.
213. Salonen, I., et al., *Serum myeloperoxidase is independent of the risk factors of atherosclerosis.* Coron Artery Dis, 2012. **23**(4): p. 251-8.
214. Hawkins, C.L., *The role of hypothiocyanous acid (HOSCN) in biological systems.* Free Radic Res, 2009. **43**(12): p. 1147-58.
215. Exner, M., et al., *Thiocyanate catalyzes myeloperoxidase-initiated lipid oxidation in LDL.* Free Radic Biol Med, 2004. **37**(2): p. 146-55.
216. Lilledahl, M.B., et al., *Combined imaging of oxidative stress and microscopic structure reveals new features in human atherosclerotic plaques.* J Biomed Opt, 2015. **20**(2): p. 20503.
217. Yang, X., et al., *Inhibition of Glutathione Production Induces Macrophage CD36 Expression and Enhances Cellular-oxidized Low Density Lipoprotein (oxLDL) Uptake.* J Biol Chem, 2015. **290**(36): p. 21788-99.
218. Agarwal, A., et al., *Renal tubular epithelial cells mimic endothelial cells upon exposure to oxidized LDL.* Am J Physiol, 1996. **271**(4 Pt 2): p. F814-23.
219. Ishikawa, K., et al., *Induction of heme oxygenase-1 inhibits the monocyte transmigration induced by mildly oxidized LDL.* J Clin Invest, 1997. **100**(5): p. 1209-16.
220. Yamaguchi, M., H. Sato, and S. Bannai, *Induction of stress proteins in mouse peritoneal macrophages by oxidized low-density lipoprotein.* Biochem Biophys Res Commun, 1993. **193**(3): p. 1198-201.
221. Kawamura, K., et al., *Bilirubin from heme oxygenase-1 attenuates vascular endothelial activation and dysfunction.* Arterioscler Thromb Vasc Biol, 2005. **25**(1): p. 155-60.
222. Otterbein, L.E., et al., *Carbon monoxide has anti-inflammatory effects involving the mitogen-activated protein kinase pathway.* Nat Med, 2000. **6**(4): p. 422-8.
223. Morita, T. and S. Kourembanas, *Endothelial cell expression of vasoconstrictors and growth factors is regulated by smooth muscle cell-derived carbon monoxide.* J Clin Invest, 1995. **96**(6): p. 2676-82.
224. Chen, S.M., Y.G. Li, and D.M. Wang, *Study on changes of heme oxygenase-1 expression in patients with coronary heart disease.* Clin Cardiol, 2005. **28**(4): p. 197-201.
225. Cheng, C., et al., *Heme oxygenase 1 determines atherosclerotic lesion progression into a vulnerable plaque.* Circulation, 2009. **119**(23): p. 3017-27.
226. Mauvoisin, D. and C. Mounier, *Hormonal and nutritional regulation of SCD1 gene expression.* Biochimie, 2011. **93**(1): p. 78-86.
227. Nakamura, M.T. and T.Y. Nara, *Structure, function, and dietary regulation of delta6, delta5, and delta9 desaturases.* Annu Rev Nutr, 2004. **24**: p. 345-76.
228. Calder, P.C., et al., *Uptake and incorporation of saturated and unsaturated fatty acids into macrophage lipids and their effect upon macrophage adhesion and phagocytosis.* Biochem J, 1990. **269**(3): p. 807-14.
229. Ibarguren, M., D.J. Lopez, and P.V. Escriba, *The effect of natural and synthetic fatty acids on membrane structure, microdomain organization, cellular functions and human health.* Biochim Biophys Acta, 2014. **1838**(6): p. 1518-28.

230. Wynn, T.A. and K.M. Vannella, *Macrophages in Tissue Repair, Regeneration, and Fibrosis.* Immunity, 2016. **44**(3): p. 450-462.
231. Gordon, S., A. Pluddemann, and F. Martinez Estrada, *Macrophage heterogeneity in tissues: phenotypic diversity and functions.* Immunol Rev, 2014. **262**(1): p. 36-55.
232. Schumann, J., *It is all about fluidity: Fatty acids and macrophage phagocytosis.* Eur J Pharmacol, 2016. **785**: p. 18-23.
233. Adolph, S., H. Fuhrmann, and J. Schumann, *Unsaturated fatty acids promote the phagocytosis of P. aeruginosa and R. equi by RAW264.7 macrophages.* Curr Microbiol, 2012. **65**(6): p. 649-55.
234. Squellerio, I., et al., *Direct glutathione quantification in human blood by LC-MS/MS: comparison with HPLC with electrochemical detection.* J Pharm Biomed Anal, 2012. **71**: p. 111-8.
235. U.D.o.H.a.H.S. Food and Drug Administration, F., Center for Drug Evaluation and Research, *Guidance for Industry: Bioanalytical Method Validation,* http://www.fda.gov/downloads/drugs/guidancecomplianceregulatoryinformation/guidances/ucm368107.pdf2013.
236. Mitro, N., et al., *Neuroactive steroid treatment modulates myelin lipid profile in diabetic peripheral neuropathy.* J Steroid Biochem Mol Biol, 2014. **143**: p. 115-21.
237. Tearney, G.J., et al., *Consensus standards for acquisition, measurement, and reporting of intravascular optical coherence tomography studies: a report from the International Working Group for Intravascular Optical Coherence Tomography Standardization and Validation.* J Am Coll Cardiol, 2012. **59**(12): p. 1058-72.
238. Wolfs, I.M., M.M. Donners, and M.P. de Winther, *Differentiation factors and cytokines in the atherosclerotic plaque micro-environment as a trigger for macrophage polarisation.* Thromb Haemost, 2011. **106**(5): p. 763-71.
239. Mantovani, A., C. Garlanda, and M. Locati, *Macrophage diversity and polarization in atherosclerosis: a question of balance.* Arterioscler Thromb Vasc Biol, 2009. **29**(10): p. 1419-23.
240. Daigneault, M., et al., *The identification of markers of macrophage differentiation in PMA-stimulated THP-1 cells and monocyte-derived macrophages.* PLoS One, 2010. **5**(1): p. e8668.
241. Eligini, S., et al., *Human monocyte-derived macrophages spontaneously differentiated in vitro show distinct phenotypes.* J Cell Physiol, 2013. **228**(7): p. 1464-72.
242. Ait-Oufella, H., et al., *Lactadherin deficiency leads to apoptotic cell accumulation and accelerated atherosclerosis in mice.* Circulation, 2007. **115**(16): p. 2168-77.
243. Thorp, E., et al., *Mertk receptor mutation reduces efferocytosis efficiency and promotes apoptotic cell accumulation and plaque necrosis in atherosclerotic lesions of apoe-/- mice.* Arterioscler Thromb Vasc Biol, 2008. **28**(8): p. 1421-8.
244. Bhatia, V.K., et al., *Complement C1q reduces early atherosclerosis in low-density lipoprotein receptor-deficient mice.* Am J Pathol, 2007. **170**(1): p. 416-26.
245. Van Vre, E.A., et al., *Apoptotic cell death and efferocytosis in atherosclerosis.* Arterioscler Thromb Vasc Biol, 2012. **32**(4): p. 887-93.
246. Szondy, Z., et al., *Transglutaminase 2-/- mice reveal a phagocytosis-associated crosstalk between macrophages and apoptotic cells.* Proc Natl Acad Sci U S A, 2003. **100**(13): p. 7812-7.
247. Fadok, V.A., et al., *Particle digestibility is required for induction of the phosphatidylserine recognition mechanism used by murine macrophages to phagocytose apoptotic cells.* J Immunol, 1993. **151**(8): p. 4274-85.
248. Szondy, Z., et al., *Transglutaminase 2 dysfunctions in the development of autoimmune disorders: celiac disease and TG2-/- mouse.* Adv Enzymol Relat Areas Mol Biol, 2011. **78**: p. 295-345.

249. Tao, H., et al., *Macrophage SR-BI mediates efferocytosis via Src/PI3K/Rac1 signaling and reduces atherosclerotic lesion necrosis.* J Lipid Res, 2015. **56**(8): p. 1449-60.
250. Thorp, E. and I. Tabas, *Mechanisms and consequences of efferocytosis in advanced atherosclerosis.* J Leukoc Biol, 2009. **86**(5): p. 1089-95.
251. Ruf, W. and T.S. Edgington, *Structural biology of tissue factor, the initiator of thrombogenesis in vivo.* FASEB J, 1994. **8**(6): p. 385-90.
252. Mallat, Z. and A. Tedgui, *[Apoptosis in the cardiovascular system].* Ann Pathol, 1999. **19**(3): p. 265-73.
253. Annex, B.H., et al., *Differential expression of tissue factor protein in directional atherectomy specimens from patients with stable and unstable coronary syndromes.* Circulation, 1995. **91**(3): p. 619-22.
254. Marmur, J.D., et al., *Identification of active tissue factor in human coronary atheroma.* Circulation, 1996. **94**(6): p. 1226-32.
255. Ardissino, D., et al., *Tissue factor in human coronary atherosclerotic plaques.* Clin Chim Acta, 2000. **291**(2): p. 235-40.
256. Borissoff, J.I., et al., *Early atherosclerosis exhibits an enhanced procoagulant state.* Circulation, 2010. **122**(8): p. 821-30.
257. Lee, C.W., et al., *Comparison of ruptured coronary plaques in patients with unstable and stable clinical presentation.* J Thromb Thrombolysis, 2011. **32**(2): p. 150-7.
258. Hutter, R., et al., *Caspase-3 and tissue factor expression in lipid-rich plaque macrophages: evidence for apoptosis as link between inflammation and atherothrombosis.* Circulation, 2004. **109**(16): p. 2001-8.
259. Toschi, V., et al., *Tissue factor modulates the thrombogenicity of human atherosclerotic plaques.* Circulation, 1997. **95**(3): p. 594-9.
260. Suefuji, H., et al., *Increased plasma tissue factor levels in acute myocardial infarction.* Am Heart J, 1997. **134**(2 Pt 1): p. 253-9.
261. Leatham, E.W., et al., *Increased monocyte tissue factor expression in coronary disease.* Br Heart J, 1995. **73**(1): p. 10-3.
262. Cimmino, G., et al., *The missing link between atherosclerosis, inflammation and thrombosis: is it tissue factor?* Expert Rev Cardiovasc Ther, 2011. **9**(4): p. 517-23.
263. Cunningham, M.A., et al., *Tissue factor and factor VIIa receptor/ligand interactions induce proinflammatory effects in macrophages.* Blood, 1999. **94**(10): p. 3413-20.
264. Yokoyama, M., *Oxidant stress and atherosclerosis.* Curr Opin Pharmacol, 2004. **4**(2): p. 110-5.
265. Uno, K. and S.J. Nicholls, *Biomarkers of inflammation and oxidative stress in atherosclerosis.* Biomark Med, 2010. **4**(3): p. 361-73.
266. Forstermann, U., N. Xia, and H. Li, *Roles of Vascular Oxidative Stress and Nitric Oxide in the Pathogenesis of Atherosclerosis.* Circ Res, 2017. **120**(4): p. 713-735.
267. Forstermann, U., *Oxidative stress in vascular disease: causes, defense mechanisms and potential therapies.* Nat Clin Pract Cardiovasc Med, 2008. **5**(6): p. 338-49.
268. Witztum, J.L. and D. Steinberg, *Role of oxidized low density lipoprotein in atherogenesis.* J Clin Invest, 1991. **88**(6): p. 1785-92.
269. Matsuoka, H., *Endothelial dysfunction associated with oxidative stress in human.* Diabetes Res Clin Pract, 2001. **54 Suppl 2**: p. S65-72.
270. Siekmeier, R., T. Grammer, and W. Marz, *Roles of oxidants, nitric oxide, and asymmetric dimethylarginine in endothelial function.* J Cardiovasc Pharmacol Ther, 2008. **13**(4): p. 279-97.
271. Cavalca, V., et al., *Glutathione, vitamin E and oxidative stress in coronary artery disease: relevance of age and gender.* Eur J Clin Invest, 2009. **39**(4): p. 267-72.
272. Biswas, S.K., et al., *Depressed glutathione synthesis precedes oxidative stress and atherogenesis in Apo-E(-/-) mice.* Biochem Biophys Res Commun, 2005. **338**(3): p. 1368-73.

273. Rosenblat, M. and M. Aviram, *Macrophage glutathione content and glutathione peroxidase activity are inversely related to cell-mediated oxidation of LDL: in vitro and in vivo studies.* Free Radic Biol Med, 1998. **24**(2): p. 305-17.
274. Mazzanti, L. and B. Mutus, *Diabetes-induced alterations in platelet metabolism.* Clin Biochem, 1997. **30**(7): p. 509-15.
275. Jones, D.P., *Redox potential of GSH/GSSG couple: assay and biological significance.* Methods Enzymol, 2002. **348**: p. 93-112.
276. Eligini, S., et al., *Nitric oxide synthetic pathway in red blood cells is impaired in coronary artery disease.* PLoS One, 2013. **8**(8): p. e66945.
277. Motohashi, H. and M. Yamamoto, *Nrf2-Keap1 defines a physiologically important stress response mechanism.* Trends Mol Med, 2004. **10**(11): p. 549-57.
278. Baird, L. and A.T. Dinkova-Kostova, *The cytoprotective role of the Keap1-Nrf2 pathway.* Arch Toxicol, 2011. **85**(4): p. 241-72.
279. Bailey-Downs, L.C., et al., *Liver-specific knockdown of IGF-1 decreases vascular oxidative stress resistance by impairing the Nrf2-dependent antioxidant response: a novel model of vascular aging.* J Gerontol A Biol Sci Med Sci, 2012. **67**(4): p. 313-29.
280. Dai, G., et al., *Biomechanical forces in atherosclerosis-resistant vascular regions regulate endothelial redox balance via phosphoinositol 3-kinase/Akt-dependent activation of Nrf2.* Circ Res, 2007. **101**(7): p. 723-33.
281. Hosoya, T., et al., *Differential responses of the Nrf2-Keap1 system to laminar and oscillatory shear stresses in endothelial cells.* J Biol Chem, 2005. **280**(29): p. 27244-50.
282. Jyrkkanen, H.K., et al., *Nrf2 regulates antioxidant gene expression evoked by oxidized phospholipids in endothelial cells and murine arteries in vivo.* Circ Res, 2008. **103**(1): p. e1-9.
283. Ungvari, Z., et al., *Resveratrol confers endothelial protection via activation of the antioxidant transcription factor Nrf2.* Am J Physiol Heart Circ Physiol, 2010. **299**(1): p. H18-24.
284. Ungvari, Z., et al., *Adaptive induction of NF-E2-related factor-2-driven antioxidant genes in endothelial cells in response to hyperglycemia.* Am J Physiol Heart Circ Physiol, 2011. **300**(4): p. H1133-40.
285. Zakkar, M., et al., *Activation of Nrf2 in endothelial cells protects arteries from exhibiting a proinflammatory state.* Arterioscler Thromb Vasc Biol, 2009. **29**(11): p. 1851-7.
286. Donovan, E.L., et al., *Phytochemical activation of Nrf2 protects human coronary artery endothelial cells against an oxidative challenge.* Oxid Med Cell Longev, 2012. **2012**: p. 132931.
287. Zhu, H., et al., *Antioxidants and phase 2 enzymes in macrophages: regulation by Nrf2 signaling and protection against oxidative and electrophilic stress.* Exp Biol Med (Maywood), 2008. **233**(4): p. 463-74.
288. Collins, A.R., et al., *Myeloid deletion of nuclear factor erythroid 2-related factor 2 increases atherosclerosis and liver injury.* Arterioscler Thromb Vasc Biol, 2012. **32**(12): p. 2839-46.
289. Ruotsalainen, A.K., et al., *The absence of macrophage Nrf2 promotes early atherogenesis.* Cardiovasc Res, 2013. **98**(1): p. 107-15.
290. Sussan, T.E., et al., *Disruption of Nrf2, a key inducer of antioxidant defenses, attenuates ApoE-mediated atherosclerosis in mice.* PLoS One, 2008. **3**(11): p. e3791.
291. Barajas, B., et al., *NF-E2-related factor 2 promotes atherosclerosis by effects on plasma lipoproteins and cholesterol transport that overshadow antioxidant protection.* Arterioscler Thromb Vasc Biol, 2011. **31**(1): p. 58-66.
292. Freigang, S., et al., *Nrf2 is essential for cholesterol crystal-induced inflammasome activation and exacerbation of atherosclerosis.* Eur J Immunol, 2011. **41**(7): p. 2040-51.
293. Huang, J., et al., *Transcription factor Nrf2 regulates SHP and lipogenic gene expression in hepatic lipid metabolism.* Am J Physiol Gastrointest Liver Physiol, 2010. **299**(6): p. G1211-21.

294. Ishii, T., et al., *Role of Nrf2 in the regulation of CD36 and stress protein expression in murine macrophages: activation by oxidatively modified LDL and 4-hydroxynonenal.* Circ Res, 2004. **94**(5): p. 609-16.
295. Burns, M.J. and M.B. Furie, *Borrelia burgdorferi and interleukin-1 promote the transendothelial migration of monocytes in vitro by different mechanisms.* Infect Immun, 1998. **66**(10): p. 4875-83.
296. Araujo, J.A., M. Zhang, and F. Yin, *Heme oxygenase-1, oxidation, inflammation, and atherosclerosis.* Front Pharmacol, 2012. **3**: p. 119.
297. Itoh, K., et al., *Keap1 represses nuclear activation of antioxidant responsive elements by Nrf2 through binding to the amino-terminal Neh2 domain.* Genes Dev, 1999. **13**(1): p. 76-86.
298. Nguyen, T., P.J. Sherratt, and C.B. Pickett, *Regulatory mechanisms controlling gene expression mediated by the antioxidant response element.* Annu Rev Pharmacol Toxicol, 2003. **43**: p. 233-60.
299. Stewart, D., et al., *Degradation of transcription factor Nrf2 via the ubiquitin-proteasome pathway and stabilization by cadmium.* J Biol Chem, 2003. **278**(4): p. 2396-402.
300. Wang, L.J., et al., *Expression of heme oxygenase-1 in atherosclerotic lesions.* Am J Pathol, 1998. **152**(3): p. 711-20.
301. Ishikawa, K., et al., *Heme oxygenase-1 inhibits atherosclerotic lesion formation in ldl-receptor knockout mice.* Circ Res, 2001. **88**(5): p. 506-12.
302. Kaneda, H., et al., *Heme oxygenase-1 gene promoter polymorphism is associated with coronary artery disease in Japanese patients with coronary risk factors.* Arterioscler Thromb Vasc Biol, 2002. **22**(10): p. 1680-5.
303. Chen, Y.H., et al., *Microsatellite polymorphism in promoter of heme oxygenase-1 gene is associated with susceptibility to coronary artery disease in type 2 diabetic patients.* Hum Genet, 2002. **111**(1): p. 1-8.
304. Schillinger, M., et al., *Heme oxygenase-1 genotype is a vascular anti-inflammatory factor following balloon angioplasty.* J Endovasc Ther, 2002. **9**(4): p. 385-94.
305. Yachie, A., et al., *Oxidative stress causes enhanced endothelial cell injury in human heme oxygenase-1 deficiency.* J Clin Invest, 1999. **103**(1): p. 129-35.
306. Kawashima, A., et al., *Heme oxygenase-1 deficiency: the first autopsy case.* Hum Pathol, 2002. **33**(1): p. 125-30.
307. Jeney, V., et al., *Pro-oxidant and cytotoxic effects of circulating heme.* Blood, 2002. **100**(3): p. 879-87.
308. Calder, P.C., *The relationship between the fatty acid composition of immune cells and their function.* Prostaglandins Leukot Essent Fatty Acids, 2008. **79**(3-5): p. 101-8.
309. Adolph, S., et al., *Unsaturated fatty acids as modulators of macrophage respiratory burst in the immune response against Rhodococcus equi and Pseudomonas aeruginosa.* Free Radic Biol Med, 2012. **52**(11-12): p. 2246-53.
310. Schoeniger, A., et al., *The impact of membrane lipid composition on macrophage activation in the immune defense against Rhodococcus equi and Pseudomonas aeruginosa.* Int J Mol Sci, 2011. **12**(11): p. 7510-28.
311. Schroit, A.J. and R. Gallily, *Macrophage fatty acid composition and phagocytosis: effect of unsaturation on cellular phagocytic activity.* Immunology, 1979. **36**(2): p. 199-205.
312. Mahoney, E.M., et al., *Response of endocytosis to altered fatty acyl composition of macrophage phospholipids.* Proc Natl Acad Sci U S A, 1977. **74**(11): p. 4895-9.
313. Fuhrmann, H., et al., *Membrane fatty acids, oxidative burst and phagocytosis after enrichment of P388D1 monocyte/macrophages with essential 18-carbon fatty acids.* Ann Nutr Metab, 2007. **51**(2): p. 155-62.

314. Rise, P., et al., *Delta5 desaturase mRNA levels are increased by simvastatin via SREBP-1 at early stages, not via PPARalpha, in THP-1 cells.* Eur J Pharmacol, 2007. **571**(2-3): p. 97-105.
315. Barlis, P., et al., *Optical coherence tomography assessment of vulnerable plaque rupture: predilection for the plaque 'shoulder'.* Eur Heart J, 2008. **29**(16): p. 2023.
316. Yabushita, H., et al., *Characterization of human atherosclerosis by optical coherence tomography.* Circulation, 2002. **106**(13): p. 1640-5.
317. Tearney, G.J., et al., *Quantification of macrophage content in atherosclerotic plaques by optical coherence tomography.* Circulation, 2003. **107**(1): p. 113-9.
318. Kume, T., et al., *Measurement of the thickness of the fibrous cap by optical coherence tomography.* Am Heart J, 2006. **152**(4): p. 755 e1-4.
319. Kume, T., et al., *Assessment of coronary arterial thrombus by optical coherence tomography.* Am J Cardiol, 2006. **97**(12): p. 1713-7.
320. Burke, A.P., et al., *Coronary risk factors and plaque morphology in men with coronary disease who died suddenly.* N Engl J Med, 1997. **336**(18): p. 1276-82.
321. Barlis, P., et al., *Assessment of culprit and remote coronary narrowings using optical coherence tomography with long-term outcomes.* Am J Cardiol, 2008. **102**(4): p. 391-5.
322. Virmani, R., et al., *Lessons from sudden coronary death: a comprehensive morphological classification scheme for atherosclerotic lesions.* Arterioscler Thromb Vasc Biol, 2000. **20**(5): p. 1262-75.
323. Kato, K., et al., *Nonculprit plaques in patients with acute coronary syndromes have more vulnerable features compared with those with non-acute coronary syndromes: a 3-vessel optical coherence tomography study.* Circ Cardiovasc Imaging, 2012. **5**(4): p. 433-40.
324. Tearney, G.J., I.K. Jang, and B.E. Bouma, *Optical coherence tomography for imaging the vulnerable plaque.* J Biomed Opt, 2006. **11**(2): p. 021002.
325. Wilcox, J.N., et al., *Localization of tissue factor in the normal vessel wall and in the atherosclerotic plaque.* Proc Natl Acad Sci U S A, 1989. **86**(8): p. 2839-43.
326. Kunsch, C. and R.M. Medford, *Oxidative stress as a regulator of gene expression in the vasculature.* Circ Res, 1999. **85**(8): p. 753-66.
327. Lafont, A., *Basic aspects of plaque vulnerability.* Heart, 2003. **89**(10): p. 1262-7.
328. Li, Y.G., et al., *Haem oxygenase-1 expression and coronary heart disease--association between levels of haem oxygenase-1 expression and angiographic morphology as well as the quantity of coronary lesions.* Acta Cardiol, 2006. **61**(3): p. 295-300.